Impacts of Climate Change on US Commercial and Residential Building Energy Demand

by

Jianhua Huang

A Dissertation Presented in Partial Fulfillment
of the Requirements for the Degree
Doctor of Philosophy

Approved February 2016 by the
Graduate Supervisory Committee:

Kevin Gurney, Chair
Matei Georgescu
Clark Miller
Sergio Rey

ARIZONA STATE UNIVERSITY

May 2016

ABSTRACT

Energy consumption in buildings, accounting for 41% of 2010 primary energy consumption in the United States (US), is particularly vulnerable to climate change due to the direct relationship between space heating/cooling and temperature. Past studies have assessed the impact of climate change on long-term mean and/or peak energy demands. However, these studies usually neglected spatial variations in the "balance point" temperature, population distribution effects, air-conditioner (AC) saturation, and the extremes at smaller spatiotemporal scales, making the implications of local-scale vulnerability incomplete. Here I develop empirical relationships between building energy consumption and temperature to explore the impact of climate change on long-term mean and extremes of energy demand, and test the sensitivity of these impacts to various factors. I find increases in summertime electricity demand exceeding 50% and decreases in wintertime non-electric energy demand of more than 40% in some states by the end of the century. The occurrence of the most extreme (appearing once-per-56-years) electricity demand increases more than 2600 fold, while the occurrence of the once per year extreme events increases more than 70 fold by the end of this century. If the changes in population and AC saturation are also accounted for, the impact of climate change on building energy demand will be exacerbated.

Using the individual building energy simulation approach, I also estimate the impact of climate change to different building types at over 900 US locations. Large increases in building energy consumption are found in the summer, especially during the daytime (e.g., >100% increase for warehouses, 5-6 pm). Large variation of impact is also found

within climate zones, suggesting a potential bias when estimating climate-zone scale changes with a small number of representative locations.

As a result of climate change, the building energy expenditures increase in some states (as much as $3 billion/year) while in others, costs decline (as much as $1.4 billion/year). Integrated across the contiguous US, these variations result in a net savings of roughly $4.7 billion/year. However, this must be weighed against the cost (exceeding $19 billion) of adding electricity generation capacity in order to maintain the electricity grid's reliability in summer.

ACKNOWLEDGMENTS

I would like to express my sincere appreciation and gratitude to my advisor, Dr. Kevin Gurney, who gave me the freedom to pursue the research topic I am interested in, and provided me with endless advice and help with my work. Without the support from him, my dissertation could never have been completed. From him, I also learned how to enjoy doing science, and how to overcome tough challenges with a can-do attitude. I would also like to thank my committee members, Dr. Matei Georgescu, Dr. Serge Rey, and Dr. Clark Miller, for their valuable comments on my proposal and in-depth suggestions for my research. Special thanks also go to the members in Gurney lab, including Risa Patarasuk, Darragh O'Keeffe, Terry Song, Maya, Hutchins, Jianming Liang, for their useful comments to my proposal, dissertation, and presentation.

During my PhD study, I have come to owe a lot to my family. Being busy with my research and far away from home, I didn't have much time for family visits. So, without the support and understanding from my parents, it would have been impossible for me to finish my PhD degree. Finally but by no means least, I owe my wife, Ting, a happy and comfortable time in the future. Since I moved from Purdue University to ASU, we had to begin a long-distance relationship. She sacrificed so much to maintain the relationship, and she has to deal with all kinds of problems in her daily life alone. I'm lucky to have Ting in my life. Her love, consideration, and encouragement kept me grounded during my PhD.

TABLE OF CONTENTS

Page

CHAPTER Page

APPENDIX Page

LIST OF TABLES

Table Page

LIST OF FIGURES

Figure Page

Figure Page

CHAPTER 1

1 INTRODUCTION

1.1 Backgrounds

Global temperature has increased by approximately 0.76°C since 1850, and eleven of the twelve warmest years were in the 1995 – 2006 time period (Solomon 2007). Global surface temperature is projected to rise 1.1 to 6.4 °C by the end of this century relative to 1980-1999 levels (Solomon 2007). Climate change will have many impacts on human activity such as human health, food supply, and water availability, to name a few. Of these, the impact of climate change on energy demand and supply has received relatively little attention. Of all the energy consuming activities, heating and cooling of indoor environments is influenced most directly by climate change. Furthermore, this activity constitutes a large proportion of total energy consumption. For example, U.S. building energy consumption accounted for 41% of primary energy consumption in 2010. Within commercial buildings, space heating and cooling together account for 30.5% building primary energy consumption, while in residential buildings, the share is 43% (DoE 2012).

The changing balance of space cooling and heating is a crucial element in determining how the energy supply sector should plan for climate change and how choices in building technology should adapt/respond to climate projections. Previous research indicates that in the most general terms, energy consumption for space cooling in the United States will increase, driven by climate change and continued expansion of air-conditioning (Wilbanks et al. 2008). At the same time, energy consumption for space heating will decrease, due to warmer mean temperatures. The precise balance, however, remains ambiguous. Much depends upon assumptions regarding climate change projections,

questions of space/time scales, research methods, emissions scenario, and energy form (on-site, or source energy) chosen, among other factors.

1.2 Past Research

1.2.1 Overview of past research

A number of approaches have been employed to study the impacts of climate change on long-term average (e.g., annual mean) and/or peak (e.g., daily maximum) energy consumption in the U.S. (Wilbanks et al. 2008; Lukas G Swan & Ugursal 2009; Edenhofer et al. 2014). These approaches can be generally classified into three categories: observation-based regression/prediction, global/regional energy modeling, and individual building energy simulation.

The observation-based regression/prediction approach takes advantage of the historical relationship between energy consumption and climate variables to predict future energy consumption under a changing climate. Because this method is based on historical data, it is self-calibrated when fitted to a model. The output resolution from this approach is usually determined by the resolution of the historical data, and the accuracy of the estimation depends on the quality of the selected regression model (usually evaluated with statistical criteria, for example R^2). This approach has been used to estimate the impacts of climate change on annual/monthly energy consumption (Sailor et al. 1998a; David J Sailor & Muñoz 1997; Sailor 2001a; Ruth & Lin 2006a) and peak energy demand (Ruth & Lin 2006a; Franco & Sanstad 2007; Alan F Hamlet et al. 2010; Sathaye et al. 2013) in some US states.

The global/regional energy modeling approach simulates energy consumption in a numerical model composed of multiple variables such as energy demand and supply, economy, technology, population, policy, and climate. The impact of climate change on building energy consumption is assessed through simulated climate change scenarios. Besides climate change, this approach can be also used to study the impact of other key variables such as population change, land use change, carbon taxes, and mitigation policy. However, the complexity and flexibility of this method comes at the expense of output resolution. Hence, this method has been employed to estimate the impacts of climate change on annual building energy consumption at the global, national, and state levels, at the finest (Isaac & Van Vuuren 2009; Stanton W Hadley et al. 2006; Zhou et al. 2013b; Zhou, Clarke, Eom, Kyle, Patel, Son H Kim, et al. 2014; Jaglom et al. 2014; McFarland et al. 2015).

The individual building energy simulation approach can be used to simulate high-frequency output (e.g., hourly) for specific building types. However, it usually requires detailed building characteristics and hourly weather data to drive the simulation. Such detailed information (e.g. building characteristics, occupants, operation schedules) is limited. As a result, this approach has been used for a few building types in particular locations only (Scott et al. 1994; Xu et al. 2012a; Dirks et al. 2015; Hong et al. 2013; Wan et al. 2012). Although Huang (Y. J. Huang 2006) and Wang *et al.* (Wang & Chen 2014) used this approach to evaluate the impact of climate change for the whole US, the results are based on building energy simulations in less than 20 cities.

In addition to the change in long-term average and/or peak energy demands, the extremes in energy demands are also affected by climate change. Numerous studies have shown

that extreme climate events (e.g. heat waves) in the future are expected to occur with greater intensity and frequency and last longer (Meehl & Tebaldi 2004; Jones et al. 2015). However, the impact and importance of more frequent and intense extreme climate events on extreme energy demand has received little attention.

A few studies have attempted to transferred the impacts of climate change on energy demands into practical financial implications based on national/international economic modeling (Linder & Inglis 1989; Stanton W Hadley et al. 2006; Rosenthal et al. 1995; Mansur et al. 2008; Mendelsohn et al. 2000; Jaglom et al. 2014). Some studies found increased costs in the energy sector, ranging from a few billion dollars to a few hundred billion dollars (Linder & Inglis 1989; Stanton W Hadley et al. 2006; Mansur et al. 2008; Jaglom et al. 2014). By contrast, other studies found savings of a few billion dollars in energy expenditures (Rosenthal et al. 1995; Mendelsohn et al. 2000). These studies, carried out at the national/international scale, usually mask the spatial variation and extremes of the impacts at the sub-national and sub-annual level, which is important for local energy consumer/suppliers and practical decision-making.

1.2.2 Shortcoming of past research

Regardless of the different approaches taken and the exact research questions asked, heating/cooling degree days (HDD/CDD) are used to relate external temperature to building energy demand in most past research. HDD (CDD) is defined as the cumulative difference between the "balance point temperature" (the outside temperature where a shift between building heating and cooling occurs) and the daily mean temperature for days in which the daily mean temperature is lower (higher) than the balance point temperature (Baumert & Selman 2003). The calculation of HDD/CDD in past research,

however, usually neglected the spatial variations in the balance point temperature and depended on a commonly-used balance point temperature (65 °F), which may result in biased estimates of climate change impact on building energy demand.

Although the impact of climate change to long-term mean/peak energy demands was explored in some past research, the impact of climate change on extreme (e.g., once per year event) energy demand was never studied. These extremes in energy demand will not only place more pressure on electricity generation and transmission, but also cause electricity system disturbance and affect electricity consumers through electricity scarcity and power outages (Miller et al. 2008). These energy security problems, in addition to the normal issues of energy demand and supply, make it especially valuable to estimate the occurrences of extreme electricity demand under a changing climate.

Due to the spatial and temporal heterogeneity of climate change, its impact on energy consumption may display strong spatial and temporal patterns, and the results could be sensitive to the spatial and temporal scales examined. However, past assessments have not comprehensively explored both the sub-national and sub-annual impacts of climate change for the whole US, making the implications of local-scale vulnerability incomplete. In addition, the population size is expected to double by the end of this century (U.S. Environmental Protection Agency 2010), and more air conditioners will be installed due to the predicted warmer temperature(Sailor & Pavlova 2003). The changes in population distribution and AC saturation, and their interaction with climate, were usually ignored in the past research, potentially underestimating energy demand increases. Finally, energy use patterns are related to building type and technology. As a result, the net impact of climate change on space heating/cooling energy consumption will be sensitive to building

type and assumed changes in future building technology. It may help to design more practical and tailored adaptation/mitigation strategies, by examining the variation of climate change impacts on different building types/technology.

1.3 Research Questions

In order to more thoroughly explore the impacts of climate change on building energy demands and overcome the shortcoming of the past research, I designed several experiments focused on different perspectives of the subject. The primary research question was: what are the impacts/implications of climate change to building energy consumption, and are these impacts/implications sensitive to other factors? More specifically, the research questions can be separated into several parts:

1) What is the impact of climate change on long-term mean (monthly/annual) building energy demand?
2) What is the impact of climate change on extreme building electricity demand?
3) Are these impacts sensitive to other factors such as, the balance point temperature, the spatial and temporal scales, the building type/technology, population change, and AC saturation change?
4) What are the financial implications of these impacts to energy consumers and suppliers?

1.4 Dissertation Structure

The dissertation consists of an Introduction, Conclusions, and four main body chapters. The main content of the body chapters are comprised of individual papers either in review or in preparation for peer-reviewed journals. Each body chapter is focused on one

or more of the research questions, and the overall Introduction and Conclusions chapters in this dissertation thread the four individual body chapters together and reflect the total narrative of my work.

The first chapter (Introduction) introduces the background of climate change and its relationship to building energy demand, provides a comprehensive literature review of past research and discusses their shortcomings, renders the research questions of this dissertation, and presents the structure of the whole dissertation.

Chapter 2 is focused on the impact of climate change to long-term mean (annual/monthly) building energy demands, and its sensitivity to spatiotemporal scales, balance point temperature, and population distribution. In order to quantify the impacts of sub-national and sub-annual US building energy demand to climate change, I derive an empirical relationship between historical monthly temperature variations and building energy demand using state-specific electricity and natural gas consumption in conjunction with an optimized balance point temperature derived from the state-level data. Based on these relationships, I employ the results of 15 high-resolution statistically-downscaled climate model simulations to estimate the vulnerability of US building energy demand to climate change. We also include changes in air-conditioning saturation levels and distinguish between "site" and "source" energy consumption with the former reflecting consumption at the end-use point and the latter reflecting the raw energy required to meet end-use demand(Energy Star 2011). With these projections complete, we test the sensitivity of the estimated impacts to three important elements of the relationship between climate change and building energy consumption: the spatiotemporal resolution of analysis, the balance point temperature methodology, and the importance of population redistribution.

Chapter 3 is focused on the impact of climate change on the frequency and intensity of extreme electricity demand. In this chapter, I develop an empirically-based regression model that links daily electricity demand to temperature-related variables (Heating/cooling degree days), and use it to quantify the impacts of climate change on the frequency and intensity of extremes in electricity demand. The model is used to estimate daily electricity demand and identify extreme events in the historical (1950-2005) and future (2006-2099) periods. The impacts of changes in long-term mean climate are isolated from the impacts due to high-frequency (daily) climate changes. The impacts of population and air-conditioning saturation levels are also assessed with the projected population and AC saturation levels data around 2050.

Chapter 4 is focused on the variation of climate change impact on building energy consumption to building type and spatiotemporal scale. In this chapter, I quantitatively explore the impact of climate change on building energy consumption using the individual building energy simulation approach. I base the building-level energy simulations on over 900 US locations distributed in 16 climate zones, providing analysis at an unprecedented spatial-temporal resolution. I include results for 15 commercial and 2 residential building types driven by current and projected climate in the decades of the 2040s and 2090s under three emission scenarios. With the high-spatiotemporal-resolution outputs, I detect the temporal (e.g., monthly and hourly) patterns of climate change impacts, identify hot spots, and calculate the differences of impacts within, as well as between climate zones, offering practical and statistically reliable insights into climate change mitigation/adaptation for different building types at local, regional, and national scales.

Chapter 5 is focused on the financial implications of climate change impacts to building energy consumers and energy suppliers. This chapter is mainly based on the state-level monthly energy demand changes found in Chapter 2. In this chapter, I quantify the financial and infrastructural changes implied by the building energy changes in ways more meaningful for energy consumers and suppliers using current consumer energy prices and energy supply reserve requirements. The energy cost differences are estimated for the state residential and commercial sector separately. The additional electricity supply capacity required to satisfy the reserve margin requirement is estimated for each North American Electric Reliability Corporation (NERC) region, which is further converted to an annual cost based on prices to build and operate new electricity capacities.

The last chapter (Conclusions) synthesizes the main findings from four body chapters, and discusses the broader implications of the findings to the audience such as climate scientist, policy makers, building designers, and energy consumers/suppliers.

The dissertation mainly consists of the following manuscripts in peer-reviewed journal format:

- Huang, J. & Gurney, K.R. Impact of climate change to building energy demand: sensitivity to spatiotemporal scales, balance point temperature, and population distribution. *Climatic Change* (*under review*)
- Huang, J. & Gurney, K.R. The impact of climate change on the frequency and intensity of extreme electricity demand. (*in preparation*)
- Huang, J. & Gurney, K.R The variation of climate change impact on building energy consumption to building type and spatiotemporal scale. *Energy* (*under review*)
- Huang, J. & Gurney, K.R. Financial implications of the climate change impacts to building energy consumers and energy suppliers. (*in preparation*)

CHAPTER 2

2 IMPACT OF CLIMATE CHANGE TO BUILDING ENERGY DEMAND: SENSITIVITY TO SPATIOTEMPORAL SCALES, BALANCE POINT TEMPERATURE, AND POPULATION DISTRIBUTION

2.1 Introduction

Global surface temperature is projected to rise 1.1 to 6.4 °C by the end of this century relative to 1980-1999 levels (Solomon 2007). Within commercial buildings, space heating and cooling together account for 31% of building primary energy consumption, while in residential buildings, the share is 43% (Kelso 2012a). A number of approaches have been employed to study the impacts of climate change on building energy consumption in the United States, including regression modeling, individual building energy simulation, and regional/national energy modeling (Wilbanks et al. 2008; Lukas G. Swan & Ugursal 2009; Edenhofer 2014; Stanton W. Hadley et al. 2006; Alan F. Hamlet et al. 2010; J. Huang 2006; Ruth & Lin 2006b; David J. Sailor & Muñoz 1997; Sailor et al. 1998b; Sailor 2001b; Xu et al. 2012b; Zhou et al. 2013a; Zhou, Clarke, Eom, Kyle, Patel, Son H. Kim, et al. 2014; Georgescu et al. 2014; Franco & Sanstad 2007). Most of the research results, however, have not comprehensively explored the US sub-national and sub-annual impacts of climate change, have not included empirically-derived "balance point" temperatures (the outside temperature where a shift between building heating and cooling occurs), and/or have not thoroughly examined the implications of population distribution effects. Each of these elements are potentially important to an accurate assessment of the full impacts in the future and hence, plans to mitigate or adapt to climate change in the building sector.

To explore a more comprehensive treatment of the impact of climate change on building energy demand, we derive an empirical relationship between historical monthly temperature and building energy demand using state-specific electricity and natural gas consumption. Based on these relationships, we employ the results of high-resolution statistically-downscaled climate model simulations to project the building energy consumption out to the year 2099. Changes in the air-conditioning (AC) saturation levels caused by higher future temperature are also included to estimate the climate change impacts. Furthermore, we distinguish between "site" and "source" energy consumption with the former reflecting consumption at the end-use point and the latter reflecting the raw energy required to meet end-use demand (Energy Star 2011).

With these projections complete, we test the sensitivity of the estimated impacts to three important elements of the relationship between climate change and building energy consumption: the spatiotemporal resolution of analysis, the balance point temperature methodology, and the importance of population redistribution. The sensitivity to spatiotemporal scales is evaluated by comparing national/annual to state/sub-annual (monthly and seasonal) results. The sensitivity to balance point temperature is evaluated by comparing the results based on state-specific balance point temperatures to the results based on the commonly-used fixed 65 °F balance point temperature. Finally, the sensitivity to population redistribution is evaluated by comparing projections that use the 2010 population distribution to the same simulation using the population distribution for the year 2090.

2.2 Methods and Data

Monthly, state-specific electricity and natural gas consumption for the 2008-2012 time period are retrieved from the Department of Energy's Energy Information Administration (EIA) (U.S. Energy Information Administration 2014a; U.S. Department of Energy 2014). This energy consumption data represents what is consumed at the "end-use" point and we refer to this as the "site" energy consumption. The energy required to provide the site energy (accounting for energy loss during production, transmission, and delivery) is referred to as the "source" energy and source-to-site ratios are used to convert between site and source energy consumption(Energy Star 2011; Deru & Torcellini 2007). The 2010 county population data is retrieved from the US Census Bureau(U.S. Census Bureau 2010b), and the 2090 county population is extracted from the Integrated Climate and Land-Use Scenarios (ICLUS) dataset (U.S. Environmental Protection Agency 2010) . Daily-mean temperature covering the 2008 to 2012 time period is retrieved from the National Center for Environmental Prediction's (NCEP) North American Regional Reanalysis (NARR) (National Center for Environmental Prediction 2014). Projected daily temperature is derived from the World Climate Research Program's (WCRP) phase 5 of the Coupled Model Intercomparison Project (CMIP5) (The World Climate Research Programme 2014). The projected daily temperature is available from 2006 to 2099 from 20 climate models (Supplementary Table S2.2) under the RCP 8.5 emission scenario (radiative forcing rises to 8.5 W/m^2 in 2100) (van Vuuren et al. 2011). The RCP 8.5 scenario is selected, because it was simulated by the greatest number of models and the temperature change was greatest, offering a wider spectrum of results and the largest signal to noise. To represent the current/projected daily temperature for U.S. counties,

necessary for the analysis in this study, the average temperature of the four closest (shortest great circle distance from the county center to the grid center) NARR/CMIP5 grid cell is used.

We use HDD/CDD to relate external surface temperature to the demand for heating/cooling in buildings. HDD (CDD) is defined as the cumulative difference between the "balance point" temperature and the daily mean temperature for days in which the daily mean temperature is lower (higher) than the balance point temperature (Baumert & Selman 2003). We compute the HDD/CDD values at the county level and apply population weighting to generate state-level means. A state-specific balance point temperature, $T_b(S)$, is estimated using total state building electricity consumption and population-weighted state temperature with a segmented regression method (Muggeo 2008) **(**Supplementary Section S2.3 and S2.6**).** The state-specific balance point temperature ranges from 51 °F in Washington to 70 °F in Florida (Figure 2.1). Generally, higher balance point temperatures occur in states with warmer climates and vice versa, possibly reflecting social norms regarding desirable interior temperatures and building thermal properties. This is consistent with previous research (de Dear & Brager 2001) and further demonstrated by the fact that the correlation coefficient between the 1970-2000 average temperature and balance point temperature is 0.71 (Figure S2.2).

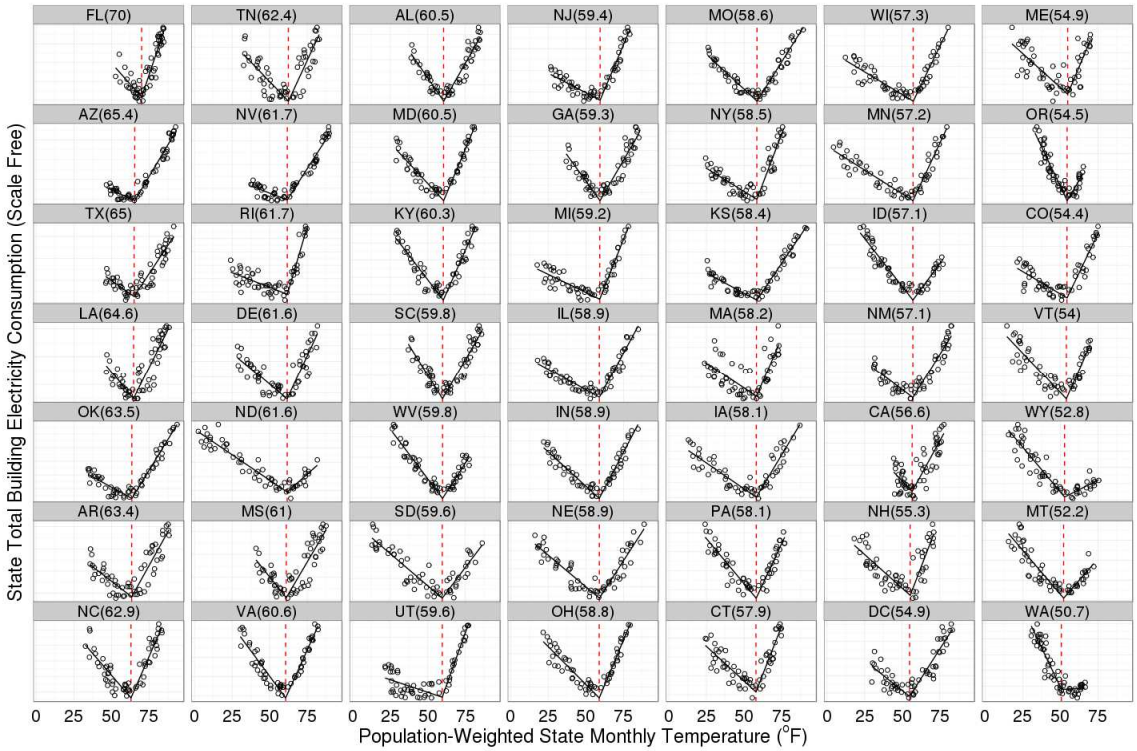

Figure 2.1 Relationship between monthly total building electricity consumption and monthly-mean, population-weighted air temperature for each US state. Black lines represent the segmented regression lines and red vertical lines indicate the balance point temperature.

To quantify the relationship between HDD/CDD and building energy consumption, a regression modeling approach is used (Supplementary Section S2.4). Electricity and natural gas consumption is modeled separately for all building sectors (residential and commercial combined) within each state over the 2008-2012 time period:

$$E^{NG}(s,m) = \alpha + \lambda(m-1) + \beta HDD(s,m) + \gamma HDD(s,m-1) + \epsilon \quad \textbf{(1)}$$

$$E^{ele}(s,m) = \alpha + \lambda(m-1) + \beta_1 HDD(s,m) + \beta_2 CDD(s,m) + \gamma_1 HDD(s,m-1) + \gamma_2 CDD(s,m-1) + \epsilon \quad \textbf{(2)}$$

where, E represents the per-capita energy consumption of natural gas (NG) or electricity (ele) for state, s, and month, m. The regression coefficients are represented by α, λ, β, and

γ, and ϵ is the error term. A trend term (m -1) is included to capture linear changes in natural gas/electricity consumption over time. A linear trend may be caused by factors that influence energy consumption and have a trend, such as population, HVAC efficiency, and natural gas/electricity prices. Finally, a time-lag is introduced through the HDD/CDD variable to reflect the thermodynamic delay impact of outdoor temperatures on indoor temperatures due to building thermal inertia (Pardo et al. 2002).

The monthly 2020-2099 per-capita and total demand for site natural gas and electricity are estimated for each state using the regression models. The estimated future energy consumption were further averaged to represent four 20-year mean datasets (2020-39, 2040-59, 2060-79, and 2080-99) with monthly resolution. The AC saturation level changes driven by higher future temperature were also accounted for by adjusting the coefficients for CDD and lagged CDD terms (Supplementary Section S2.5).

Besides natural gas and electricity, other fuels are also used in residential and commercial buildings, including propane, distillate fuel oil, kerosene, and wood. However, the state-level monthly consumption for these fuels contains considerable amounts of missing data making it challenging to build regression models and estimate the future consumption for these fuel types. Instead, the consumption of these fuels is calculated based on their ratios to annual total state natural gas consumption in the residential and commercial sectors as provided in the EIA's State Energy Data System (SEDS) for the mean 2008-2012 time period (U.S. Energy Information Administration 2014b). These ratios are fixed for the present and future years, and the same ratio is applied to all months for each state. The total consumption for all fuel types, other than electricity, is referred as non-electric fuel consumption.

Because the population is critical element in generating the energy consumption in the future, changes in the state/national building energy consumption will be sensitive to the changes in spatial distribution and size of the population. We control for total population size, isolating the impact of the spatial distribution of population size on the relationship between climate and building energy consumption. Because climate change exhibits specific spatial patterns, the interaction of the population spatial redistribution with climate change spatial patterns is worth examination.

2.3 Results and Discussion

2.3.1 Sensitivity to spatial and temporal scales

Table 2.1 presents the national total median (as well as minimum and maximum) annual energy consumption difference between four future 20-year periods and the 2008-12 average based on 20 climate models (state-specific balance point temperatures and 2010 population spatial patterns are used). Source and site building electricity consumption increases due to higher cooling demand in all four future time periods under the RCP 8.5 emission scenario, reaching a 9.4% increase in source electricity demand by the 2080-99 time period. By contrast, non-electric (including natural gas, propane, distillate fuel oil, kerosene, and wood) source and site energy consumption exhibit declines, reaching reductions of nearly -27% in the 2080-99 time period. Because the reduction of non-electric site fuel consumption outweighs the net increase in site electricity consumption, total site energy consumption decreases in all four future periods (up to -9% in 2080-99). However, due to the large source-to-site ratio of electricity (Supplementary Table S2.1),

the decline in total source energy consumption is less, approaching zero in the 2080-99 time periods.

Table 2.1 Annual national (site and source) energy consumption differences between four future time periods and the 2008-12 time period. Results represent the relative difference (%, upper line), and difference (Trillion btu, lower line) for each time period. The difference values represent the median of the 20 climate models; values within the parenthesis represent the minimum and maximum.

	Site Electricity	Source Electricity	Site Non-electricity	Source Non-electricity	Total Site	Total Source
2020-39	0.6 (-0.7, 2.1) 60 (-68, 195)	0.7 (-0.7, 2.2) 199 (-217, 636)	-8.7 (-14.8, -2.2) -872 (-1489, -219)	-8.7 (-14.9, -2.2) -907 (-1547, -228)	-4 (-7.5, -1.2) -766 (-1453, -226)	-1.7 (-3.6, -0.1) -671 (-1417, -24)
2040-59	2.9 (0.9, 4.8) 272 (79, 445)	3 (0.9, 4.9) 879 (254, 1427)	-14.7 (-22.2, -7.3) -1472 (-2224, -729)	-14.7 (-22.2, -7.3) -1529 (-2310, -758)	-5.8 (-10, -3.1) -1117 (-1932, -590)	-1.3 (-3.8, -0.2) -510 (-1483, -78)
2060-79	5.9 (3.2, 8) 542 (299, 739)	6 (3.3, 8.1) 1736 (951, 2358)	-20.8 (-29.2, -11.6) -2083 (-2926, -1166)	-20.8 (-29.2, -11.6) -2164 (-3039, -1211)	-7.9 (-11.7, -4.3) -1514 (-2254, -834)	-1 (-3.1, 0.3) -391 (-1237, 102)
2080-99	9.3 (4.8, 12.6) 857 (448, 1161)	9.4 (4.9, 12.7) 2730 (1422, 3694)	-26.8 (-37.1, -18) -2690 (-3720, -1807)	-26.8 (-37.1, -18) -2794 (-3864, -1877)	-9 (-13.3, -6.9) -1729 (-2559, -1325)	-0.4 (-2.8, 2) -161 (-1093, 802)

In contrast to the relatively small net changes in annual national energy consumption, larger changes are found when consumption is examined on a sub-annual basis. Figure 2.2 shows the absolute and relative national energy consumption difference at the monthly timescale between the four future time periods and the 2008-2012 period. The annual difference is also shown for comparison. Total source energy demand increases during the warmer months (May—October) by up to 10% (285 Trillion btu) in September during the 2040-59 time period and up to 23% (662 Trillion btu) during the 2080-99 time period. This larger seasonal change is driven by an increase in electricity demand during the warmer months with maximum departures of 11.5% and 26.7% in the 2040-59 and 2080-99 time periods, respectively. By contrast, total source energy consumption demand shows a decrease during the colder months (November—April) with maximum departures of -10.5% (-460 Trillion btu) in the 2040-59 time period and -18.9% (827

trillion btu) during the 2080-99 time period. This is driven by large declines in non-electric fuel demand during all months with maximum declines of -16.2% (January) and -34.9% (October) during the 2040-59 and 2080-99 time periods, respectively. Source electricity demand also declines during the colder months, albeit to a lesser degree than the source non-electric fuel demand.

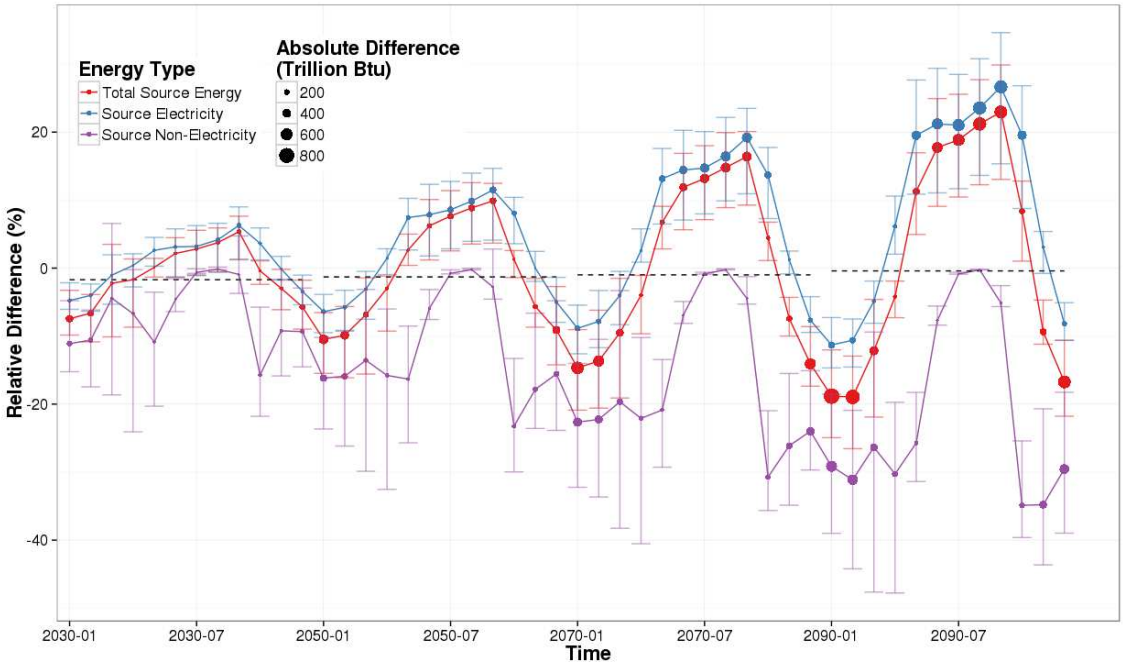

Figure 2.2 Monthly national source energy consumption difference (relative difference on y-axis, absolute difference reflected in symbol size) between future time periods and the 2008-12 time period. Points represent the median, and the whiskers represent minimum and maximum relative difference values from the of 20 climate model. The dashed black lines indicate the annual relative source energy consumption difference for the four future periods.

As with the comparison between annual and monthly changes, there are greater changes in building energy demand at the state level compared to national totals (Figure 2.3). The total annual source electricity consumption increases in most states due to increased future cooling needs, except in a few northwest states where cooling demand remains low

(Figure 2.3a) driven by the fact that electricity-based heating declines outweigh the small increase in cooling demand. The change in electricity consumption is driven primarily by the direct impact of increased cooling demand on current air-conditioning saturation levels and ranges from -3% in Washington to +13.6% in Massachusetts. Increased electricity consumption from added air-conditioning capacity is relatively small (Supplementary Figure S2.3).

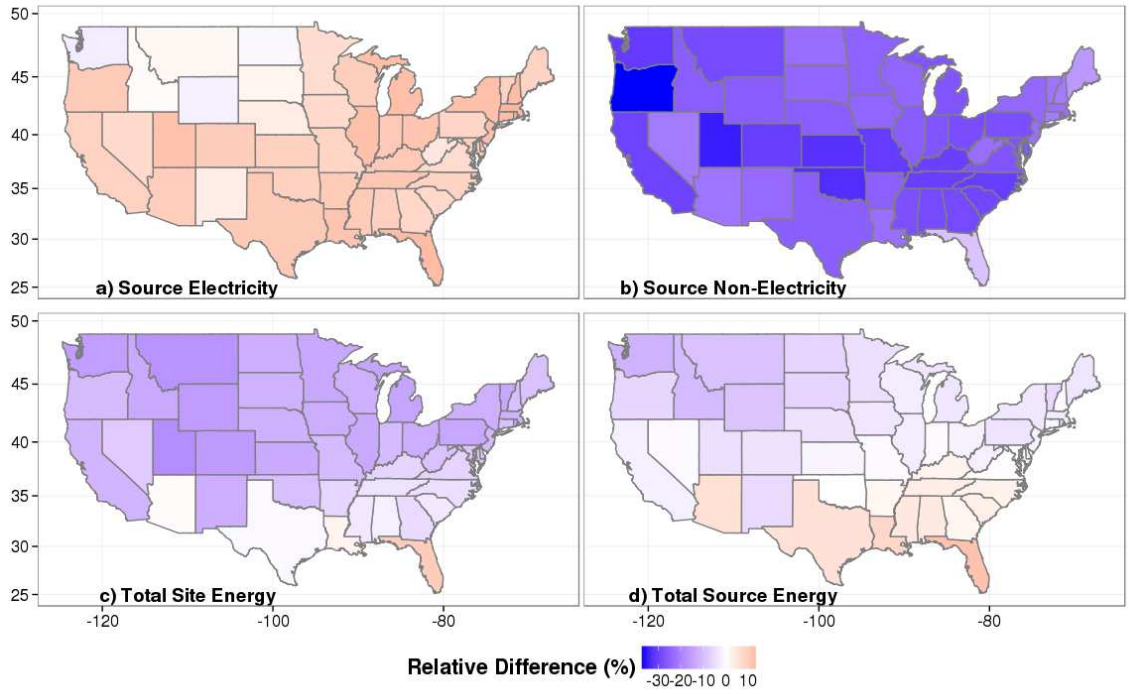

Figure 2.3 Annual building energy consumption relative differences (%) between the 2080-99 time period and 2008-12 time period. a), source electricity consumption; b), source non-electric consumption; c), total site energy consumption; d), total source energy consumption. Results represent the median of 20 climate model.

The total annual source non-electric fuel consumption declines in all states (Figure 2.3b), driven by lower heating requirements in the future, with the largest declines in the West and mid-latitude regions and relatively smaller decreases in the South and the upper

Great Plains. The decrease in annual source non-electric consumption across all US states ranges from -9.3% in Florida to -36.7% in Oregon.

Because the decline in site non-electric fuel consumption exceeds the increase in site electricity consumption, the total site energy consumption decreases in most states except Florida, Louisiana, and Arizona (Figure 2.3c). However, the total source energy demand increases in more states beyond these three, because of the high source-to-site ratios of electricity (Figure 2.3d). The increase in total source energy consumption in these states (e.g. +11.5% in Florida) combined with the decrease in source energy consumption in states with colder climates (e.g. -11.8% in Washington) results in the small national source energy consumption difference noted in Table 2.1, in spite of these opposing individual state-level changes.

These spatial variations in energy demand become further pronounced when examined on a seasonal basis (Figure 2.4). For example, electricity demand increases by +50% in Oregon during the summer months of the 2080-99 time period. Conversely, South Carolina shows an electricity consumption decrease of -16.3% during the winter months. Non-electric fuel consumption similarly shows much greater changes when examined on a seasonal basis, with the largest decline of -48% appearing in Oregon during the spring. Oregon displays the most dramatic electricity consumption changes mostly driven by the large increase in air-conditioning capacity (Table S2.5 and Figure S2.3)

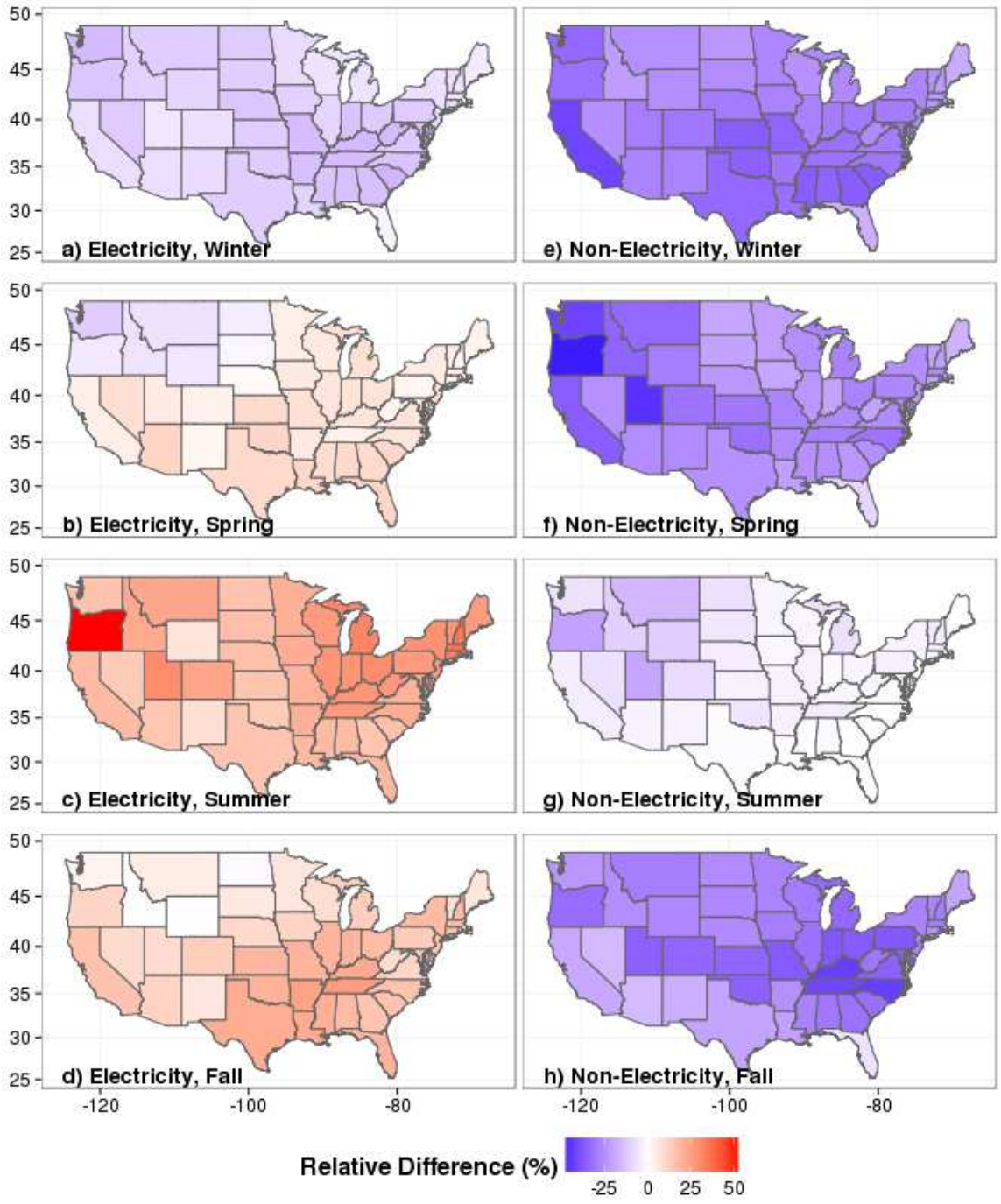

Figure 2.4 Seasonal relative difference (%) in building source electricity and source non-electric energy demand between the 2080-99 time period and 2008-2012. a), Winter (Dec-Feb); b), Spring (Mar-May); c), Summer (Jun-Aug); and d), Fall (Sep-Nov). Panels e) through h) provide the same sequence but for source non-electric fuel consumption. Results represent the median of 20 climate model.

2.3.2 Sensitivity to balance point temperature

A key distinction in the present study versus previous work and an important ingredient in the robustness of the results is the use of a state-specific "balance point" temperature rather than a fixed national balance point temperature (see Methods and Supplementary Section S2.3 and S2.6). The use of the state-specific balance-point temperature versus a fixed value, changes the regression relationship between building energy consumption and temperature and improves the regression model performance (higher adjusted R-squared values) in most states for both electric and non-electric fuels (Supplementary Section S2.6). As shown in Figure 2.5, the use of a fixed 65 °F balance point temperature leads to larger source electricity consumption changes in most states, except Florida, Arizona, and Texas. The largest difference is seen in the state of Oregon where the relative difference (The difference between the future and current energy demands, divided by the current energy demand. It is referred to as RD) of total source energy consumption is 13.7 percentage points higher (7.7% versus -6%) when using a fixed 65 °F balance point temperature. As a result of the overestimated change in most states, the change in national total source energy consumption is 2.1 percentage points higher (1.6% versus -0.4%) based on a fixed 65 °F balance point temperature. Finally, given that HDD/CDD is commonly used in end-use energy consumption modeling, the empirically-based state-specific balance point temperature methodology outlined here would likely lead to more accurate estimation of end-use energy consumption in energy consumption modeling.

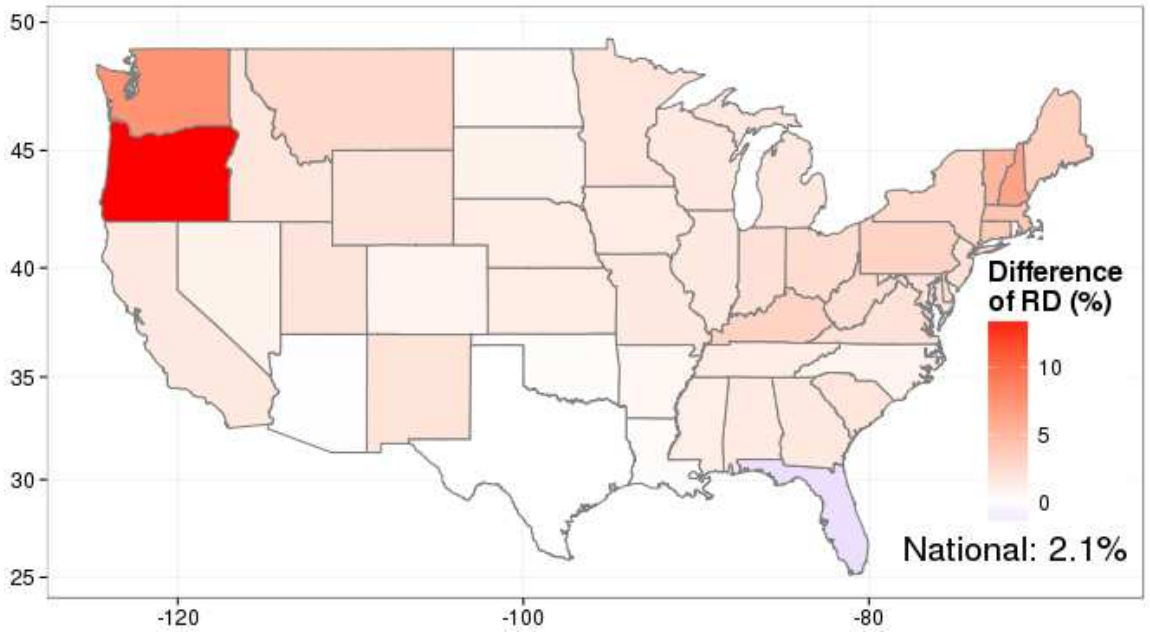

Figure 2.5 RD of source energy consumption between the 2080-99 time period and 2008-2012 when based on a fixed 65 °F balance point temperature subtracted from the RD based on a state-specific balance point temperature. Values reflect the median of 20 climate models.

2.3.3 Sensitivity to population distribution

The U.S. population is expected to exceed 600 million by the end of this century with more people inhabiting coastal areas and parts of the country with warmer temperatures (Figure S2.4) (U.S. Environmental Protection Agency 2010).

Figure 2.6 shows the RD between the 2080-99 time period and 2008-2012 using a 2010 population distribution subtracted from the RD between the 2080-99 time period and 2008-2012 using a 2090 population distribution (the state-specific balance point temperature is used in both). The use of the 2090 population distribution causes energy consumption increases in the warmer areas to be amplified and the energy consumption declines in colder areas to be diminished. For example, the 11.5% increase of total source energy consumption in Florida is further increased by an additional 5.3 percentage points,

while the 9.2% decline in Wyoming is lessened by 8.2 percentage points. The two effects (intensified increases and diminished decreases) result in greater RD values in most states. As a result, the change in national total source energy consumption is 1 percentage point higher under the 2090 population distribution, altering the national RD from a negative (-0.4%) to a positive value (0.6%).

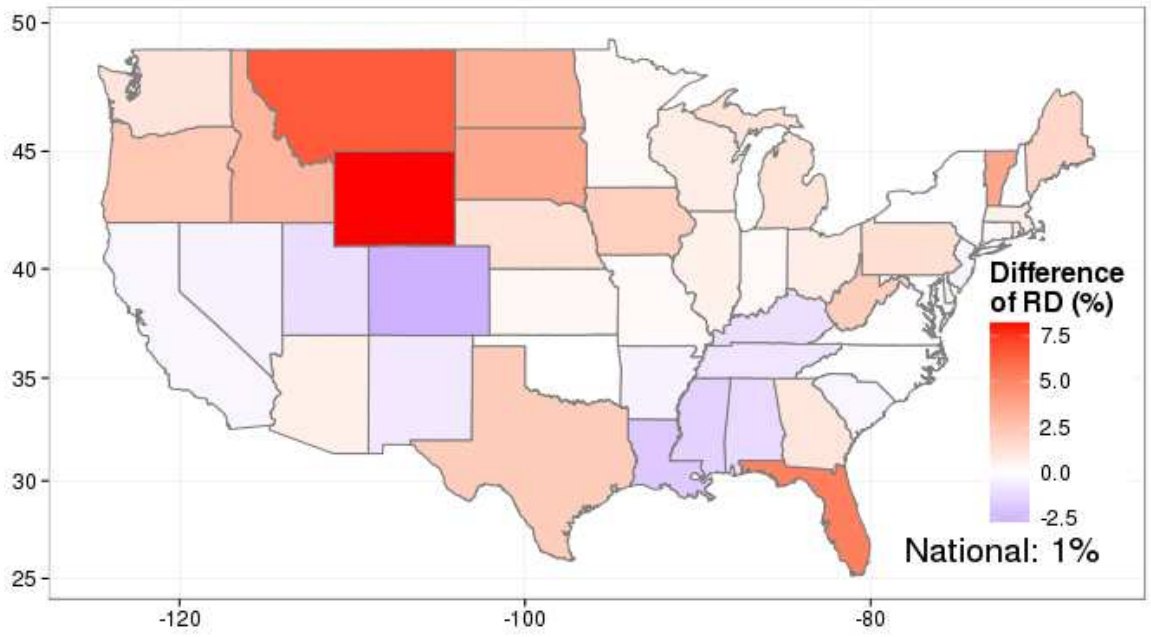

Figure 2.6 RD of source energy consumption between the 2080-99 time period and 2008-2012 when based on a 2010 population distribution subtracted from the RD based on a 2090 population distribution. Values reflect the median of 20 climate models.

2.4 Conclusions

In this study, we have quantified the sensitivity of the relationship between climate change and building energy demand to three elements of analysis. First, we tested how influential the consideration of space and time resolution is to estimates of national, annual building energy consumption under a changing climate. We show that there are large changes at the state spatial scale and the monthly/seasonal time scales (+/- 50%)

which are masked by analysis reporting only national/annual results. Second, we examined the sensitivity to the method used in determination of the balance point temperature. We find that the use of a fixed 65 °F balance point temperature versus a state-specific value leads to an overestimate of the energy consumption changes in most states with a maximum change in the state of Oregon equal to almost 14 percentage points. Integrated over the US, the more accurate state-specific balance point temperature reduces the national total source energy consumption relative difference by slightly over 2 percentage points. We recommend the state-specific balance point temperature method as an accurate means to assess the impact of climate change on building energy demand. Finally, we test the impact of population spatial structure, finding that currently available population projections when combined with modeled spatial projections of temperature, exacerbates the increase in warmer areas (e.g., enhancing the increase in Florida by 5.3 percentage points), while lessening the decreases in colder states (e.g., reducing the decrease in Wyoming by 8.2 percentage points). As a result, the national total source energy consumption changes from a net decrease (less energy needed) to a net increase (more energy needed).

Of the three elements tested, we find the largest sensitivity residing with the use of state/month space/time scales versus national/annual. Given the space/time variations in building heating/cooling demand and the space/time variations in projected climate change, the intersection of these two leads to changes that are significantly hidden by national/annual averaging. Next in importance is the impact of assumed spatial distribution of population. While population distribution is challenging to predict, shifts between cold versus warm regions in the US, could have significant impacts on the

anticipated building energy demand and the consequential supply considerations. Last among these three sensitivity tests, is the method by which the balance point temperature is represented. Though having the least impact, the state-specific balance point temperature developed here has implications for other research applications such as energy consumption analysis currently performed for predicting energy supply capacity changes and studies exploring the socioeconomic drivers of energy demand.

It is important to note that the present study is not aimed at predicting future building energy consumption but rather to highlight the sensitivity to some of the key assumptions used to make those projections. Given the sensitivity analysis here, research addressing the impact of climate change on building energy consumption should be performed at relevant spatiotemporal scales, rely on accurate balance point temperatures, and account for changes in the distribution of population.

Policies aimed at reducing energy consumption within the building sector may best be focused on the rise in electricity demand and driven by increasing cooling needs, particularly in the summer and among the lower tier of states in the US. Furthermore, with the advent of policy occurring at sub-national scales, such as the Clean Power Plan recently enacted in the US, a better understanding of the impacts of climate change and state-specific mitigation opportunities is paramount.

The sub-national/annual changes estimated here can be combined with the spatial distribution of current electricity generation capacity, to provide practical guidance for planning future electricity generation capacity. Our results also suggest that further disaggregation of the temporal domain may be important. For example, understanding the interaction of change in high frequency and extreme events (e.g., heat waves) associated

with climate change and building energy consumption may illuminate further stress points in the demand and supply of energy in this sector. Finally, recent research(Georgescu et al. 2012) has indicated that some US urban areas will experience additional temperature increases due to the Urban Heat Island effect. Such changes could potentially compound the implications outlined here.

2.5 Acknowledgements

We would like to thank the National Science Foundation CAREER award 0846358, the Department of Energy grant #DE-SC0006105 and Amazon cloud computing resources provided by Amazon Climate Research Grant Program. We would also like to thank Matei Georgescu for helpful insights.

CHAPTER 3

3 THE IMPACT OF CLIMATE CHANGE ON THE FREQUENCY AND INTENSITY OF EXTREME ELECTRICITY DEMAND

3.1 Introduction

Climate change consists of both changes in the long-term mean and variations about the mean state (Meehl & Tebaldi 2004). Among the changes in variability, numerous studies have shown that heat waves in the future are expected to occur with greater intensity, frequency and duration (Meehl & Tebaldi 2004; Jones et al. 2015). Because of the direct relationship between air temperature and building space cooling/heating increases in heat wave frequency and intensity will result in sudden, large increases in electricity demand. These increases in demand, in turn, place considerable pressure on electricity supply and the balance between baseload and peak demand delivery. Previous research has considered the impacts of climate change on the long-term average (Zhou et al. 2013b; Sailor 2001a; Zhou, Clarke, Eom, Kyle, Patel, Son H Kim, et al. 2014; Isaac & Van Vuuren 2009) and regular peak electricity demand (e.g., diurnal maximum) (Dirks et al. 2015; Hong et al. 2013; Miller et al. 2008). However, the impact and importance of heat waves on extreme (e.g., once per year event) electricity demand in the future has received little attention.

Sudden, large increases in electricity consumption associated with intense heat waves not only places more pressure on electricity generation and transmission, but can lead to electricity scarcity and power outages (Miller et al. 2008). For example, the elevated electricity demand associated with the 1996 heat wave in the Western United States led to blackout events, interrupting service to about 7.5 million electricity customers (Council

2002). The economic cost of such blackouts is estimated to be up to $50/kWh in some sectors (De Nooij et al. 2007) and the direct economic loss during the 1996 blackout event was estimated to be more than $1 billion in California alone (Douglas 2000). In addition, heat waves can impair electricity generation capacity and cause unscheduled shutdowns in thermo-electric power plants due to warmer cooling water, further increasing the risk of electricity scarcity and outage. For example, the 2003 European heat wave forced some powerplants to reduce electricity generation and several French nuclear powerplants had to be shut down, leading to increases in French electricity imports, decrease in exports, and a reduced supply to the industrial sector (Salagnac 2007). The implications of sudden large increases in electricity demand justify an exploration of how longer, more frequent and more intense heat waves resulting from climate change may significantly alter future electricity demand.

In this study, we develop an empirically-based regression model that links daily electricity demand to weighted heating/cooling degree days. The model is used to estimate daily electricity demand in historical and projected future time periods. Two different metrics – the probability ratio (PR) and relative difference (RD) - are used to evaluate the likelihood and magnitude of large increases in electricity demand driven by heat wave events. We separate the influence of long-term annual/monthly changes in climate from short, high-frequency changes, to isolate their impacts. Because population changes and growth in air-conditioning (AC) saturation (i.e. the percentage of buildings installed with AC) are critical elements in estimating these future impacts, we test the relative contribution of our estimated impact to these two variables. Other factors

associated with electricity supply and demand, such as the system capacity, prices, and technological change are assumed constant.

3.2 Methods and Data

An empirically-based relationship between daily electricity demand and daily heating/cooling degree days (HDD/CDD) is developed for the 2007-2013 time period. HDD/CDD is defined as the absolute difference between outdoor temperature and a balance point temperature for days in which the temperature is lower/higher than the balance point temperature (Baumert & Selman 2003). The 2007-2013 daily electricity demand in each Balancing Authority Area (BAA, a regional area contributing to the reliable operation of the electricity system) was aggregated from the hourly electricity demand data extracted from the Federal Energy Regulatory Commission (FERC) Form 714. To calculate the 2007-2013 daily HDD/CDD, daily 2-meter temperature with a spatial resolution of 32 km x 32 km was extracted from the gridded North American Regional Reanalysis (NARR) generated by the National Center for Environmental Prediction (NCEP) (National Center for Environmental Prediction 2014). The state-specific balance point temperature developed by Huang *et al.* (2016) is used to calculate the daily HDD/CDD for each US census tract. Because most census tracts are smaller than a NARR grid cell, the daily HDD/CDD of the closest NARR grid cell (shortest distance between the tract center and the NARR grid cell center) is used to represent the daily HDD/CDD for each census tract. The census tract HDD was multiplied by the census tract population to get a population-weighted HDD (referred to as *PH*). Because space cooling is primarily provided by electricity-driven air-conditioning (AC) and the

AC saturation values vary substantially across the United States, the census tract CDD is multiplied by both population and AC saturation values to get the population-and-AC-weighted CDD (*PAC*). The census tract *PH* and *PAC* are, hence, calculated as follows:

$$PH_{tr} = P_{tr} \times HDD_{tr} \quad (1)$$

$$PAC_{tr} = P_{tr} \times A_{tr} \times CDD_{tr} \quad (2)$$

where *P* represents population, *A* represents the AC saturation level, *HDD/CDD* represents heating/cooling degree days, and *tr* identifies the US census tract. The census tract *PH/PAC* can be spatially integrated to achieve a *PH/PAC* for the whole US.

The 2010 census tract population data is retrieved from the US Census Bureau (U.S. Census Bureau 2010a). The AC saturation levels were extracted from the 2009 Residential Energy Consumption Survey (RECS) data for each census division (covering one or multiple states), and hence, the census tracts within one division share the same AC saturation level. Because there is little research to support AC saturation changes in other sectors, we use AC saturation levels from the residential sector only.

In order to relate electricity consumption to PH and PAC, the daily electricity consumption in each BAA, and the census-tract PH and PAC are aggregated to the US total. Since electricity can be used for both heating and cooling, a linear regression model is developed to relate daily electricity demand to daily *PH* and *PAC*. Because we aim to estimate electricity demand extremes caused by heat waves during warmer months, colder months (November-March) with small amounts of space cooling and associated electricity consumption are excluded in the regression model. However, since space heating demand persists throughout the year, particularly in the northern US, *PH* is also included as an independent variable in the model. In addition, the US local time changes

(daylight saving vs standard time) appear in March and November during 2007-2013, which may cause inconsistent relationships between electricity demand and PH/PAC. The exclusion of the five winter months eliminates such inconsistencies and improves the regression model performance. The full regression model, including 21 independent variables, is described as follows:

$$E_d = C + \alpha * T + \beta * BD + \gamma 1 * PH_{d+1} + \gamma 2 * PH_d + \cdots \gamma 8 * PH_{d-5} + \lambda 1 * PAC_{d+1} + \lambda 2 * PAC_d + \cdots \lambda 8 * PAC_{d-5} + \theta 1 * PH_{d+1}^2 + \theta 2 * PH_d^2 + \kappa 1 * PAC_{d+1}^2 + \kappa 2 * PAC_d^2 + \varepsilon \quad (3)$$

where *E* represents electricity demand for date *d*, *C* represents a constant (intercept) term, *T* represents the electricity demand annual trend (ranging from 1 to 7, corresponding to the 2007 to 2013 time period), *BD* is a categorical variable indicating whether the date is a weekday (1) or weekend/holiday (0), ε represents error term, and α, β, γ, λ, θ, and κ are coefficients of interest.

Because the Coordinated Universal Time (UTC) used by the NARR is several hours ahead of the local time used by FERC, the FERC-based electricity demand in day *d* corresponds to the NARR-based *PH/PAC* in part of day *d* and part of day *d+1*. Thus, the *PH/PAC* for both the current (*d*) and following day (*d+1*) are included in the full regression model. In order to capture the non-linear effect observed between electricity demand and PH/PAC, the squared terms (PH^2 & PAC^2) for *d* and *d+1* are also included. Because previous research found lagged effects of HDD/CDD on electricity demand for up to 5 days (Pardo et al. 2002), lagged *PH/PAC* values (up to 5 days) are included in the model. Since the energy consumption patterns are different between weekdays and weekends/holidays, a categorical variable (*BD*) is used to capture their differences. The

holidays are defined by North American Electric Reliability Corporation (NERC) and include New Year's Day, Memorial Day, Independence Day, Labor Day, Thanksgiving, and Christmas. A trend term (*T*) is included to capture the annual trend of electricity demand that can be caused by any factor that tends to have a long-term trend, such as population and HVAC efficiency.

The best model is selected from 2^{21} candidate models based on their Bayesian Information Criterion (BIC) values. The BIC value is calculated based on model likelihood and imparts a large penalty to the number of variables included in a model, so that preference is given to the models with smaller numbers of dependent variables, reducing the risk of over-fitting (Burnham & Anderson 2004). The best model has an adjusted-R^2 of 0.98, and includes 9 independent variables, all of which are statistically significant with p-values approaching zero (Table S3.1). Similar to the findings in previous research, the *PAC* lag is significant for up to 5 days, while the *PH* lag extends to 1 day only (Pardo et al. 2002).

The selected regression model is used to predict daily electricity demand in a historical period (1950-2005) and a future period (2006-2099) based on daily climate model outputs extracted from the Coupled Model Intercomparison Project Phase 5 (CMIP5) at the 0.125 degree resolution (Brekke et al. 2013). The downloaded CMIP5 output is already biased-corrected using the quantile mapping technique. Generally, the cumulative distribution function (CDF) of the modeled temperature is paired with the CDF of the observed temperature in the historical period. At each quantile, the difference between the modeled temperature and the observed temperature is viewed as bias. In the historical period, this bias is corrected by assigning the observed temperature to the corresponding

modeled temperature at each quantile. The relative difference between the modeled temperature and observed temperature in the historical period is then used to adjust the temperature in the future period. This bias-correction process guarantees that the systematic climate model errors are eliminated, and there is no statistical bias associated with the CMIP5 climate model outputs (Brekke et al. 2013). The temperature from 20 climate models (Table S3.1) is used, and each of them is available in both the (Representative Concentration Pathways) RCP 4.5 (radiative forcing reach 4.5 W/m2 in 2100) and RCP 8.5 (radiative forcing reach 8.5 W/m2 in 2100) emission scenarios (van Vuuren et al. 2011).

Two metrics, the "probability ratio" (PR) and the "Relative Difference" (RD), are used to compare the large departures in daily electricity demand between the future and historical periods. The PR and RD are defined as follows:

$$PR = count\left(E_{ft} \geq E_{hs,n}\right)/N \quad (4)$$

$$RD = \left(E_{ft,n} - E_{hs,n}\right)/E_{hs,n} \quad (5)$$

where E represents the daily electricity demand in the historical period, *hs*, and the future period, *ft,* and n represents the *Nth* largest (e.g., top 1, 10, and 30) daily electricity demand in the given time period. For example, when N equals 2, the PR value reflects the number of days in which future electricity demand are larger than, or equal to, the second largest daily electricity demand in the historical period, divided by 2. Using the same example, the RD is defined as the difference between the second largest future single-day electricity demand and the second largest historical single-day electricity demand, divided by the second largest historical single-day electricity demand. Because the historical period covers 56 years, the PR and RD are calculated from a moving 56-year

time period (e.g., 2006-2061, 2007-2062……2044-2099). The *PR* and *RD* are calculated for *N* ranging from 1 to 56, representing extreme event frequencies ranging from once per 56 years to once per year (Table S3.3).

In order to evaluate the sensitivity of climate change impacts on electricity demand, to the temporal resolution of climate change (e.g., daily, monthly, and annual), we integrate the daily temperature to monthly and annual averages. The temperature is integrated within each gridcell under the RCP 8.5 scenario in the historical period (1950-2005) and a future period (2022-2077, 56-year time period centering at 2050). Because daily temperature is needed for the regression model, we reconstruct the 2022-2077 monthly/annual temperature to daily resolution by adding the monthly/annual temperature difference between 2022-2077 and 1950-2005, to the 1950-2005 daily temperature. As a result, the reconstructed 2022-2077 daily temperature has the same daily temperature distribution (around the mean) as the 1950-2005 data, but with different monthly/annual averages. The original 2022-2077 daily temperature extracted from the CMIP5 climate models represents the high-frequency (daily) temperature change, while the reconstructed 2022-2077 daily temperature retains only the long-term mean (monthly/annual) temperature changes. In the remainder of this paper, analysis using the high-frequency (daily) temperature change will refer to the underlying temperature changes as "daily climate change", while the longer-term mean (monthly, annual) temperature changes are referred to as "monthly climate change" or "annual climate change".

Because population and AC saturation levels are used in the calculation of *PH* and/or *PAC*, we also explore the contribution of these factors to the overall results. We do this

for the 2022-2077 period under the RCP 8.5 scenario only. The projected 2050 population data is retrieved from the Integrated Climate and Land Use Scenarios (ICLUS) dataset (U.S. Environmental Protection Agency 2010), and the estimated 2050 AC saturation levels are derived from Huang *et al.* (2016). The individual impact of temperature, population, and AC saturation, respectively, are evaluated by setting two of the three variables constant while varying the third. The combined impact (in terms of the RD) is estimated by varying all three variables simultaneously. The impact of the interaction between the three variables (e.g., the effect of increased temperature to the increased population) is calculated as the difference between the combined and the sum of three individual impacts.

If we assume that the individual impacts caused by temperature, population, and AC saturation level changes are independent of each other, the hypothetical combined and interaction impacts can be calculated as follows:

$$RD_C^* = (1 + RD_T)(1 + RD_P)(1 + RD_A) - 1$$

$$= RD_T + RD_P + RD_A + RD_T * RD_P + RD_P * RD_A + RD_T * RD_A + RD_T * RD_P * RD_A \quad (6)$$

$$RD_I^* = RD_C^* - (RD_T + RD_P + RD_A)$$

$$= RD_T * RD_P + RD_P * RD_A + RD_T * RD_A + RD_T * RD_P * RD_A \quad (7)$$

where *RD* represents the relative difference due to temperature (*T*), population (*P*), and the AC saturation level (*A*) changes. *RD** represents the hypothetical relative difference due to the combined impact (*C*) and the interaction impact (*I*).

3.3 Results and Discussion

Various time periods (e.g., 1 day, 3 days, and 10 days) have been used to measure the integrated impact of heat waves (Meehl & Tebaldi 2004; Jones et al. 2015). Since

electricity demand in our model is affected by the *PAC* values over the current and previous seven days (from *d*+1 to *d*-5) (Table S3.2), a 7-day duration is the most appropriate time period to evaluate the integrated impact of heat waves on electricity demand.

3.1 Contribution of climate change

Under the situation of daily climate change (without population or AC saturation level change), sudden, large increases in electricity demand are likely to appear more often in the future due to more frequent and longer-lasting heat wave events (Figure 3.1). Based on the results from 20 climate models under the RCP 8.5 scenario, the occurrence of the most extreme electricity demand event will increase from 1-per-56 years to a median value of 463-per-56 years (model range: 73-1099) in the 2006-2061 running bin. This translates to an occurrence of one extreme electricity demand event every 44 days, on average. In the last 56 year running bin of the 21st century (2044-2099), as climate change intensifies, these events increase from 1-per-56 years to 2600-per-56 years (model range: 696-4255) or an equivalent occurrence of one large event every 8 days. In the RCP 4.5 scenario, the equivalent PR ratios are 210 and 740, respectively. Not surprisingly, large electricity demand events which historically occur more frequently, see less dramatic increases in the future. For example, the probability of one-per-year demand events, increases to 70-per-year in the last 56 year running bin under the RCP 8.5 scenario.

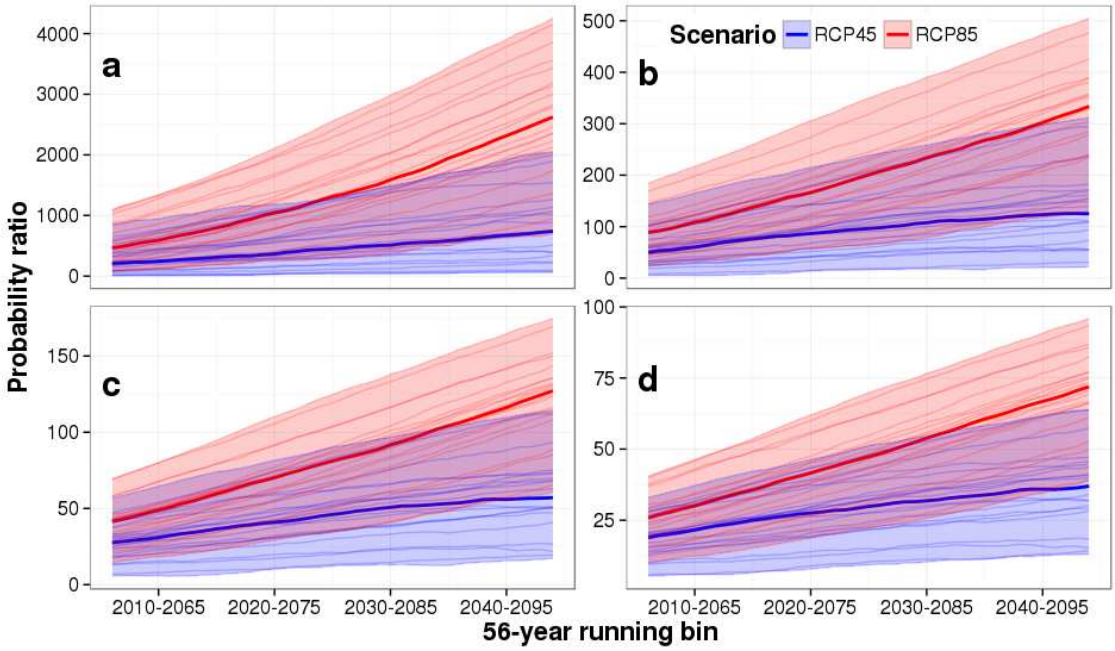

Figure 3.1 The probability ratio of extreme electricity demand events in the future relative to the 1950-2005 time period for four representative event frequencies: a. 1-per-56-years, b. 10-per-56-years, c. 30-per-56-years, and d. 56-per-56-years. The thin lines represent the estimate for a single climate model. The thick line represents the median estimate, and the shaded area represents the range of estimates for all climate models.

In addition to the increased likelihood of large electricity demand events, these events are more intense (the magnitude of the daily electricity demand during a heat wave event). The median daily electricity demand of the 1-per-56 year event is 11% higher (model range: 7% - 18%) in the 2006-2061 running bin period compared to the historical (1950-2005) time period under the RCP 8.5 scenario (Figure 3.2a). This rises to a 25% increase (model range: 14% - 35%) in the last 56 year running bin of the 21st century. In contrast to the sensitivity of the large event likelihood to the event frequency, the relative difference of the event intensities show little change across the range of event frequencies (Figure S3.2).

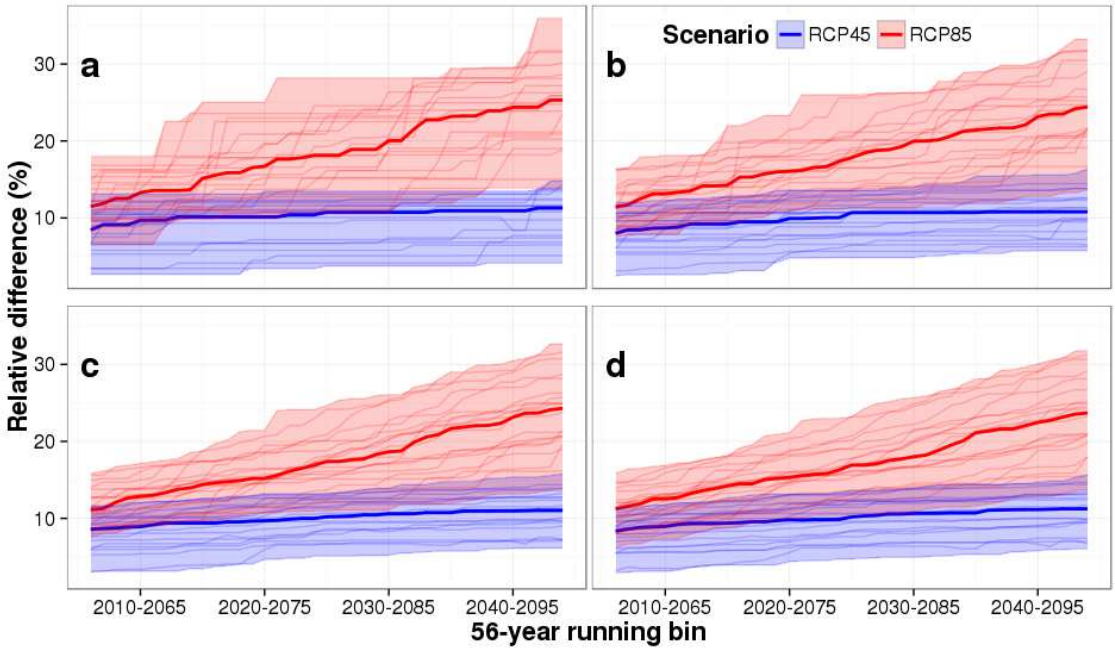

Figure 3.2 The relative difference of extreme electricity demand intensity in the future relative to the 1950-2005 time period for four representative event frequencies: a. 1-per-56-years, b. 10-per-56-years, c. 30-per-56-years, and d. 56-per-56-years. The thin lines represent the estimate for a single climate model. The thick line represents the median estimate, and the shaded area represents the range of estimates for all climate models.

If one assumes that the current electricity generation capacity is able to meet the historical one-per-56 year event, 25% more electricity generation capacity, and transmission lines sufficient to deliver the additional generation, will be needed in the latter half of the 21st century to meet the greater daily electricity demand, all else being equal. Furthermore, these large demand events will come more often (2600x in the most extreme event case) which has implications for the structure of electricity supply and how baseload versus peaking capacity is managed.

3.2 Sensitivity to temporal resolution

A key element in quantifying the future likelihood of large electricity demand events is the averaging period or resolution of the underlying temperature data. Much climate

change impact research uses annual/monthly mean climate variables, especially in the past one or two decades when high-resolution climate model output were not available due to the limitation of computational resources. However, heat wave events and the subsequent electricity demand occur on timescales of hours to days. We assess the importance of the high temporal-resolution climate model outputs by repeating the above analysis using the reconstructed daily temperature based on monthly and annual climate change (See Methods and data).

For different frequencies of extreme events, the PR values caused by monthly climate change is very close to the corresponding values due to daily climate change, but the PR values due to annual climate change is usually smaller (Figure 3.3). For example, the median PR value based on monthly climate change is almost the same as the value based on daily climate change (43.7 vs. 43.6) for the once per year extreme electricity demand, while the PR value based on annual climate change is about 15% smaller (37.4 vs. 43.6) under the RCP 8.5 scenario in the mid-century (2022-2077, centering at 2050). For the most extreme event (1-per-56 years), the daily, monthly, and annual climate change will increase the odds by 1140, 1210, and 950 fold, respectively.

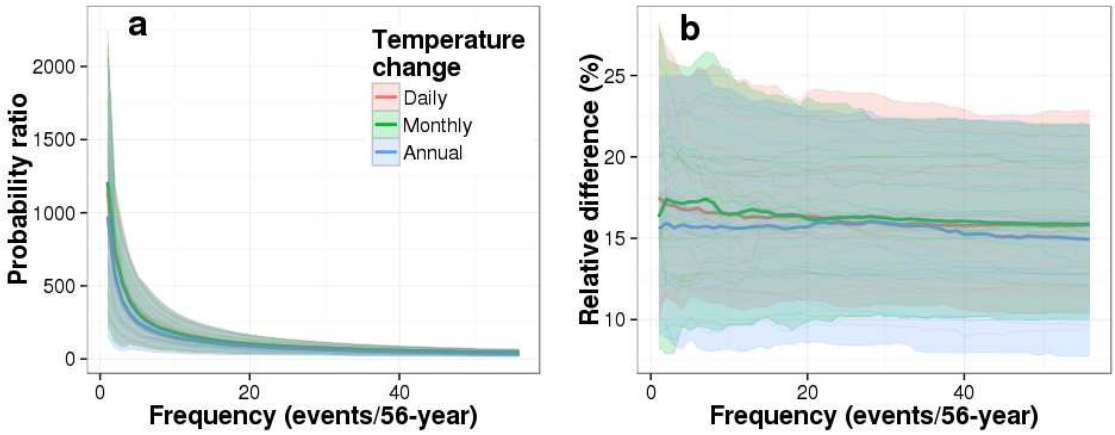

Figure 3.3 Probability ratio and relative difference of extreme electricity demands caused by daily, monthly, and annual temperature changes in 2022-2077 relative to 1950-2005, under the RCP 8.5 emission scenario. Each thin line represents the estimate for a single climate model. The thick line represents the median estimate, and the shaded area represents the range of estimates for all climate models.

Similar to the pattern of PR values, the RD values resulting from monthly climate change are similar to those driven by daily climate change. This is particularly true for the more common, less extreme electricity demand events. RD values resulting from extreme variations in annual climate change are expectedly lower (Figure 3.3b). The median RD based on annual climate change is about 2 percentage points smaller (15.6% vs. 17.5%) than the value based on daily climate change for the most extreme (1-per-56 years) electricity demand events, and the difference reduces to 1 percentage point (14.9% vs. 15.8%) for the once per year event. The comparison of PR and RD values between the long-term (annual/monthly) mean and daily climate changes suggests that the impacts of long-term monthly climate change can be used to approximate the impacts of daily climate change, at least for the less extreme electricity demand events. However, the impact of future heat waves on extreme electricity demand may be systematically underestimated by using annually averaged temperature change. These findings further

suggest that the differences of intra-month climate variability between the future and historical periods are negligible, while the intra-annual climate variability in the future period is higher than the variability in the historical period.

3.3 Contribution of population and AC saturation changes

Electricity demand during heat wave events is not only a function of higher temperature or changes in heat wave duration. A number of other factors will determine future demand during heat waves such as electricity prices, electricity conservation policy, population and demand technology, among others. Of these, we include two factors that are both critical and lend themselves to assessment in the current scope of this study: population and AC saturation levels. The impact of temperature, population, and AC saturation level changes to the extreme event probability and intensity are estimated separately for the 2022-2077 time period under the RCP 8.5 scenario (Figure 3.4a). During this mid-century time period, population accounts for roughly the same increase in extreme event frequency as temperature; each increasing the likelihood of the 1-per-56 year event by over 1000 folds. The AC saturation change, by contrast, has a much smaller contribution, increasing the likelihood by about 20 times.

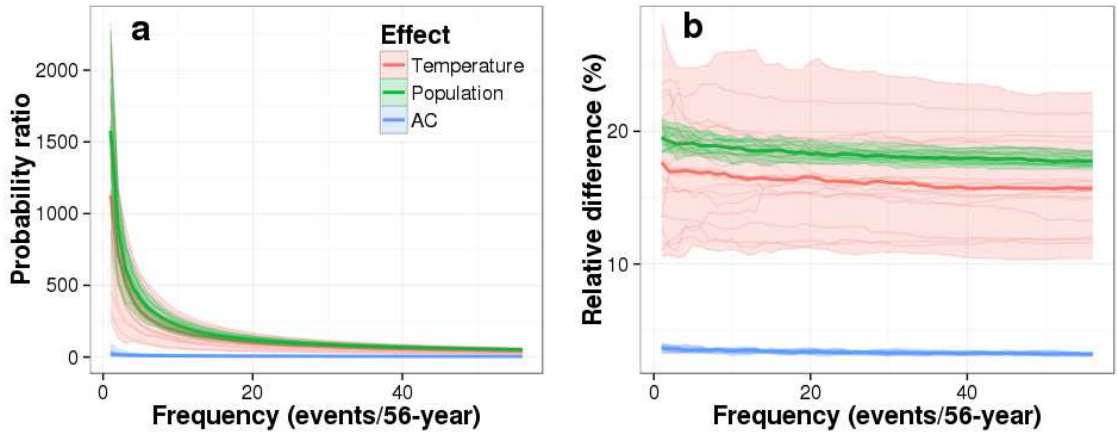

Figure 3.4 The probability ratio (a) and relative difference (b) of large electricity demand events attributed separately to changes in temperature, population, and AC saturation levels. Results are calculated for 2022-2077 relative to 1950-2005 under the RCP 8.5 scenario. Each thin line represents the estimate for a single climate model. The thick line represents the median model estimate, and the shaded area represents the range of estimates for all climate models.

The intensity can be similarly ascribed to temperature, population and AC saturation levels separately. The RD values due to population and temperature changes are consistently larger than 15% across the range of extreme event frequencies, while the RD due to an increase in AC saturation levels is usually less than 4% (Figure 3.3b).

The PR/RD increases resulting from an increase in AC saturation levels are small, probably because warmer climates of the US are already near 100% AC saturation. Although the increase of AC adoption is relatively large in colder climates (e.g., from 43% historically to 66% mid-century in Oregon), the total space cooling demand is generally low in these climates. As a result, the increase in AC saturation alone, leads to a small change in electricity demand US-wide.

In addition to examining the contribution of temperature, population and AC saturation changes in isolation of one another, the impact of these three variables can be examined in combination. This highlights the potential for interactions between these variables in

exacerbating the large electricity demand impacts. The interaction impact (e.g., the effect of increased temperature to the increased population) is calculated as the combined impact minus the sum of three (temperature, population, and AC saturation changes) individual impacts. With the concurrent changes of all three components, the most extreme electricity demand events (1-per-56-year) will increase more than 58% in the period of 2022-2077 under the RCP 8.5 scenario. The interaction impact (18%) is about the same as the impact due to temperature or population change, alone. The combined impact drops to 52% for the once per year extreme event, and the interaction impact drops to 15%. The high interaction impact indicates that the combined impact can't be simply calculated as the sum of each single component's impacts, and it is important to consider the interaction between different components.

One of the challenges of estimating the impact of climate change on electricity demand derives from the complicated, nonlinear, and spatially-heterogeneous interactions between the impacts of climate change and other components. The hypothetical combined/interaction impacts are calculated based on the impacts of three single components with simplified assumptions (See Methods and data). The hypothetical interaction impact is about 13 percentage points smaller than the real interaction impact (5% vs. 18%) for the most extreme event (1-per-56-year), so is the hypothetical combined impact (45% vs. 58%) (Figure 3.5). This indicates that the assumptions used for the hypothetical calculations strongly violate real conditions. The violation is mainly due to the spatially-heterogeneous interactions between three components. For example, the population increases faster in the warmer area than the cold area, resulting in higher

space cooling and electricity demand than the results based on the assumption that there is no spatial variation of population change.

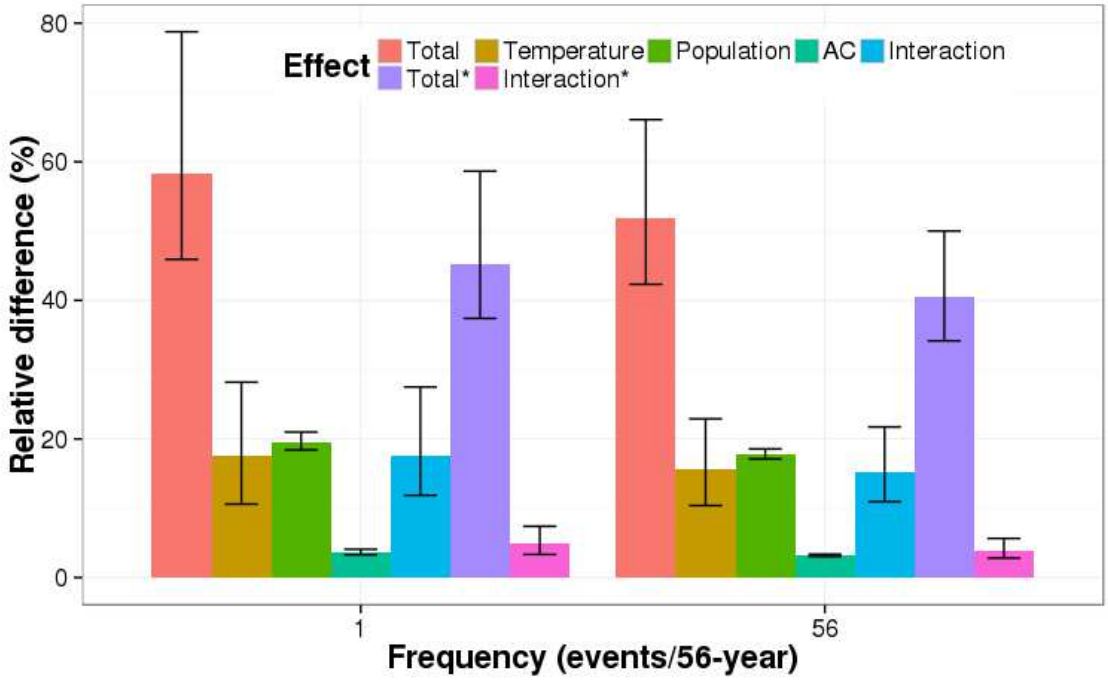

Figure 3.5 Decomposition of the total relative difference into three single components (temperature, population, and AC saturation level) and their interaction. The Total* and Interaction* represent the hypothetical total and interaction effects calculated based on RD values of three single components (See Methods). The histogram represents the median value, and the error bar represents the minimum and maximum values from 20 climate models. The relative difference is calculated between 2022-2077 and 1950-2005 under the RCP 8.5 emission scenario.

3.4 Conclusions

We develop a framework that evaluates the relationship between US heat waves associated with climate change and subsequent large electricity demand. We employ two different metrics that represent the change in frequency and intensity of large electricity demand events in the future as heat waves become more frequent, intense, and of longer duration. The impact of these heat wave events, when averaging temperatures over daily, monthly and annual time periods, are estimated based on an empirically-based model.

Given the importance of both population growth (in space and time) and the ongoing penetration of air-conditioning technology to the electricity demand response, we also explore the influence of these changes on future impact. The impact that occurs from the combination and interaction of changing temperature, population, and AC saturation levels are also evaluated by changing these variables simultaneously. Lastly, we explore the simulated combined/interaction impacts when compared to hypothetical combined/interaction impacts based on simplified assumptions.

Using the CMIP5 daily climate model RCP 8.5 scenario projections, we find that the occurrence of the most extreme electricity demand event (one-per-56 year) over our 56 year time window increases more than 2600-fold in the 2044-2099 time period. The more common one-per-year extreme demand event increases more than 70-fold in the same future time period. The estimated relative difference in the integrated electricity consumption across the extreme demand events is relatively constant at +25% regardless of the extreme event frequency.

The sensitivity of results to the temporal resolution of climate change is assessed using the reconstructed daily temperature that represents the long-term mean (monthly/annual) climate change. The impact caused by daily climate change can be approximated with the impact due to monthly climate change, while it may be underestimated using the impact based on annual climate change. The impact caused by daily climate change can be approximated with the monthly climate change data, while it may be underestimated using the annual climate change data. Compared to the results based on daily climate change, the PR of the once per year extreme electricity demand is underestimated by about 15% (37.4 vs. 43.6) using the annual climate change data, and the corresponding

RD is underestimated by about 2 percentage points (15.6% vs. 17.5%) in the 2022-2077 period.

The impacts caused by population and temperature change are similar to each other, while the impact caused by AC saturation change is smaller. Around mid-century, the change in population will increase the most extreme electricity demand by more than 15%, while the change in AC saturation will only increase the demand by 4%. Under the concurrent changes of temperature, population, and AC saturation, the largest electricity demand events will increase about 58%, with 18 percentage points of that change attributed to the interaction of the three tested variables. The hypothetical combined/interaction impacts of the three components are also estimated, based on the hypothesis that the three variables change uniformly over space and they are independent of each other. As a result, the hypothetical combined/interaction impacts are about 13 percentage points smaller than the corresponding estimates that accounts for the spatially-heterogeneous interactions between the three components.

Since the regression model is built for the whole United States, it contains the assumption that the electricity can be transmitted within the whole US without limitation. In fact, the contiguous US is separated into three interconnection regions, and the transmission lines are usually limited between and within regions. The adjusted-R^2 indicates that the model works well for the whole US domain. However, due to the spatial heterogeneity of the projected climate change, we may be able to find the spatial pattern of changes in extreme electricity demand when the regression model is run at smaller spatial scale. Since the historical damage (e.g., economic losses) associated with extreme electricity demand were rarely documented and explored, the PR and RD values calculated here

can't be linked to the actual damages. More research and better documentation of losses are required to explore the damages caused by extreme electricity demand, and offer more practical insights into the implications of PR and RD values (Pendleton et al. 2013).

3.5 Acknowledgements

We would like to thank the National Science Foundation CAREER award 0846358, the Department of Energy grant #DE-SC0006105 and Amazon cloud computing resources provided by Amazon Climate Research Grant Program.

CHAPTER 4

4 THE VARIATION OF CLIMATE CHANGE IMPACT ON BUILDING ENERGY CONSUMPTION TO BUILDING TYPE AND SPATIOTEMPORAL SCALE

4.1 Introduction

Energy consumption in commercial and residential buildings accounted for 41% of US primary energy consumption in 2010, of which 37% was used for space heating and cooling. Within the commercial sector, space heating and cooling together account for 31% of building primary energy consumption, while in residential buildings, the share is 43% (Kelso 2012b). Building energy consumption, especially space cooling and heating, is directly influenced by climate change.

Different methods have been utilized to study the impact of climate change on residential and/or commercial building energy consumption (Wilbanks et al. 2008; Lukas G Swan & Ugursal 2009; Edenhofer et al. 2014). These methods can be generally classified into three categories: observation-based regression/prediction, global/regional energy modeling, and individual building energy simulation.

The observation-based regression/prediction approach takes advantage of the historical relationship between energy consumption and climate variables to predict future energy consumption under a changing climate. Because this method is based on historical data, it is self-calibrated when fitted to a model. The output resolution from this approach is usually determined by the resolution of the historical data, and the accuracy of the estimation depends on the quality of the selected regression model (usually evaluated with statistical criteria, such as R^2). This approach has been used to estimate the impacts

of climate change on annual/monthly energy consumption (Sailor et al. 1998a; David J Sailor & Muñoz 1997; Sailor 2001a; Ruth & Lin 2006a) and peak energy demand (Ruth & Lin 2006a; Franco & Sanstad 2007; Alan F Hamlet et al. 2010; Sathaye et al. 2013) in some US states. For example, Huang *et al.* used this method to estimate the building energy demand changes and financial implications of climate change at the state/month scale in the contiguous US (Huang & Gurney 2015).

The global/regional energy modeling approach simulates energy consumption in a numerical model composed of multiple variables such as energy demand and supply, economy, technology, population, policy, and climate. The impact of climate change on building energy consumption is assessed through simulated climate change scenarios. Besides climate change, this approach can be also used to study the impact of other key variables such as population change, land use change, carbon taxes, and emissions mitigation policy. However, the complexity and flexibility of this method comes at the expense of output resolution. Hence, this method has been employed to estimate the impacts of climate change on building energy consumption at annual timescales and at global, national, and state spatial scales, at the finest (Isaac & Van Vuuren 2009; Stanton W Hadley et al. 2006; Zhou et al. 2013b; Zhou, Clarke, Eom, Kyle, Patel, Son H Kim, et al. 2014; Jaglom et al. 2014; McFarland et al. 2015).

The individual building energy simulation approach can be used to simulate high-frequency output (e.g., hourly) for specific building types. However, it usually requires detailed building characteristics and hourly weather data to drive the simulation. Such detailed information (e.g. building characteristics, occupants, operation schedules) is limited. As a result, this approach has been used for a few building types in particular

locations only (Scott et al. 1994; Xu et al. 2012a; Dirks et al. 2015; Hong et al. 2013; Wan et al. 2012). Although Huang (Y. J. Huang 2006) and Wang *et al.* (Wang & Chen 2014) used this approach to evaluate the impact of climate change for the whole US, the results are based on building energy simulations in less than 20 cities.

Although the impact of climate change on energy consumption across different building types has been explored down to the monthly temporal scale and for spatial scales down to climate zones (covering several to hundreds of counties) (Wang & Chen 2014; Y. J. Huang 2006), the importance of sub-monthly timescales and variation within climate zones has rarely been studied. Given the spatial and temporal heterogeneity of climate change, the impacts on building energy consumption can vary substantially within climate zones at sub-monthly timescales.

In this study we quantitatively explore the impacts of climate change on building energy consumption using the individual building energy simulation approach. Our focus is on the examination of impact variation across different building types at multiple time scales (e.g., annual, monthly, and hourly) and spatial scales (e.g., national, climate zone, and location). We quantify these impacts at over 900 US locations across the 16 US climate zones. We also explore the variation of the impact across 15 commercial building types (each with three different age classes, representing different building technology) and 2 residential building types. High spatiotemporal-resolution combined with building energy consumption simulation at over 900 locations allows us to detect the temporal and spatial patterns of the impacts. Consideration of different building age classes, allows us to compare the sensitivity to the differing levels of building technology. These analyses are based on large amounts of simulations ensure the estimates are statistically reliable, and

can offer more localized and practical insight into climate change mitigation/adaptation options.

The remainder of this paper is divided into three parts: methodology, results and discussion, and conclusions. The methodology section includes a description of the building energy simulation model, the weather data and building prototypes used to drive the energy consumption simulations, calibration of results, and the metrics used for comparing results. The variation of building energy consumption impacts to building types/technology at different spatial and temporal scales are explored in the results and discussion section. The main findings, caveats, and the potential for future work are discussed in the conclusions section.

4.2 Methods and Data

4.2.1 Building energy simulation model

EnergyPlus, a well-known building energy simulation tool developed by the US Department of Energy (DOE), is used to simulate building energy consumption. EnergyPlus has been extensively tested and validated for the ANSI/ASHRAE standards and is widely used by engineers and scientists to model building energy consumption (Crawley et al. 2001). EnergyPlus requires hourly weather data (e.g., temperature, humidity, and solar radiation) and hundreds of building characteristics (e.g., heating, ventilating, and air conditioning system, building materials, and occupancy) associated with specific building prototypes to drive the energy simulations. It produces hourly energy consumption by end use and fuel type for a given building prototype.

4.2.2. Weather data

The current hourly weather data used in EnergyPlus is retrieved from the third (and the latest) Typical Meteorological Year (TMY3) collection (Wilcox & Marion 2008). Each TMY3 file includes hourly weather data in one year duration for a specific location, which is developed based on 1991-2005 weather data or 1976-2005 weather data, if the latter exists. The meteorological data is available for 925 locations in the contiguous US, most of which reflect the 1991-2005 weather data. Future monthly weather is derived from the World Climate Research Programme's (WCRP) Coupled Model Intercomparison Project phase 3 (CMIP3) (The World Climate Research Programme n.d.). The monthly temperature change between a future time period and the present for each TMY3 location is represented as the average temperature change of its four closest CMIP3 neighbor grid cells. The average temperature change at each location is calculated for two future periods (2040s and 2090s, relative to 1991-2005), each under three IPCC emission scenarios (A2, A1B, and B1 representing high, medium and low emissions respectively (Nakicenovic & Swart 2000)) with an ensemble of 15 climate model outputs. These average monthly temperature differences are then added to the current hourly TMY3 temperature data to generate the future hourly weather conditions for each location, similar to the procedure taken in other studies (Scott et al. 1994; Y. J. Huang 2006; Xu et al. 2012a).

The projected temperature change for the decades of the 2040s and 2090s are spatially heterogeneous with the temperature change magnitude dependent upon emissions scenario (Figure 4.1). Generally, inland locations see larger temperature increases than coastal areas, and high latitude regions show greater differences than low latitude regions. In the 2040s, the temperature increase is less than (or around) 2 °C in all emission

scenarios for most locations. In the 2090s, the temperature change shows larger variation across the emission scenarios, with more than a 4 °C increase in most US locations under the A2 scenario and about a 2.5 °C increase under the B1 scenario. The temperature change is always smallest under the B1 scenario, and it is largest under the A1B and A2 scenarios in the 2040s and 2090s, respectively. These spatial patterns are consistent with previous research (Karl 2009).

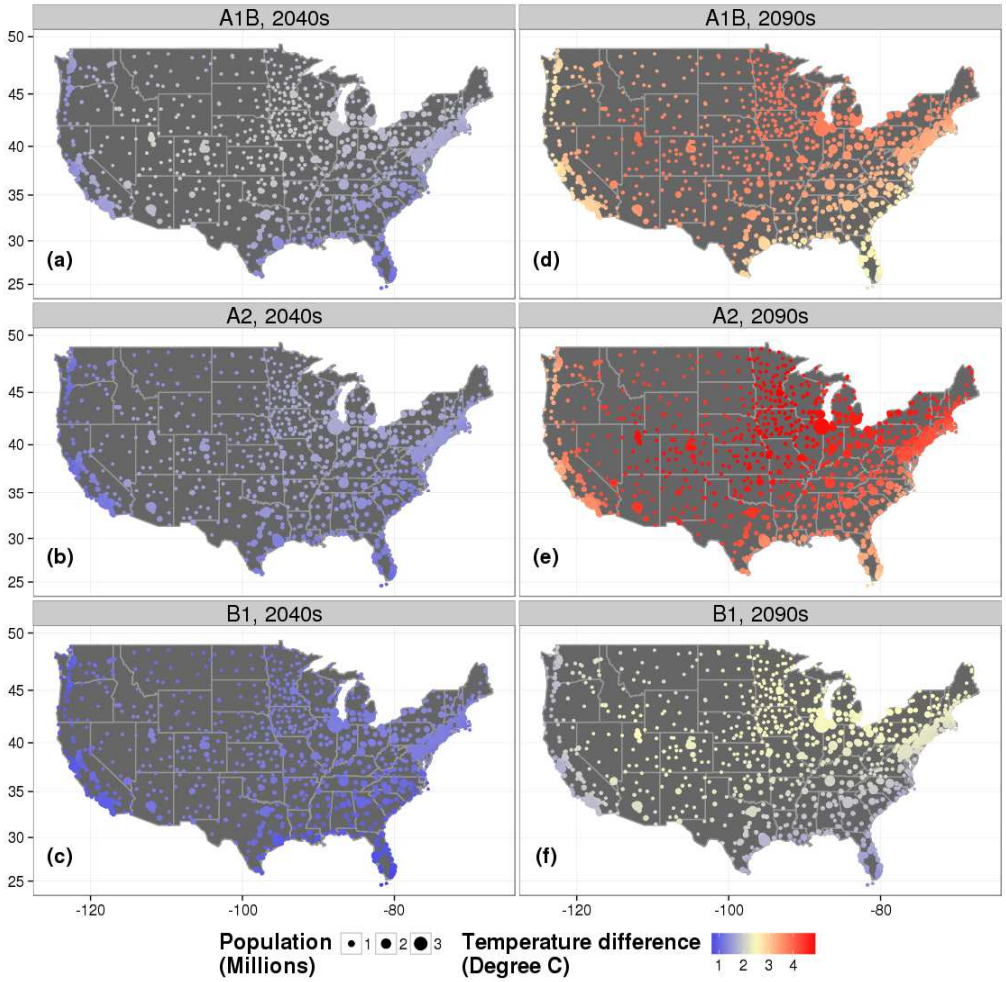

Figure 4.1. Population (for 2010) and temperature difference (°C) between future time periods (2040s and 2090s) and the current time period (1991-2005) under three IPCC emission scenarios at 925 TMY3 locations in the US. Symbol color represents temperature change, symbol size represents population.

4.2.3 Building prototypes

The US DOE developed 16 commercial building prototypes for the EnergyPlus model (Table 4.1), reflecting three different age classes (pre-1980, post-1980, and new-2004), located in 15 reference cities. For each of the 16 building prototypes, there are multiple age classes and/or building characteristics, but they share the same floor area and number of floors. These 16 building types account for 70% of the existing commercial floor area in the U.S., while the 15 reference locations represent all U.S. climate zones (Figure 4.2). The climate zones are based on the number of heating/cooling degree days (HDD/CDD), average temperature, and precipitation (Baechler et al. 2010). Each climate zone is represented as a combination of a thermal zone (number) and a hydrological zone (letter). The thermal zone numbers range from 1 to 7 representing large CDD to small CDD (or small HDD to large HDD). The letters "A", "B", and "C" represent moist, dry, and marine hydrological zones, respectively.

The three building age classes are used as a proxy for building technology as they represent progressively newer, more efficient standards. The pre-1980 building prototype represents building technology up to 1979, the post-1980 building prototype represents building technology from 1980 to 2003, and the new-2004 building prototype represents building technology following the ANSI/ASHRAE/IESNA Standard 90.1-2004 guidelines (Deru et al. 2011). Buildings with newer technology have more energy-efficient equipment and better insulation to mitigate the impact of non-optimal outside temperature. For example, the wall R-value (resistance to heat flow) in the new-2004 building class is about twice that of the pre-1980 building class. Furthermore, the energy intensity of interior lighting in the new-2004 building class is approximately 50% smaller and new buildings are usually equipped with more energy-efficient HVAC system (Deru

et al. 2011). All of the DOE commercial building prototypes are used for energy simulation except the "midrise-apartment" prototype, for which the calibration data is not available (see section 2.4 for calibration details). Two of the reference cities, Los Angeles and Las Vegas, are located in the same climate region - 3B. Los Angeles is used to represent the 3B region within California (3B-CA) and Las Vegas is used to represent the 3B region outside of California ("3B-non-CA"). For each TMY3 location, the commercial building prototypes developed for the reference city within the same climate region, are used to simulate energy consumptions.

Table 4.1 US average building floor area and average number of floors for residential and commercial building prototypes (Mendon et al. 2013; Deru et al. 2011).

Building Type	Floor Area (ft2)	Number of Floors
Residential		
Single-family House	2,400	2
Multi-family Apartment	21,600	3
Commercial		
Large Office	498,588	12
Medium Office	53,628	3
Small Office	5,500	1
Warehouse	52,045	1
Stand-alone Retail	24,962	1
Strip Mall	22,500	1
Primary School	73,960	1
Secondary School	210,887	2
Supermarket	45,000	1
Quick Service Restaurant	2,500	1
Full Service Restaurant	5,500	1
Hospital	241,351	5
Outpatient Health Care	40,946	3
Small Hotel	43,200	4
Large Hotel	122,120	6
Midrise Apartment	33,740	4

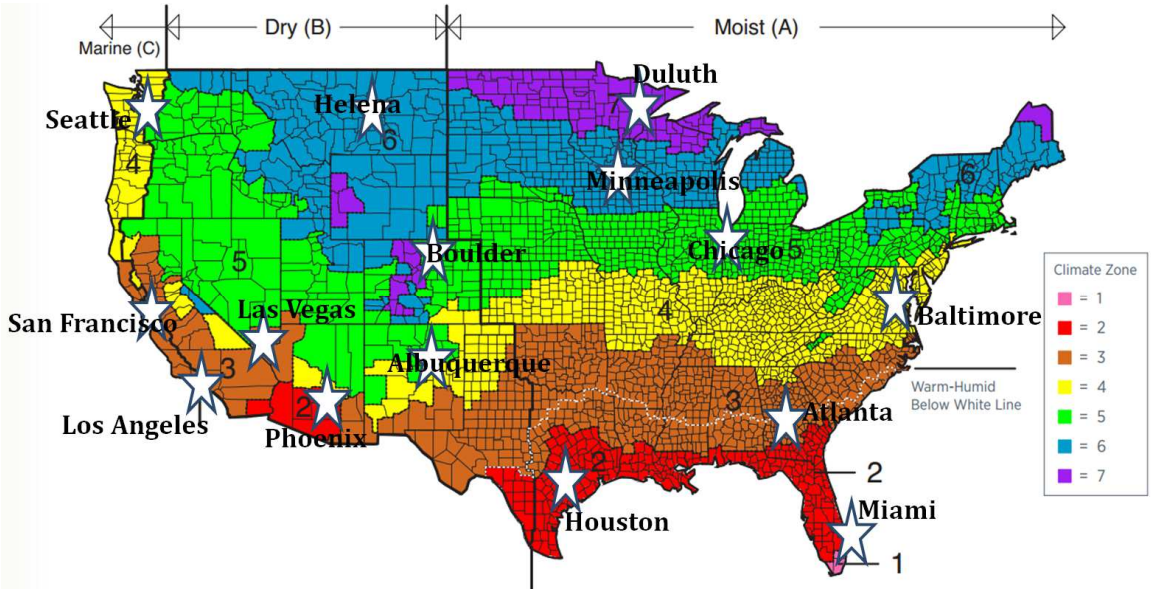

Figure 4.2 Energy Information Administration (EIA) climate zones and reference cities for the commercial building prototypes (Baechler et al. 2010).

The DOE also developed prototypes for residential buildings based on the International Energy Conservation Code (IECC). These prototypes are not disaggregated into different age classes (such as done for commercial buildings) but reflect new construction only. There are two residential prototypes: single-family (SF) detached houses and multi-family (MF) low-rise apartment buildings (Table 4.1). Each of these prototypes was modified to represent three types of heating systems (electric resistance, gas furnace, and heat pump), resulting in 6 residential sub-prototypes for each representative city. Unlike the commercial building prototypes, which were developed for 15 representative cities, the residential building prototypes were developed for 119 representative locations. For each of the 925 TMY3 locations, the residential building prototypes associated with the closest representative city within the same state and climate zone are used.

4.2.4 Calibration to survey data

"Site energy" and "source energy" are usually used to describe end-use energy consumed in a building and the raw energy required to meet the on-site demand, respectively. Because source energy accounts for the energy loss during production and delivery, it reflects the total energy consumption more comprehensively and it is more comparable across different fuel types. In this study, we chose source energy as the comparison target, and converted the site energy consumption generated by EnergyPlus to source energy consumption using source-to-site ratios (Star 2009).

The simulated commercial building energy consumption and floor area are calibrated (EnergyPlus estimates are constrained to match the survey data) with the 2003 Commercial Buildings Energy Consumption Survey (CBECS) (U.S. Department of Energy n.d.) for each building type and age class within a census division. Similarly, the residential output is calibrated with the 2009 Residential Energy Consumption Survey (RECS) (U.S. Department of Energy n.d.) data for each building type and heating system in each RECS survey domain (typically covering one or more states). Within a division/domain, energy consumption and building area are distributed to each TMY3 location by population, which is calculated as the total population in the census tracts (U.S. Census Bureau 2010b) that are closest (shortest distance from tract center to TMY3 location). The annual energy consumption in each location is further distributed to each month or hour according to the time-structure output from EnergyPlus. Because new-2004 commercial buildings are not available in the 2003 CBECS data, the EnergyPlus output for new-2004 commercial buildings are not calibrated and they are not used for most analysis except in section 3.7 where the impact of building technology changes are discussed (see section 3.7 for details).

The annual energy consumption intensity from the EnergyPlus model is close to the RECS/CBECS survey data for most building types except the *full service restaurant* and *outpatient* building types (Figure 4.3). The energy consumption intensity in residential buildings is generally less than commercial buildings, with the smallest RECS/CBECS energy consumption intensity appearing in the *single-family house* building type (86 kBtu/sq-ft) and the largest RECS/CBECS energy consumption intensity occurring in the *quick service restaurant* building type (1103 kBtu/sq-ft). In contrast, the *warehouse building type* exhibits *the* smallest EnergyPlus energy consumption intensity (88 kBtu/sq-ft), while the *quick service restaurant* building type exhibits the largest (1286 kBtu/sq-ft).

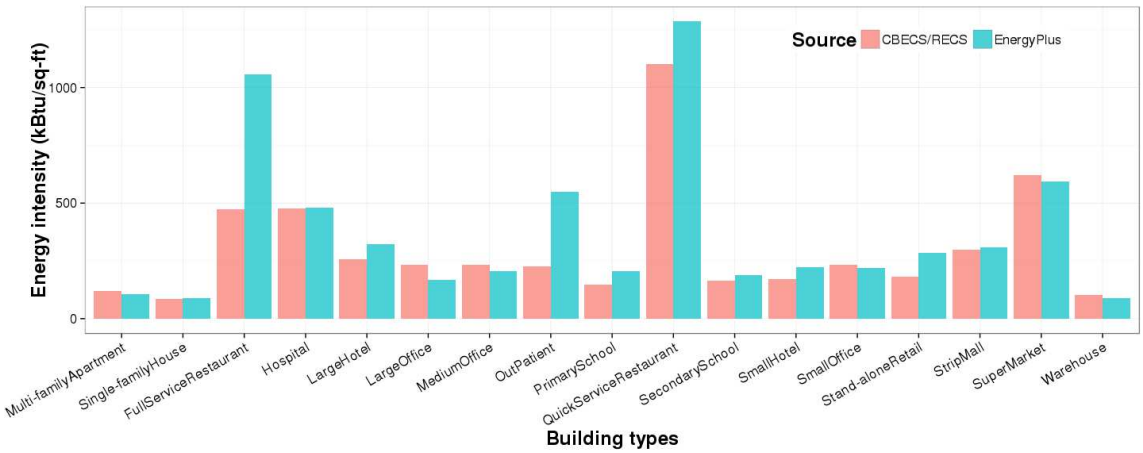

Figure 4.3 Comparison of the 1991-2005 energy intensity for commercial and residential building types for the CBECS/RECS survey data and the EnergyPlus model.

The discrepancies between the EnergyPlus model output and the RECS/CBECS survey data may be caused by several factors. First, simulated output will always differ from actual data, because the model cannot account for all the factors that determine building energy consumption and energy thermodynamics. Second, the building prototypes were developed based on the most commonly used technologies/building characteristics in the survey data, which may not correctly represent the energy consumption patterns and fuel

mixes of the real building stock. Finally, the definition/measurement of floor area may differ between the survey data and the EnergyPlus model, resulting in energy consumption intensity differences. Because both the energy consumption and floor area are calibrated in this research, the calibrated energy consumption intensity from EnergyPlus, in the end, is required to match the intensity value derived from the survey data exactly at the scale of census division/domain.

4.2.5 Comparison metrics

Relative difference (RD) and intensity difference (ID) are used to quantify the impact of climate change on building energy consumption. RD (%) represents the relative change in energy consumption, defined as the energy consumption difference between the future and current period, divided by the energy consumption in the current period:

$$RD = \left(E_{ft} - E_{cr}\right)/E_{cr} \quad (1)$$

where E is the energy consumption in the current (*cr*) and future (*ft*) periods.

ID (KBTU/sq-ft) represents the change in energy consumption intensity, calculated as the calibrated current energy consumption intensity, multiplied by the RD:

$$ID = RD \times EI'_{cr} \quad (2)$$

where EI' is the calibrated current energy consumption intensity (KBTU/sq-ft).

To capture aggregated results, the RD and ID values are summed for each combination of commercial building type and age class, and each combination of residential building type and heating system, weighted by their current energy consumptions. RD and ID values for two of the three age classes (pre-1980 and post-1980) are aggregated (weighted by their calibrated current energy consumption) to get the RD and ID for each commercial building type. Similarly, the RD and ID values for the three heating systems

(electric resistance, gas furnace, and heat pump) are aggregated to get the RD and ID values for each residential building type. RD and ID values for all commercial/residential building types are further aggregated to calculate the RD and ID values for the integral of all commercial/residential buildings. Since the current energy consumption is used as the denominator in equation (1), the RD tends to be big for the building types with small current energy consumption (e.g., warehouse). However, the ID avoids this problem, because it includes a multiplier which accounts for the energy consumption intensity in the current period. The combination of RD and ID, reflecting both the relative and absolute changes, comprehensively depict the impact of climate change.

In section 3.3, the median and quantile values (25%-75%, and 0%-100%) of the 925 ID values are compared between the three building technologies (pre-1980, post-1980, and new-2004) to study the sensitivity of climate change impact to building technology improvement such as building thermal efficiency and HVAC efficiency. Because the new-2004 buildings cannot be calibrated with the 2003 CBECS data, the energy consumptions for the three building technologies are not calibrated in section 3.3. Since section 3.3 is not aimed at studying the impacts of climate change in future periods relative to 1991-2005, but the impact of building technology changes, the calibration of energy consumption in the current period is less important.

4.2.6 Cluster analysis

Local Indicators of Spatial Association (LISA) is used to identify spatial clustering of climate change impact. LISA depends on the statistics of the Local Moran's I, which is calculated as follows (Anselin 1995):

$$I_i = (x_i - \bar{x}) \sum_{j=1}^{n} w_{ij}(x_j - \bar{x}) \quad (3)$$

where, x is the observation value, I is the local Moran's I value for observation i, n is the total number of observations, w_{ij} is the weighting matrix defining the weight of observation j on observation i.

For each observation i, equal weights are given to all of its neighbors, and 0 for non-neighbors. Neighbors are defined as the observations that are within a distance of 175 km to the observation i. The distance limit is set as 175 km, because it is the smallest distance that guarantees each weather location has at least one neighbor. With the given distance limit (175 km), each observation has about 12 neighbors on average. A larger distance limit increases the number of neighbors and assumes low climate change impact spatial heterogeneity. Given the observed spatial variation of climate change (Figure 4.1) and RD/ID values, it is not appropriate to use a larger distance limit.

A LISA map usually contains five categories: high-high (high values surrounded by high values), low-low (low values surrounded by low values), high-low (high values surrounded by low values), low-high (low values surrounded by high values), and insignificant (the p-value of local Moran's I is not statistically significant). The observation value, the local Moran's I, and the significance of local Moran's I (p-value ≤ 0.05 is deemed significant) are used to decide which category a given observation belongs to with the following rules (Anselin 1995):

- high-high: $x_i > \bar{x}$, $I_i > 0$, and p-value ≤ 0.05
- low-low: $x_i < \bar{x}$, $I_i > 0$, and p-value ≤ 0.05
- high-low: $x_i > \bar{x}$, $I_i < 0$, and p-value ≤ 0.05
- low-high: $x_i < \bar{x}$, $I_i < 0$, and p-value ≤ 0.05
- insignificant: p-value > 0.05

Because no results belong to the high-low or low-high category in this research, these two categories are not displayed on the LISA map.

4.3 Results and Discussion

The impact of climate change on building energy consumption varies across building types, and the strength of variation depends on the spatial scale, temporal scale, and the building technology. The impacts are estimated and compared across building types at three time scales (annual, monthly, and hourly), three spatial scales (national, climate zone, and location), and for three building technologies (pre-1980, post-1980, and new-2004).

4.3.1. Climate change impact: variation across building types & temporal scales

4.3.1.1 The annual time scale

The national annual energy consumption ID and RD values driven by the difference between future and present climate, vary by building type, emissions scenario, and future time period (Table 4.2). The differences for "all" buildings (the weighted sum of the individual building types – see section 2.5) show very small increases in the 2040s under all three emission scenarios. Because residential buildings consume more energy than commercial buildings, the ID and RD values for the *all* buildings category are dominated by the differences in the residential buildings, which are comparatively small.

Table 4.2 US average annual building energy consumption intensity difference (kBtu/sq-ft) and relative difference (%, value in parentheses) between two future time periods and the current time period (1991-2005).

Building Type	**2040s**			**2090s**		
	A1B	A2	B1	A1B	A2	B1
Residential	0.2(0.2)	0(0)	0.1(0.1)	0.8(0.9)	1.9(2.1)	0.1(0.1)
Multi-family Apartment	0.3(0.2)	0(0)	0.2(0.1)	1(0.8)	2.1(1.8)	0.2(0.2)
Single-family House	0.2(0.2)	0(0)	0.1(0.1)	0.8(0.9)	1.8(2.1)	0.1(0.1)
Commercial	1.7(0.7)	1.1(0.5)	1.1(0.5)	4.3(1.9)	7.2(3.2)	1.9(0.9)
Full Service Restaurant	5.6(1.2)	4.3(0.9)	3.4(0.7)	12.1(2.6)	17.6(3.7)	6.4(1.3)
Hospital	2(0.4)	1.6(0.3)	1.3(0.3)	4.5(1)	6.9(1.5)	2.4(0.5)
Large Hotel	7.3(2.8)	6.1(2.4)	4.7(1.8)	14.8(5.8)	19.9(7.8)	8.9(3.5)
Large Office	3.8(1.7)	3(1.3)	2.5(1.1)	8.6(3.7)	12.8(5.5)	4.7(2)
Medium Office	3.1(1.3)	2.2(1)	2(0.9)	7.1(3.1)	11(4.7)	3.7(1.6)
Out Patient	0.1(0)	0(0)	0.1(0.1)	0.4(0.2)	1(0.4)	0.1(0.1)
Primary School	2.8(1.9)	2.2(1.5)	1.8(1.2)	6.2(4.2)	9.2(6.3)	3.4(2.3)
Quick Service Restaurant	6.1(0.6)	4.2(0.4)	3.6(0.3)	14.7(1.3)	23.7(2.1)	6.6(0.6)
Secondary School	3.4(2.1)	2.5(1.5)	2.2(1.4)	7.9(4.8)	12(7.3)	4.1(2.5)
Small Hotel	3.3(1.9)	2.7(1.6)	2.2(1.3)	7.2(4.2)	10.6(6.2)	4.1(2.4)
Small Office	2.6(1.1)	1.8(0.8)	1.6(0.7)	6.2(2.7)	9.7(4.2)	3(1.3)
Stand-alone Retail	1.8(1)	1.3(0.7)	1.1(0.6)	4.3(2.4)	7(3.8)	2(1.1)
Strip Mall	3.1(1)	2.2(0.7)	1.8(0.6)	7.3(2.5)	11.5(3.9)	3.4(1.2)
Super Market	6.2(1)	4.6(0.7)	4(0.6)	13.7(2.2)	20.5(3.3)	7.3(1.2)
Warehouse	-4.8(-4.6)	-4.4(-4.3)	-3.1(-3)	-8.4(-8.1)	-9(-8.7)	-6.1(-5.9)
All buildings	0.5(0.4)	0.2(0.2)	0.3(0.3)	1.5(1.3)	3(2.5)	0.5(0.4)

There exists little building energy consumption change in future decades for the two residential building types, particularly in the decade of the 2040s where the changes are close to zero. By contrast, the building energy consumption differences in the commercial buildings are larger and vary to a greater extent across the different commercial building types. The large commercial building increases usually appear in the buildings with high

space cooling demands (e.g., *hotel* and *restaurant*), while the decreases appear in the buildings with low space cooling demands (e.g., *warehouse*). For example, in the decade of the 2040s, the RD values for commercial buildings range from -4.6% (*warehouse*) to 2.8% (*quick service restaurant*) under the A1B scenario. By the end of this century, the RD variation increases, ranging from -8.7% (*warehouse*) to 7.8% (*large hotel*) under the A2 scenario.

4.3.1.2 The monthly time scale

The impact of climate change on building energy consumption analyzed at the annual scale masks larger changes estimated at smaller timescales (Figure 4.4). Although the annual ID/RD values are positive for all except the warehouse building type, the monthly differences show both positive and negative values for each building type, with the largest positive difference in July/August and the largest negative difference in January. The monthly ID values for the two residential building types are similar, with values ranging from -1.4 kBtu/sq-ft in January to +1.7 kBtu/sq-ft in August for both building types. In percentage terms, the *single-family house* building type show larger variation (ranging from -14% in January to 23% in August) than the *multi-family apartment* building type (ranging from -11% in January to 17% in August), due to the smaller energy consumption intensity in the *single-family house* building type under the current period.

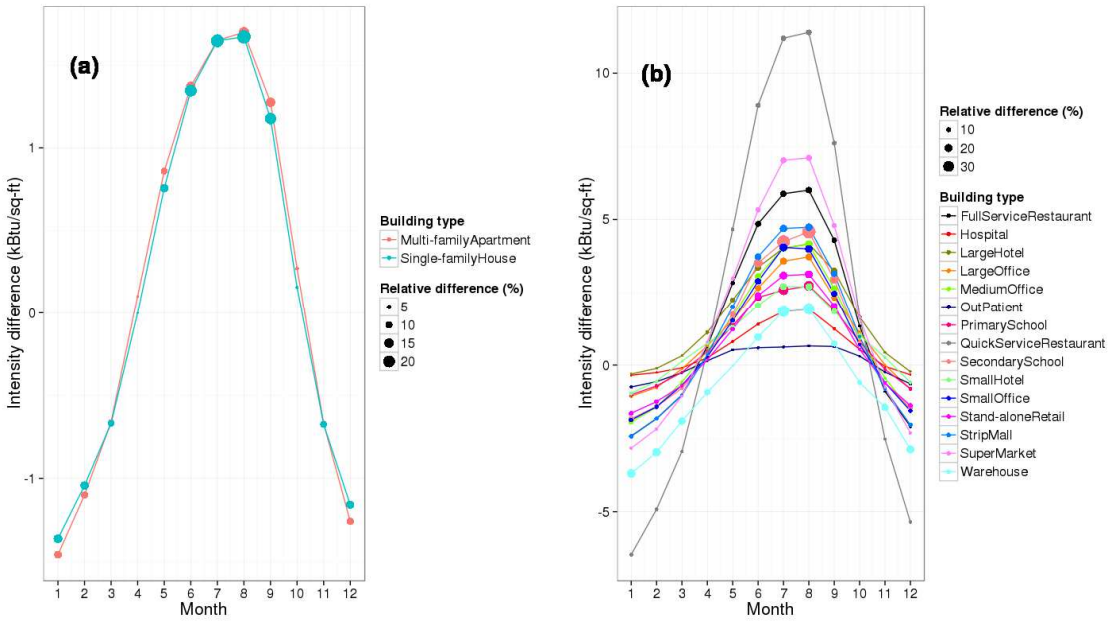

Figure 4.4 US average monthly ID and RD building energy consumption values between the 2090s and the 1991-2005 time period under the A2 emission scenario for (a) residential and (b) commercial building types

Compared to the relatively small monthly ID/RD values for the residential buildings, commercial buildings usually show larger monthly ID/RD values with greater variation among the different building types. The positive ID values in August range from 0.7 kBtu/sq-ft (*outpatient* building) to 11.4 kBtu/sq-ft (*quick service restaurant*). The negative ID values in January range from -0.3 kBtu/sq-ft (*large hotel*) to -6.5 kBtu/sq-ft (*quick service restaurant*). These are accompanied by a large variation in RD values with a maximum percent increase in August of 39% (*secondary school*) and a maximum percent decrease in January of -22% (*warehouse*). The large ID values usually appear in building types with high energy intensity (e.g., *restaurant*), while the large RD values appear in the building types with low energy intensity (e.g., *warehouse*).

4.3.1.3 The hourly time scale

Since the largest increase in energy consumption usually appears in the July/August timeframe, a more detailed examination of the hourly ID/RD values and their variation across building types in this time period is worthwhile. Figure 4.5 shows the average hourly ID/RD values during July and August in the 2090s under the A2 emissions scenario. In contrast to the monthly change patterns described in section 3.1.2 where the building consumption differences matched the seasonal cycle (increased energy demand in warmer months and decreased energy demand in colder months), the hourly changes are more diverse and show larger variations across building types. Unlike the monthly case where the two residential building types had very similar monthly ID/RD values, the hourly ID/RD values for the *single-family house* building type shows greater variation within the 24 hour cycle than the *multi-family apartment* building type, with both the largest hourly ID (2.6 Btu/sq-ft) and RD (37.7%) values appearing in the *single-family house* building type. This is probably because *single-family houses* typically have a larger surface to volume ratio, thus the inside temperature and space heating/cooling demand is more influenced by fluctuations in the outside temperature via faster thermal heat transmission (Smeds & Wall 2007). The two maximum ID values appear around 10-11 am and 7-8 pm for residential buildings, probably due to the high internal heat gain (heat emitted from any source/equipment inside the building, for example, lighting, cooking, and human metabolism) during these two periods, when the buildings are occupied and/or most appliances (e.g., clothes washer, clothes dryer, bathroom, and lighting) are used to a greater extent (Mendon et al. 2013). The increased temperature caused by climate change, on top of the two periods with high internal heat gain, requires more space cooling and leads to larger ID values compared to other hours. By contrast, the

maximum RD values usually appear at midnight. This is probably because the energy consumption is low during late night hours driven by low appliance use and space cooling demands (Mendon et al. 2013). This, in turn, results in a small denominator within the RD calculation and a high RD value. The different diurnal patterns of ID and RD demonstrate the importance of including both ID and RD in analysis of climate change impacts on building energy consumption.

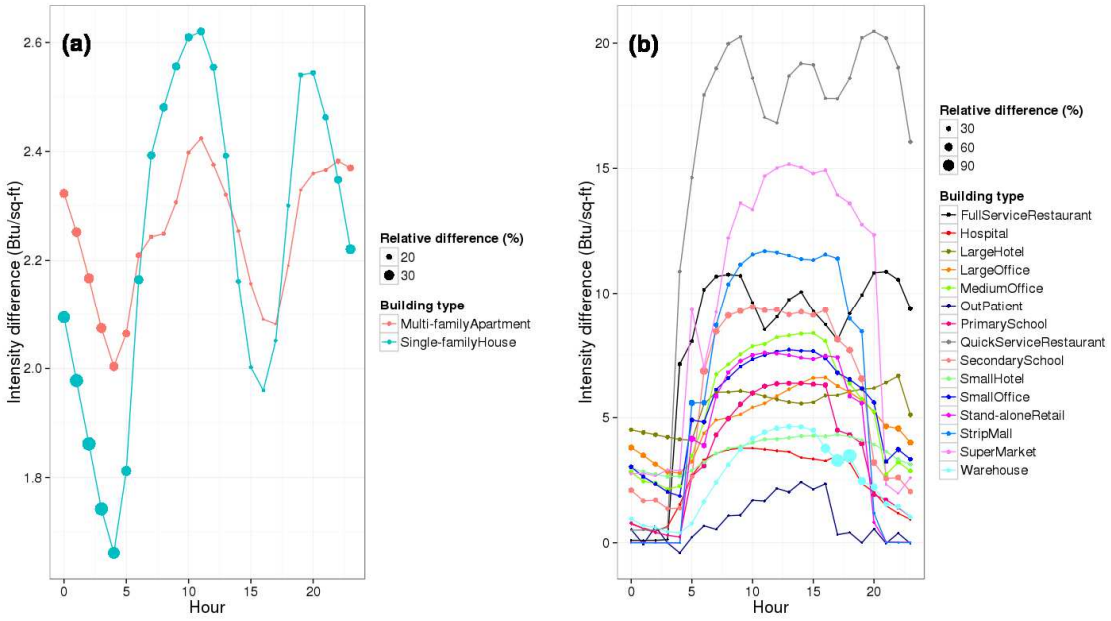

Figure 4.5 US average hourly ID/RD values in July and August between the 2090s and the 1991-2005 time period under the A2 emission scenario for residential and commercial buildings.

The commercial buildings show greater hourly ID and RD variation both within and across the commercial building types. ID values range from 0 to 20 Btu/sq-ft and RD values range from 0% (midnight, for multiple building types) to 110% (5-6 pm, in the *warehouse*). The maximum ID appears in the *quick service restaurant* building type for which the energy consumption intensity is the largest, while the maximum RD value occurs in the *warehouse* building type for which the energy consumption intensity is the

smallest (Figure 4.3). The maximum ID values for commercial buildings usually appear around midday due to the high occupancy and equipment use, and the subsequent high space cooling demands during business hours (Deru et al. 2011). There are some building-specific maxima appearing in other hours. For example, the maximum ID values for the *full service restaurant* and the *quick service restaurant* building types appear around 9 am, 2 pm, and 8 pm consistent with maximum customer patronage in these two building types. The maximum ID value for large hotels appears around 10 pm likely due to the high activity of hotel guests, lighting, and equipment use (Deru et al. 2011). In contrast to the changes during the daytime, the nighttime ID/RD values are usually small.

4.3.2 Climate change impact: variation across building types & spatial scales

4.3.2.1 The climate zone scale

The impact of climate change on building energy consumption also displays a strong spatial variation at the spatial scale of climate zones. Figure 4.6 shows the climate-zone-scale annual RD values for each of the residential/commercial building types in the 2090s under the A2 emission scenario. Although the annual/national RD values for both the *multi-family apartment* and *single-family house* building types are very small (< 2% in most cases), the RD values across the climate zones show large variation, ranging from -5.8% to 11.3% in the *multi-family apartment* building type and -6.2% to 14.7% in the *single-family house* building type.

For commercial buildings, the majority of RD values across all climate zones show net increases in energy consumption with the *secondary school* building type showing a maximum energy demand increase of 20.9% (climate zone 1A). The *warehouses* building type is an exception with negative RD values as large as -16.6% (climate zone 7A).

Within each building type, the warmer climate zones usually show a net increase in energy consumption due to space cooling demand increases, while colder climate zones display a net decrease driven by declines in space heating demand. For example, the RD values in the *warehouse* building type range from a net decrease of -16.6% in climate zone 7A to a net increase of 12.4% in climate zone 1A. Within each climate zone, the RD values also display strong variation across building types. For example, the RD values in climate zone 4A range from -8.4% in the *warehouse* building type to 8.1% in the *secondary school* building type. Relatively small variations of climate-zone-level RD values exist in the *hospital* (ranging from -1.1% to 2.7%) and *outpatient* building types (ranging from -2% to 2.4%) compared to other commercial building types. This could be due to the stricter ventilation requirements for healthcare (*outpatient* and *hospital*) building types (Deru et al. 2011). The strict ventilation requirements weaken the impact of outside temperature change on the indoor environment, and result in small RD values

over the whole US.

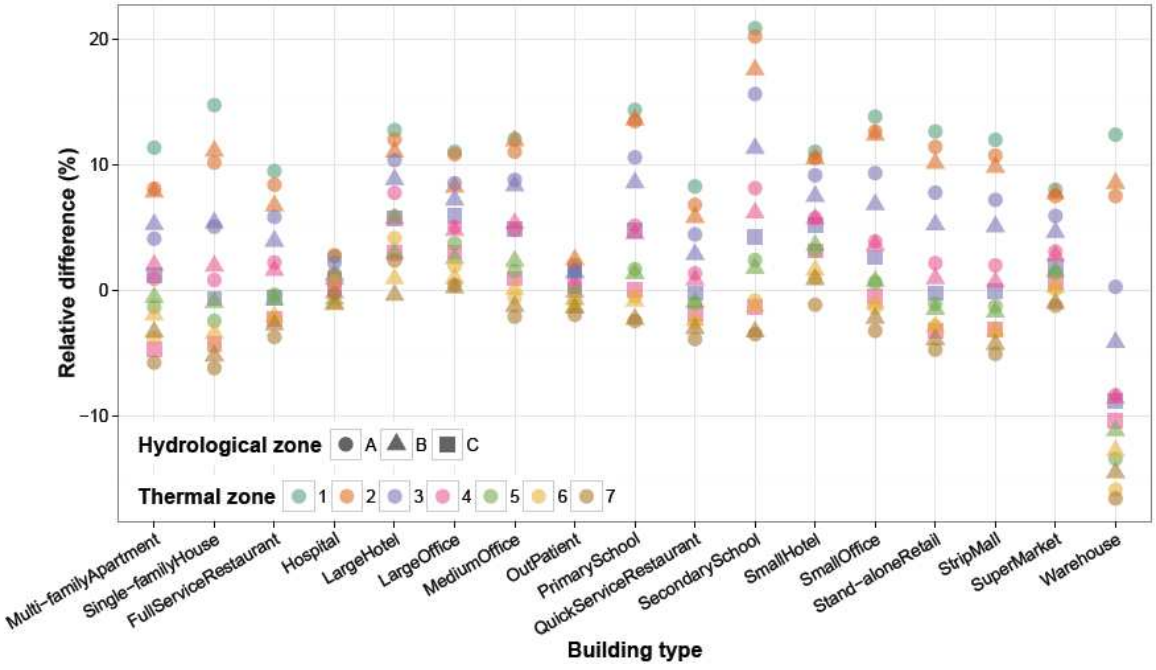

Figure 4.6 Climate-zone (thermal and hydrological zones) scale annual building energy consumption relative difference (%) between the 2090s and the 1991-2005 time period under the A2 emission scenario for residential and commercial building types.

4.3.2.2. The local scale

Even larger annual RD variations are found at the local scale (Figure 4.7), with the largest increase in energy consumption (+24%) appearing in the *secondary school* building type (in Aroostook, Texas, climate zone 2A) and the largest decrease (-20%) appearing in the *warehouse* building type (in Aransas, Maine, climate zone 7A). Within each climate zone and building type, there still exists a large variation in local-scale RD values, especially in the climate zones covering large areas. For example, the local-scale RD values in the *secondary school* building type range from -11.8% to 5.8% (17.6 percentage point span) in climate zone 6A, covering 8 climate-zone-scale RD values for this building type. The strength of such variation also depends on building type. For

example, in the same climate zone (6A), the local-scale RD values in the *warehouse* building type only range from -19% to -11% (8 percentage point span), covering only 5 climate-zone-scale RD values. The variation of RD values within climate zones indicates that these within climate zone differences can be larger than the differences between climate zones, and hence systematic bias could result from representing the changes in a climate zone from a single reference location.

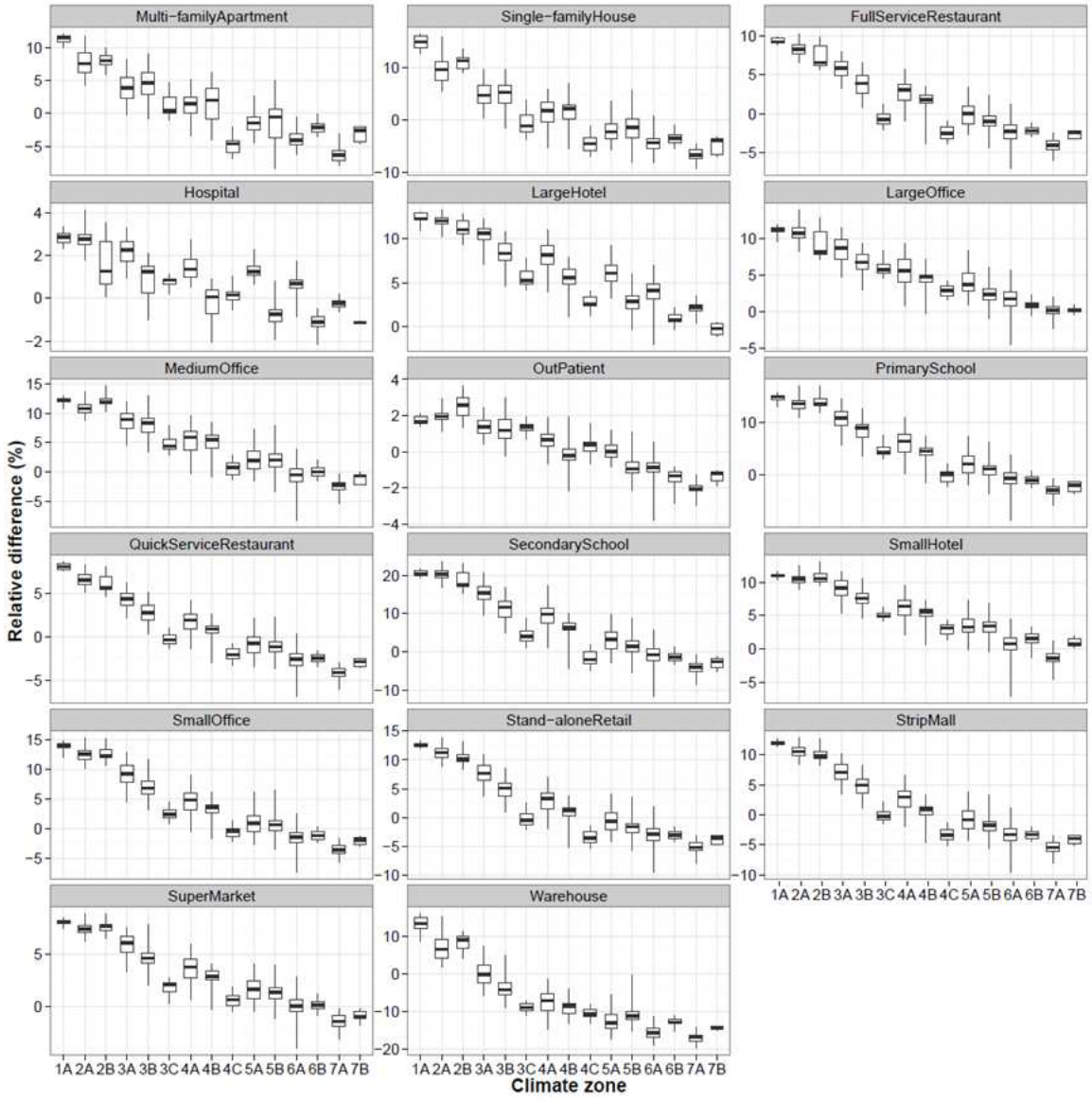

Figure 4.7 Local-scale annual building energy consumption relative difference (%) between the 2090s and the 1991-2005 time period under the A2 emission scenario for all residential and commercial building types. Each quantile plot displays the intensity differences at 925 TMY3 locations, with the middle bar representing the median value, the box representing the 25% – 75% quantiles, and the whiskers representing the 0% and 100% quantiles.

4.3.2.3 Spatial clustering

Despite the RD variation across spatial scales and building types, LISA maps display consistent patterns—high values cluster in climate zones 1, 2, and 3, low values cluster in

climate zones 6 and 7, with insignificant values in climate zones 4 and 5 (Figure 4.8). Although coastal locations typically show small temperature increases compared to inland locations (Figure 4.1), they often display large changes in energy consumption. The high-high result is found mostly in climate zones 1A and 2A. This may be due to three reasons. Firstly, the current outdoor temperatures are typically higher than the cooling thermostat set-point temperature (less or equal to 75 °F for different building types) in climate zone 1A and 2A, especially during summer (National Oceanic and Atmospheric Administration n.d.). Thus any temperature increase in the future will require additional space cooling. By contrast, the current outdoor temperature in the North is usually lower than the set-point temperature, even in summer. Hence, the future temperature increase may require little, or no, additional space cooling. Secondly, the humidity is usually high in coastal areas, and it requires additional energy to dehumidify the air in order to maintain a comfortable indoor environment (Mazzei et al. 2005). Finally, the buildings in warmer climate zones usually have smaller wall and ceiling insulation R-values compared to the colder climate zones (Deru et al. 2011; Mendon et al. 2013). This implies that warmer climate zones have buildings that are more vulnerable to the increased outside temperature and will require more space cooling.

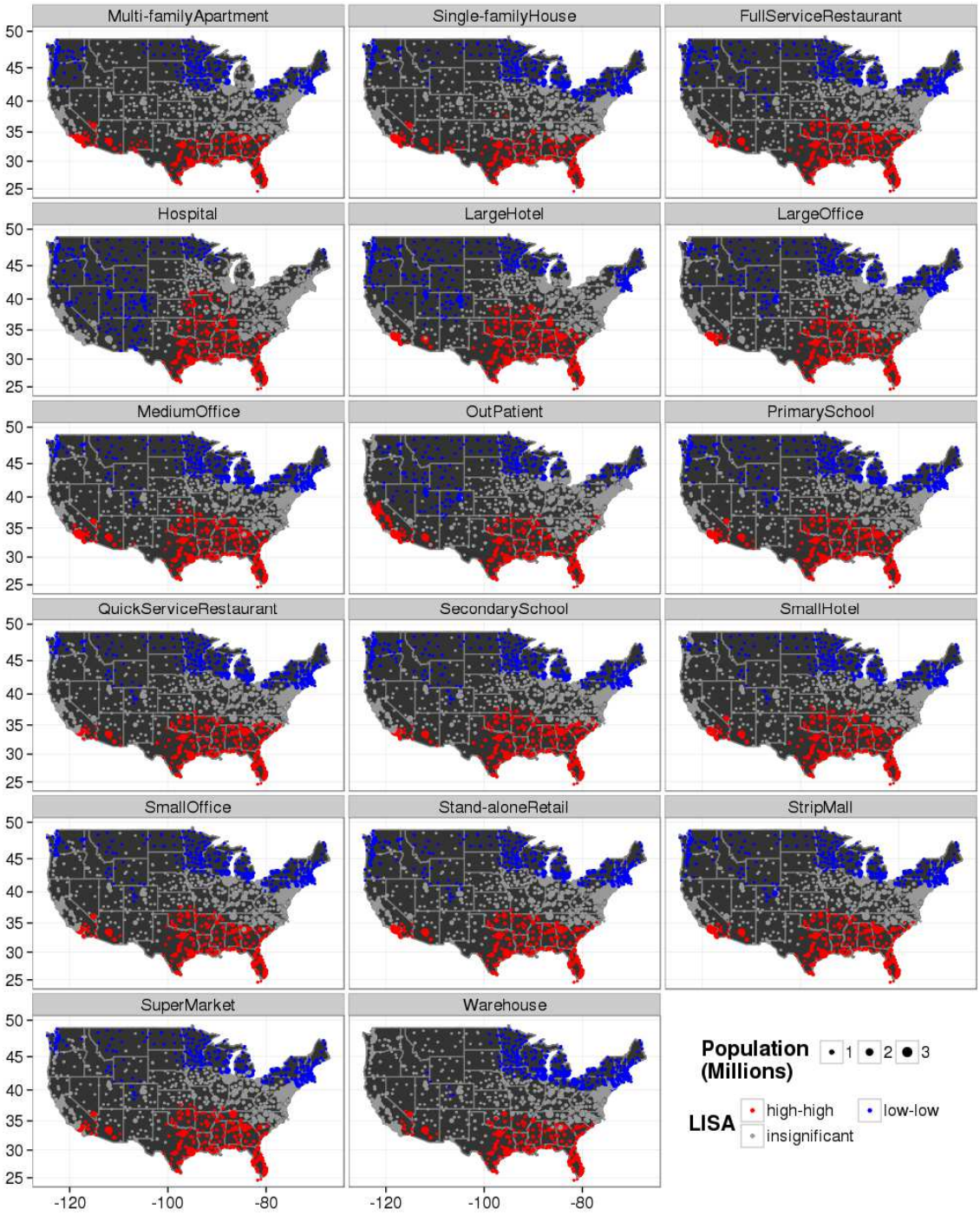

Figure 4.8 Local Indicators of Spatial Association (LISA) map of annual building energy consumption RD values (%) between the 2090s and the 1991-2005 time period under the A2 emission scenario.

4.3.2.4 Drivers of spatial variation

In order to explore the drivers of the spatial variation in energy consumption changes, we use the results for the *quick service restaurant* building type (the building type with the largest energy intensity) and examine the RD values in comparison to projected surface temperature change within and across climate zones (Figure 4.9). When examining the RD at the climate zone-scale (Figure 4.9a), values decrease along the climate zones from 1 to 7, indicating that the spatial variation of altered energy consumption is primarily caused by the current HDD/CDD gradient variation across the climate zones. For example, the positive RD values appear in the high-CDD zones due to the dominance of increased cooling demands, while the negative RD values occur in the high-HDD zones due to the dominance of reduced heating demands. Within each climate zone, the RD values for hydrological zone C (marine) are usually less than zone A and B due to moderated climate change along coastal areas. The RD values for hydrological zone B (dry) are typically less than zone A (wet) because less energy is required to dehumidify the air in drier climates.

In contrast to the variation across climate zones, the variation of RD values within climate zones is related to projected temperature change. RD values are positively correlated with temperature changes within most climate zones except 2A and 2B, and the correlation coefficients are greater than 0.5 in about half of the climate zones. This indicates that temperature change is the major driver of RD variation within each climate zone, and large temperature changes usually lead to large RD values. Were the temperature to further increase after the 2090s, the locations seeing net decreases in energy consumption will likely switch to net increases. This is because there is a limit to

space heating declines, which can't drop below zero. There is no limit for space cooling increases, however. When the temperature further increases, the dominance of space heating reductions in cold climates will weaken, and the space cooling increase will eventually outweigh the space heating decrease.

Although the analysis in this section is based on the *quick service restaurant* building type, it represents the general pattern seen for all building types (Figure S4.1 and S4.2 in Appendix).

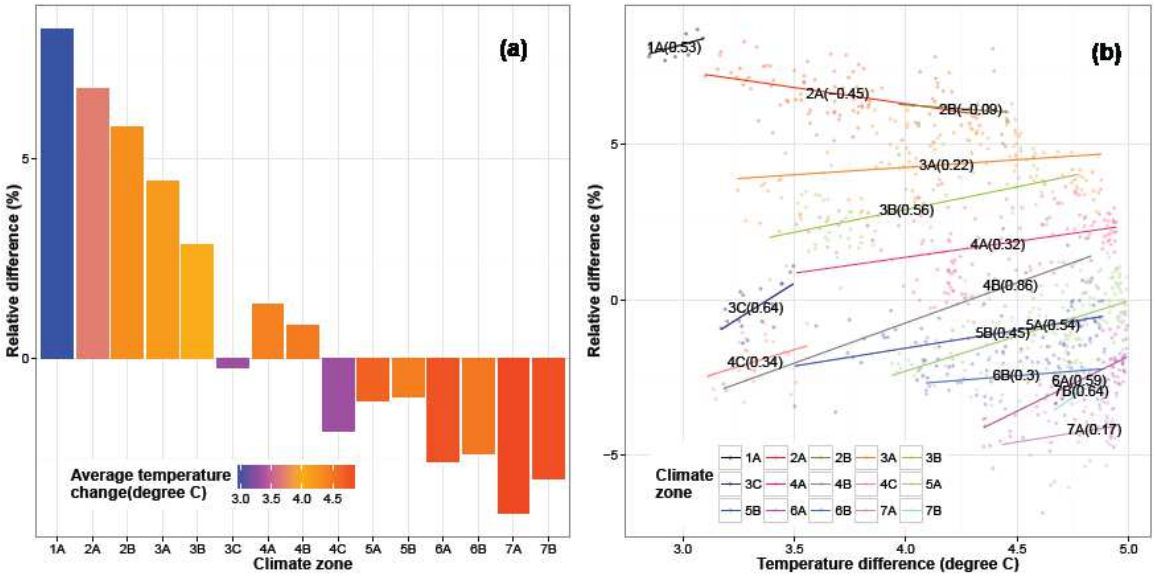

Figure 4.9 Quick service restaurant energy consumption RD (%) variation between the 2090s and the 1991-2005 time period under the A2 emission scenario. (a) RD across climate zones (sorted from high CDD to low CDD); (b) RD versus temperature change within each climate zone (each point represents a TMY3 location). The number within parenthesis represents the correlation coefficient between RD and temperature change in each climate zone.

4.3.3 Variation across building technology

Building technology plays an important role in determining building energy efficiency and consumption. Advanced technologies (e.g., efficient HVAC, well-insulated walls) can mitigate the impact of climate change on the indoor environment. To quantify the

potential effectiveness of new building technology in mitigating the impact of climate change, we show the median and quantiles (25%-75%, and 0%-100%) of the 925 ID values for the three different age classes of building in Figure 4.9. Effective building technology that can reduce the impacts of climate change on building energy consumption will be represented by a small median ID value and/or narrow quantiles.

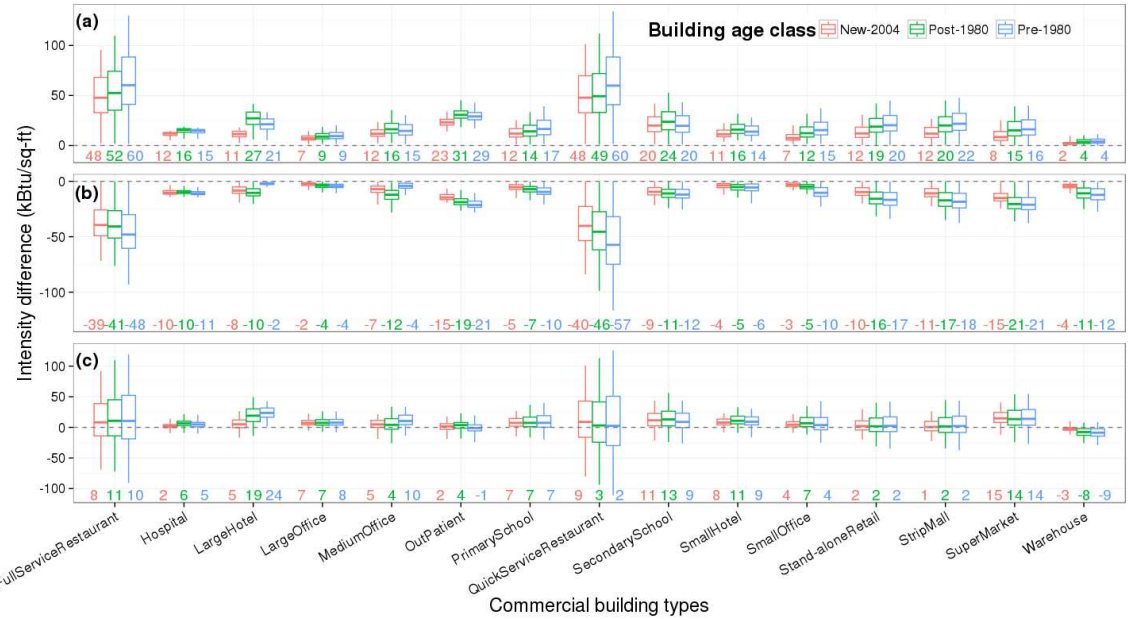

Figure 4.10 Space cooling (a), space heating (b), and total (c) energy consumption intensity differences (kBtu/sq-ft) for commercial buildings between the 2090s and the 1991-2005 time period under the A2 scenario. Each quantile plot displays the intensity differences in 925 TMY3 locations, with the middle bar representing the median value, the box representing 25% – 75% quantiles, and the whiskers representing the 0% and 100% quantiles. The red, green, and blue numbers are the median values (kBtu/sq-ft) for new-2004, post-1980, and pre-1980 buildings respectively.

The median space cooling demand increases in the pre-1980 buildings are similar to the post-1980 building values. However, the new-2004 buildings consistently exhibit the smallest median increase (Figure 4.10a). The median space heating demand decreases are usually greatest in the pre-1980 buildings, followed by the post-1980 buildings. The new-2004 buildings generally have the smallest median space heating demand decrease

(Figure 4.10b). Besides the smaller space cooling/heating median changes, the new-2004 buildings also display narrower 25%-75% and 0%-100% quantiles for both space cooling and space heating. The median IDs for total energy consumption show less of a range among the different building technology due to the cancellation between increased cooling demands and decreased heating demands (Figure 4.10c). However, the new-2004 buildings still show the narrowest quantile values (25%-75% and 0%-100%) for most building types. These results confirm the expectation that the buildings equipped with newer technology are more efficient in maintaining a comfortable indoor environment and less sensitive to outdoor temperature changes due to the stronger insulation.

4.4 Conclusions

This paper estimates the impact of climate change on building energy consumption for 2 residential and 15 commercial building types at 925 U.S. locations. This research is aimed at isolating the sensitivity of building energy consumption to climate change, and highlights the variations across building types at different spatial and temporal scales, so that it is more helpful to the implementation of localized and specialized adaptation/mitigation policy to climate change.

We find a small national annual energy consumption increase for residential building types, but a large increase (up to 8%) for commercial building types by the decade of the 2090s. Larger variations are found across different building types, when the impacts are examined at the monthly/hourly temporal scales. At the monthly scale, the national energy consumption increases up to 39% in August for the *secondary school* building type, while it decreases up to 22% in January for the *warehouse* building type. At the

hourly scale during summer, the variation is even larger, ranging from 0% change at the midnight for multiple building types to 110% increase at 5-6 pm for the *warehouse* building type.

Strong variations are also found within and between building types, when impact is examined at sub-national spatial scales. At the climate zone scale, the RD value increases up to 21 % in the *secondary school* building type (climate zone 1A), while it decreases up to 17% in the *warehouse* building type (climate zone 7A). Larger variations are found across building types at the location scale, ranging from -20% to 24%. There also exists large variations within climate zones in individual building types (e.g., the RD values range from -12% to 6% in the climate zone 6A for the *secondary school* building type), suggesting potential bias when representing the impacts of climate change in each climate zone with a single reference location. The clustering analysis suggests that large energy consumption changes are mainly clustered in areas with warm-humid (Southeast) climates. The variation of current CDD/HDD in different climate zones is the major driver of the spatial variation in energy consumption changes between climate zones, while the variation of local-scale temperature change is strongly related to the variation of local-scale energy consumption change within each climate zone. Energy consumption for different commercial building technologies indicates that the new-2004 building types are less sensitive to climate change, compared to the pre-1980 and post-1980 building types.

It is worthwhile to note that the residential building prototypes were developed following the IECC guidance, not based on the historical building characteristics. As a result, the impacts of climate change on residential buildings should be interpreted as the impact on

future residential buildings constructed according to the IECC rules, instead of reflecting impacts on current residential building stock. The building stock used here represents the current spatial distribution and mix of building types. In future analysis, it may be useful to update these building stock attributes with projected land use datasets such as the Integrated Climate and Land-Use Scenario (ICLUS) (U.S. Environmental Protection Agency 2010).

In this study, the impacts of climate change on building energy consumption are only explored with the CMIP3 climate model long-term monthly temperature changes. One may be able to estimate the complete climate change impacts more comprehensively with higher resolution and/or more contemporary climate model outputs (for example, CMIP5 and North American Regional Climate Change Assessment Program). Besides long-term temperature changes, increases in extreme events and changes in mean humidity will also alter building energy consumption. Some research has suggested that climate change will result in more intense and frequent heat waves, of longer duration (Meehl & Tebaldi 2004). Because it requires a large amount of energy to satisfy cooling demand during heat waves and the electricity grid is vulnerable to extreme events, it is important to study the impacts of extreme events on energy consumption, energy supply, and energy security. Along with increasing temperatures, a positive trend in specific humidity has been observed in the United States (Gaffen & Ross 1999). Since dehumidification requires considerable amounts of energy, it is also worthwhile to explore the impact of humidity changes on building energy consumption. With the detailed spatio-temporal energy consumption changes estimated here, potential mitigation/adaptation strategies

specific to the particularly vulnerable building types (e.g., restaurants) at the most vulnerable times of the year could be explored.

4.5 Acknowledgements

We would like to thank the funding support from National Science Foundation CAREER award 0846358 and the Department of Energy grant #DE-SC0006105. We would also like to thank Amazon Climate Research Grant Program for providing cloud computing resource.

CHAPTER 5

5 FINANCIAL IMPLICATIONS OF THE CLIMATE CHANGE IMPACTS TO BUILDING ENERGY CONSUMERS AND ENERGY SUPPLIERS

5.1 Introduction

Energy consumption in residential and commercial buildings is affected by climate change directly through the impact on space cooling and heating. More than 40% of 2010 US primary energy was used by buildings, of which 23% was used for space heating and 15% was used for space cooling (Kelso 2012b). A number of studies have assessed the impacts of climate change on building energy consumption within the US domain. Some of these studies estimated the impacts based on historical relationships between climate variables and energy consumption (David J Sailor & Muñoz 1997; Sailor et al. 1998a; Sailor 2001a; Ruth & Lin 2006a; Alan F Hamlet et al. 2010; Sathaye et al. 2013). Others evaluated the impacts with energy simulation models, either at the building level (Scott et al. 1994; Xu et al. 2012a; Y. J. Huang 2006; Wang & Chen 2014; Dirks et al. 2015) or the regional/international level (Zhou et al. 2013b; Zhou, Clarke, Eom, Kyle, Patel, Son H Kim, et al. 2014; Isaac & Van Vuuren 2009; Stanton W Hadley et al. 2006; McFarland et al. 2015). In general, these studies found a net increase of energy consumption in the warmer regions of the US due to increased cooling demand. In colder regions, they found a net decrease in energy consumption due to lower heating demand. When integrated over the whole US domain, however, study results varied from a net increase to a net decrease in building energy consumption and depended upon the research methods, future time period, emissions scenario, and energy form (on-site or source energy) chosen. Most importantly, there has been little systematic translation of these energy demand

changes into the practical implications for the population ultimately affected: building energy consumers and energy suppliers.

The few studies that have attempted such translation have estimated the financial impacts of climate change to the US energy sector based on national/international economic modeling (Linder & Inglis 1989; Stanton W Hadley et al. 2006; Rosenthal et al. 1995; Mansur et al. 2008; Mendelsohn et al. 2000; Jaglom et al. 2014). Some studies found increased costs in the energy sector, ranging from a few billion dollars to a few hundred billion dollars (Linder & Inglis 1989; Stanton W Hadley et al. 2006; Mansur et al. 2008; Jaglom et al. 2014). By contrast, other studies found a savings of a few billion dollars in energy expenditures (Rosenthal et al. 1995; Mendelsohn et al. 2000). These studies, mostly carried out at the national/international and annual scales, usually mask the spatial and temporal variation and extremes of the impacts at the sub-national and sub-annual level, which is important for local energy consumers/suppliers and practical estimates of climate change damage cost. Furthermore, the heating/cooling degree days used in these researches usually depended on a commonly-used 65 °F balance point temperature (the external temperature at which no heating/cooling is required to maintain a comfortable building environment), which may cause biased estimates.

Huang et al (2015) attempted to explore the importance of the sub-national and sub-annual impacts of climate change on building energy demand and supply using observationally-based relationships between energy consumption and temperature and a state-specific balance point temperature. Huang et al examined the whole US at the state spatial scale and month temporal scale. The impact on electricity and non-electric

(including natural gas, distillate fuel oil, kerosene, propane, and wood) fuel consumption was quantified in the residential and commercial building sectors in four future periods (2020-39, 2040-59, 2060-79, and 2080-99), each with an ensemble of 20 climate model outputs under the Representative Concentration Pathways (RCP) 8.5 emission scenario (radiative forcing rises to 8.5 W/m^2 in 2100). In some states, the summer electricity demand increased by more than 50% and the winter non-electric demand decreased by up to 48% by the end of this century. These opposing extremes canceled when examined at the national/annual scale, ending up with energy demand changes approaching zero in all future time periods. Hence, the estimate at the whole US domain and the annual timescale masked extremes of impact at smaller space/time scales.

Based on the state-level monthly energy demand changes found in Huang et al (Huang & Gurney 2015), this study quantifies the financial and infrastructural changes implied by the building energy changes in ways more meaningful for energy consumers and suppliers using current consumer energy prices and electricity capacity reserve requirements. The energy cost differences are estimated for the state residential and commercial sector separately. The additional electricity capacity required to satisfy the reserve margin requirement is estimated for each North American Electric Reliability Corporation (NERC) region, which is further converted to an annual cost based on prices to building and operate new electricity capacities. These estimates, based on historical relationship and state monthly energy consumption changes, can provide more accurate estimates of the climate change damage and the social cost of carbon in the building sector.

5.2 Methods and Data

5.2.1 Consumer cost difference

The financial implications for building energy consumers given the changes to electricity and non-electric energy demand are explored through examination of state-level consumer energy prices. The EIA SEDS provide state-level end-use energy consumption (MMbtu) and end-user energy prices (USD/MMbtu) by fuel type, state, and sector (U.S. Energy Information Administration n.d.). The electricity price (USD/MMbtu) is calculated as the average of 2008-12 electricity prices weighted by annual end-use electricity consumption (Table 5.1). Similarly, the non-electric price is calculated as the average of 2008-12 non-electric fuel prices weighted by annual end-use consumption of each non-electric fuel (including natural gas, propane, distillate fuel oil, kerosene, and wood). The state energy prices are combined with the changes to building energy demand to arrive at an estimate of state-level residential and commercial building expenditure were climate change to be imposed on consumers experiencing current pricing.

Table 5.1 Electricity and non-electric consumer energy prices (2008-2012 average) and annual cost difference between 2080-99 and 2008-12 for the residential and commercial sectors. Currency in 2008-2012 US dollars ($).

State	*Electricity price ($/mmBtu)*		*Non-electric price ($/mmBtu)*		*Cost difference (million $)*		
	Residential	**Commercial**	**Residential**	**Commercial**	**Residential**	**Commercial**	**Total**
AL	31.76	16.44	30.01	15.11	80	53	133
AZ	31.85	16.86	27.41	12.83	164	143	307
AR	26.70	12.63	22.09	10.20	10	-29	-19
CA	43.02	10.91	38.39	9.75	-703	522	-181
CO	31.62	9.57	26.19	9.00	-251	-14	-265
CT	55.43	20.17	47.33	12.98	-205	109	-96
DE	40.49	18.66	32.93	14.83	-18	-1	-19
DC	38.85	14.18	37.86	12.74	-33	18	-15
FL	34.23	18.04	29.42	14.04	1649	1062	2711
GA	30.66	15.97	27.26	12.38	-207	85	-122
ID	23.02	11.01	18.82	10.42	-94	-50	-144
IL	33.43	9.99	27.16	9.39	-565	19	-546
IN	28.43	11.19	24.86	9.62	-175	-16	-191
IA	30.01	12.05	22.57	9.41	-175	-73	-248

KS	29.55	11.62	24.37	10.60	-172	-8	-180
KY	25.48	11.92	23.43	10.41	-24	26	2
LA	26.18	12.94	24.89	11.91	177	137	314
ME	45.47	19.86	36.27	18.79	-102	-39	-141
MD	40.64	15.34	34.10	11.81	-133	54	-79
MA	46.04	17.99	43.58	14.17	-513	71	-442
MI	36.50	11.93	29.03	9.67	-687	15	-672
MN	30.88	10.74	24.41	8.87	-296	-111	-407
MS	29.83	13.29	27.91	11.56	53	40	93
MO	26.69	12.10	21.87	11.05	-287	-64	-351
MT	27.59	12.18	25.60	9.75	-111	-58	-169
NE	26.20	10.86	22.27	8.07	-106	-44	-150
NV	35.51	12.57	28.35	10.12	-16	-8	-24
NH	47.40	19.75	41.34	16.74	-83	9	-74
NJ	47.23	14.45	40.14	10.81	-316	161	-155
NM	31.06	11.31	25.83	8.85	-104	-37	-141
NY	53.01	16.69	46.63	12.21	-1204	391	-813
NC	29.76	15.76	23.73	12.85	-67	27	-40
ND	23.98	13.12	21.44	11.42	-62	-46	-108
OH	32.38	12.23	27.96	10.28	-520	-33	-553
OK	26.82	11.61	21.69	10.71	-95	-37	-132
OR	26.58	12.15	22.75	10.95	-113	-27	-140
PA	36.19	16.49	28.42	12.80	-1125	-284	-1409
RI	45.52	19.72	38.92	15.84	-118	5	-113
SC	31.42	15.40	26.36	12.64	60	30	90
SD	26.48	12.29	22.02	9.64	-54	-26	-80
TN	27.85	12.27	28.76	11.11	116	96	212
TX	34.53	12.08	27.16	9.69	871	622	1493
UT	26.02	8.71	21.23	8.37	-120	-38	-158
VT	45.83	19.64	39.36	18.26	-87	-19	-106
VA	30.70	14.98	22.90	11.63	-196	-14	-210
WA	23.47	13.13	21.24	11.91	-541	-314	-855
WV	25.18	10.85	21.74	10.77	-67	-46	-113
WI	36.54	11.65	29.17	9.53	-263	-21	-284
WY	26.10	11.60	21.88	10.27	-59	-45	-104
US total	33.79	13.40	29.76	11.04	-6889	2193	-4696

A per household annual cost difference is calculated for the residential sector as follows:

$$\mathrm{CD} = (\mathrm{P_{ele}} \times \mathrm{SD_{ele}} + \mathrm{P_{nele}} \times \mathrm{SD_{nele}})/\mathrm{HH} \quad (1)$$

where the cost difference per household, *CD*, is a function of the price, *P*, (USD/MMbtu) for electricity, *ele*, and non-electric fuel, *nele*. The on-site energy difference, *SD*, (mmBtu), and the number of households (U.S. Census Bureau n.d.), *HH*.

Because there is a general trend towards electricity demand increases and non-electric demand decreases in the future, a high price ratio of electricity to non-electric fuel will

generally lead to higher future consumer expenditures. The price ratios of electricity/non-electric fuel are calculated for state residential and commercial sectors separately, which are used to explore the cost difference patterns in the two sectors.

5.2.2 Electricity generation capacity and cost

Peak electricity demand typically occurs during summer months and Huang et al. (2015) show that summer electricity consumption will increase more than 20% in some states during the 2080-99 period. As a result, additional electricity generation capacity will likely be required to meet the increased peak electricity demand. The North American Electric Reliability Corporation (NERC) is a nonprofit organization tasked with maintaining reliable electricity supply for the North America. There are eight NERC regions within the contiguous United States: Florida Reliability Coordinating Council (FRCC), Midwest Reliability Organization (MRO), Northeast Power Coordinating Council (NPCC), Reliability First Corporation (RFC), SERC Reliability Corporation (SERC), Southwest Power Pool, RE (SPP), Texas Reliability Entity (TRE), and Western Electricity Coordinating Council (WECC). The electricity generated in one region is primarily supplied to energy consumers in the same region; the inter-region electricity trade is small and limited by the available transmission lines (North American Electric Reliability Corporation n.d.). NERC publishes a Summer Reliability Assessment for each assessment area annually, which provides the estimated summer electricity demand, generation capacity, and reserve margin. The reserve margin is defined as the difference between generation capacity and electricity demand, divided by the electricity demand. NERC recommends a 15% reserve margin to maintain electricity system reliability. In the 2008-2010 assessment reports, each assessment area belongs to one NERC region.

Starting in 2011, the assessment areas were redistricted, with some assessment areas overlapping multiple NERC regions. This makes it impossible to attribute each assessment area to one NERC region and calculate the NERC level reserve margin. As a result, we only use the 2008-2010 assessment reports to calculate the average electricity demand, generation capacity, and reserve margin for each NERC region in the current period. In future periods, because electricity demand is estimated at the state level and state boundaries do not coincide with the NERC boundaries, we downscale the state-level electricity demand to the county level by population and assign each county a NERC region. Most counties are assigned NERC regions based on the Emissions & Generation Resource Integrated Database (eGRID) (U.S. Environmental Protection Agency n.d.). If a county is missing from eGRID, it is assigned to the NERC region according to the affiliation of its closest neighbors (majority affiliation). We have compared the results achieved from choosing a different number of neighbors in this calculation (e.g., 1, 3, 5, and 7), and the NERC borders are most well-defined and reasonable when three neighbors are used. The county level summer electricity demand is then aggregated to the NERC level in order to calculate the reserve margin for each NERC region in future periods. The future energy demand and reserve margin are further used to calculate the additional generation capacity needed to satisfy the 15% research margin requirement.

The Levelized Cost Of Electricity (LCOE) is usually used to estimate the per unit cost ($/MWh) of constructing and operating a new powerplant during its whole life cycle (U.S. Energy Information Administration n.d.). LCOE consists of fixed costs (including capital cost, fixed operation & management cost, transmission investment, and subsidy), and

variable operation & management (VOM) costs that depend on electricity generation. The cost for building and operating additional capacities is calculated as follows:

$$TC = FC \times GC \times 8760 \times CF + VC \times GC \times OH \quad (2)$$

where *GC* represents the additional generation capacity (MW) required, *FC* represents the per unit fixed cost ($/MWh), *VC* represents the per unit VOM cost ($/MWh), *CF* represents the capacity factor (%), *OH* represents the operational hours, and *TC* is the annual total cost ($).

Because population is used to weight energy consumption difference, the sensitivity of cost and reserve margin changes to population is also evaluated using the 2090 population extracted from the Integrated Climate and Land Use Scenarios (ICLUS) dataset (U.S. Environmental Protection Agency 2010). In order to exclude the pure effect of population size change, the 2090 national population is hold at the 2010 level. As a result, only the change of population distribution is considered for the sensitivity analysis.

5.3 Results and Discussion

5.3.1 Impact on energy consumers

The spatiotemporal changes in building energy demand have important financial and strategic implications for building energy consumers. In 2080-99, all else being equal, the residential and commercial sectors in the warmer states would see increases in annual energy costs. For example, using current consumer energy prices, the annual building energy costs would increase $2.7 billion ($1.6 billion increase in the residential sector and $1.1 billion increase in the commercial sector) in Florida. By contrast, consumers in colder states would see energy cost declines. For example, the state of Pennsylvania

would see a savings of $1.4 billion ($1.1 billion savings in the residential sector and $284 million savings in the commercial sectors) in annual building energy costs. For the US economy as a whole, the residential sector would experience a net energy savings of $6.9 billion/year while the commercial building sector would see energy costs rise $2.1 billion/year. Across the two sectors this would amount to a net savings of $4.7 billion/year.

The residential energy cost difference can be represented at the mean household level within each state. Figure 5.1 shows the annual state mean residential household energy cost difference change between the 2080-2099 time period and the current time period. The consumers in the warmer states would see an energy cost increase, while the consumers in the colder states would see an energy cost decline (Figure 5.1). The annual household energy cost differences range from -$340/household (savings) in Vermont to +$231/household in Florida (cost increase).

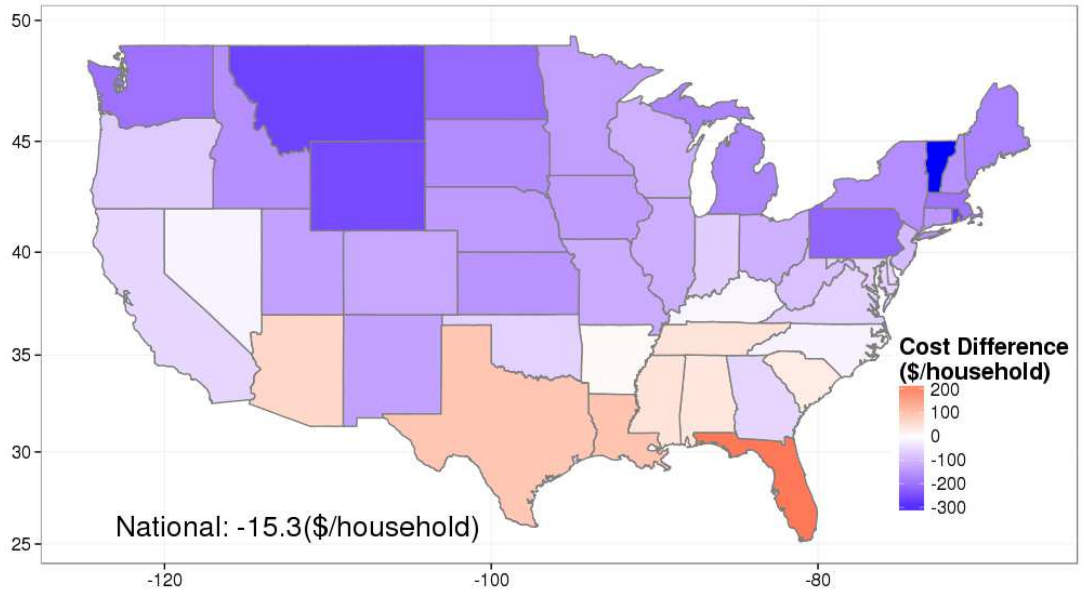

Figure 5.1 Annual state mean residential household energy cost difference (USD/household) between the 2080-99 time period and 2008-2012.

Figure 5.2 shows the price ratios of electricity/non-electric fuels for each state. In the colder states, the ratio of electricity to non-electric fuel price is typically large, but the total site energy change is dominated by the decline in non-electric fuel needs. As a result, the greater electricity price is more than offset by the non-electric fuel demand decline, resulting in net savings. In the warmer states, the ratio of electricity to non-electric fuel price is usually small (Figure 5.2). Although these states show greater increases in electricity demand, the low price ratios mean that the increased electricity cost does not overwhelm the non-electric fuel savings. The high price ratios of electricity/non-electric fuels in the colder states and the low price ratios in warmer states result in a net savings for the whole US. Because the price ratio in the commercial sector is usually larger than the residential sector, and commercial buildings typically use less non-electric fuel for heating after business hours, there is a net increase in commercial sector building energy cost but a net savings in the residential sector building energy cost when integrated across the United States.

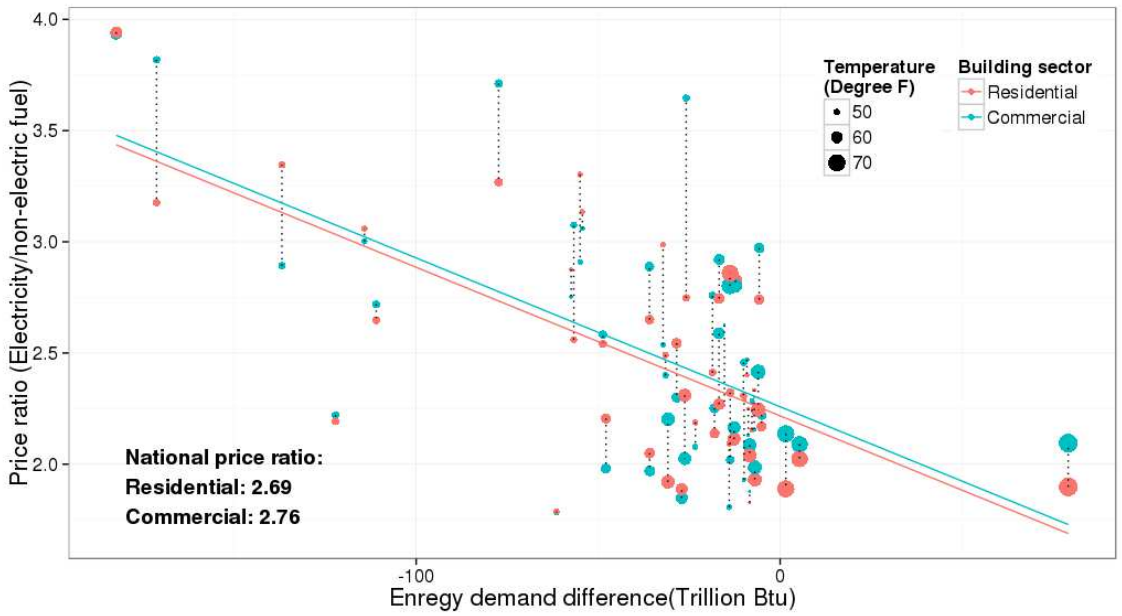

Figure 5.2 Relationship between the price ratio (Electricity price/non-electric fuel price) and the site energy difference (2080-99 minus 2008-2012). Point size represents the annual average temperature in 2008-2012. Each pair represents one state. The national price ratio is the mean value of all states weighted by state population.

5.3.2 Impacts on energy suppliers

Energy supply capacity must also consider the physical and financial implications of altered future building energy needs in spatiotemporal detail. In the current period (2008-2012), all NERC regions have enough (>15%) reserve margins to maintain the reliability of electricity supply during summer (Figure 5.3). The current reserve margins range from 16.7% in TRE to 26.2% in WECC, with reserve margins in most NERC regions greater than 20%.

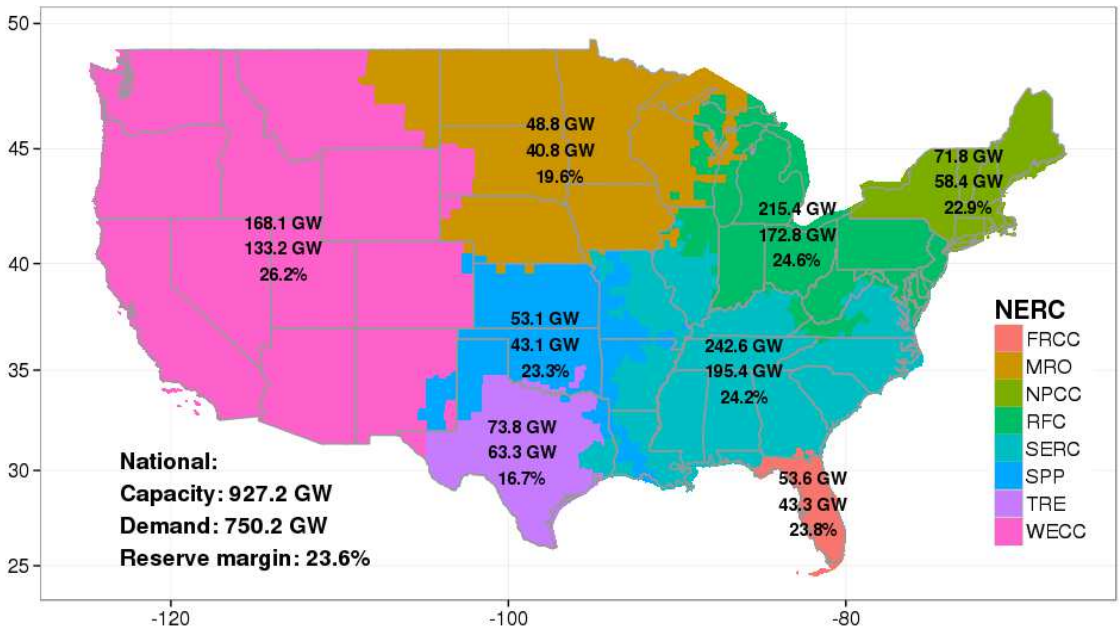

Figure 5.3 NERC region electricity generation capacity, electricity demand, and reserve margin during the 2008-12 summer. The top, middle, and bottom numbers in each NERC region represent generation capacity (GW), electricity demand (GW), and reserve margin (%), respectively.

Under the estimated building electricity demand increases, summer regional reserve margins fall below 15% in different future time periods for different NERC regions (Table 5.2), with the NPCC passing this threshold first (2020-39). By the end of this century, the reserve margins in all of the eight NERC regions fall below 10% during the summer season, with the smallest (-2.9%) reserve margin in NPCC. For the US as a whole, the reserve margin passes the 15% threshold in 2060-79, and it reaches 5.9% by the end of this century. In order to maintain the 15% reserve margin, 80.6 GW of additional capacity would be needed for the whole US in the period of 2080-99, with the greatest capacity need in the RFC region (23.2GW).

Table 5.2 Electricity supply capacity reserve margin (%) in future periods, and additional capacity (GW, within parenthesis) required to meet the 15% requirement.

NERC	2020-39	2040-59	2060-79	2080-99
FRCC	22.1	17	11(1.9)	5.1(5.1)
MRO	16.5	12.5(1.1)	8.6(2.9)	5(4.6)
NPCC	13.9(0.7)	8.1(4.6)	2.1(9.1)	-2.9(13.2)
RFC	18.9	13.7(2.5)	8.5(12.9)	3.8(23.2)
SERC	22.5	18	13.1(4.1)	7.8(16.1)
SPP	23.1	19.1	14.6(0.2)	9.6(2.6)
TRE	17.9	13.8(0.8)	9.5(3.7)	4.3(7.6)
WECC	23.4	18.8	14.3(1.1)	9.6(8.2)
US Total	20.5(0.7)	15.7(9)	10.8(35.9)	5.9(80.6)

The Levelized Cost of Electricity (LCOE) is used to estimate the cost of building and operating additional US electricity grid capacity. Using contemporary estimates of the LCOE, an additional capacity of 80.6 GW would constitute a fixed cost ranging from 7.1 billion $/year to 65.3 billion $/year (Table 5.3). If this new capacity is used for electricity generation during the summer and VOM cost is considered for those times, the total cost would range from 19.2 billion $/year to 72.1 billion$/year. Natural gas-fired powerplants (e.g., conventional combined cycle, advanced combined cycle, and advanced combustion turbine) are the most plausible plant types to satisfy the increased summer electricity demand, given that they are reliable, consistent, and can be operated at relatively low cost. Although some non-dispatchable plant types (e.g., wind and solar photovoltaic) also show low total costs, their energy sources are intermittent and it is less likely that these technologies will be used to supply electricity during the peak summer season. Even with the cheapest option ($19.2 billion), the estimated annual cost of adding and operating 80.6 GW of electricity capacity is substantially higher than the annual consumer savings

noted above. Hence, it is possible that the ultimate cost of building additional powerplants may be passed to electricity consumers. As a result, some states for which the net building energy demand changes resulted in savings, may end up with a net cost increase after accounting for the cost of adding capacity. The estimation of how energy supply and new facility costs are passed to consumers could be achieved with more sophisticated economic supply/demand modeling but that was considered beyond the scope of this study.

Table 5.3 The Levelized Cost Of Electricity (LCOE) for new electricity generation capacity in the US (2012 $/MWh) (U.S. Energy Information Administration).

Plant type[1]	Capacity factor (%)	Fixed cost ($/MWh)	VOM cost ($/MWh)	Fixed cost for 80.6 GW (billion $/year)	Total cost for 80.6 GW[2] (billion $/year)
Dispatchable					
Conventional Coal	85	65.4	30.3	39.2	44.6
IGCC	85	84.2	31.7	50.5	56.1
IGCC with CCS	85	108.8	38.6	65.3	72.1
Natural Gas-Fired					
Conventional CC	87	17.2	49.1	10.6	19.2
Advanced CC	87	18.9	45.5	11.6	19.6
Advanced CC with CCS	87	35.7	55.6	21.9	31.7
Conventional CT	30	46.4	82	9.8	24.3
Advanced CT	30	33.4	70.3	7.1	19.5
Advanced Nuclear	90	74.3	11.8	47.2	49.3
Geothermal	92	44.4	0	28.8	28.8
Biomass	83	63.1	39.5	37.0	44.0
Non-dispatchable					
Wind	35	80.3	0	19.8	19.8
Wind-Offshore	37	204	0	53.3	53.3
Solar PV	25	118.5	0	20.9	20.9
Solar Thermal	20	223.6	0	31.6	31.6
Hydro	53	78.1	6.4	29.2	30.4

[1] Abbreviation for plant type: CC—Combined Cycle, IGCC—Integrated Coal-Gasification Combined Cycle, CCS—Carbon Control and Sequence, CT—Combustion Turbine

[2] Total cost assumes that the 80.6 GW capacity is used for generation during the summer only (*OH* = 2190 hours)

5.3.3 sensitivity to population distribution

There is a general trend of population shifting from the inland and colder areas to the costal and warmer areas by the end of this century (U.S. Environmental Protection Agency 2010). This spatial pattern of population redistribution lessens the impacts of climate change in the colder areas, while exacerbates the impacts in the warmer areas. Based on the 2090 population distribution, the estimated cost changes are higher in most states compared to the results based on the 2010 population distribution (Figure 5.4.a). For example, the cost change is increased from +$2.7 billion to +$3.9 billion in Florida, resulting in an extra of $1.2 billion cost change based on 2090 population distribution. As a result of the higher changes in most state, the national savings is reduced by $3.4 billion (from -$4.7 to -$1.3 billion) based on the 2090 population distribution.

The reserve margins also vary due to the change of population distribution. Generally, the reserve margins in the southern and western regions are further reduced due to the increased population, while the reserve margins in the northern regions are increased due to the decreased population. Compared to the results based on 2010 population, the reserve margin based on 2090 population is reduced by 7 percentage points (pp) in FRCC, while it is increased by 3.8 pp in MRO. At the national level, these large changes cancel each other, resulting in slightly larger reserve margin based on the 2090 population.

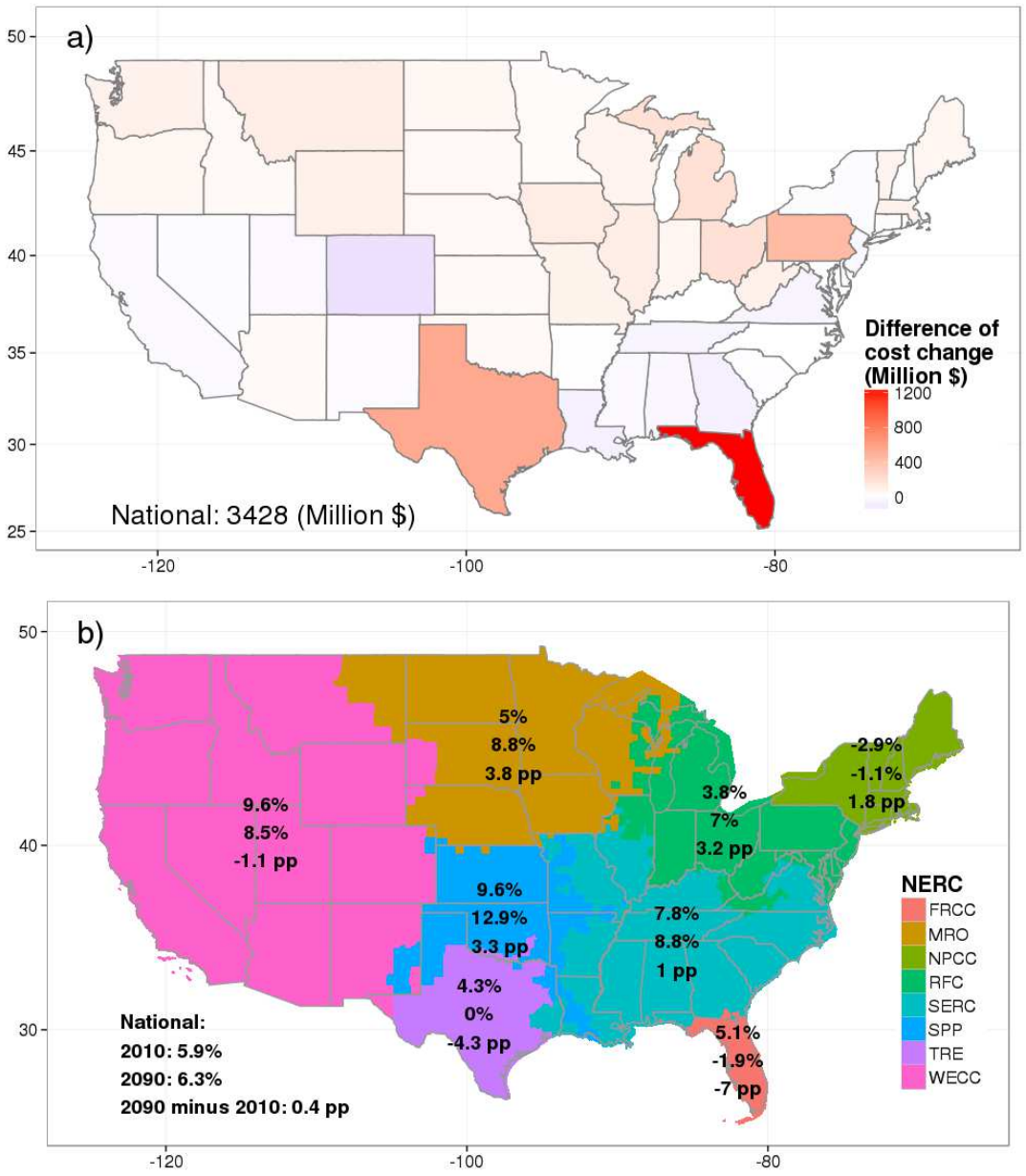

Figure 5.4 Sensitivity of consumer costs and reserve margins to population distribution in 2080-99 time period. a) shows the difference of cost changes, and b) shows the difference of reserve margins between the results based on 2090 and 2010 population. The top, middle, and bottom numbers in b) represent the reserve margin (%) based on 2010 population, the reserve margin (%) based on 2090 population, and their difference (2090 minus 2010, with the unit of percentage point (pp)).

5.4 Conclusions

Based on the state-level monthly energy demand changes, we evaluate the implications of climate change to energy consumers and suppliers. We found increased energy costs in warmer states and decreased energy costs in colder states. The residential sector sees a savings about $7 billion/year for the whole US, while the commercial sector sees a net increase of $2.2 billion/year. At the average household level, changes in annual residential energy cost range from -$340/household in Vermont to +$231/household in Florida.

To meet the increased electricity demand needed in summer while simultaneously maintaining safe reserve margins, utilities will need to add capacity. In order to meet the 15% reserve margin requirement, 80.6 GW capacity is needed for the whole US, which amounts to $19.2– $72.1 billion/year to build and operate this additional capacity. Were these costs passed to consumers, the net savings found in some states due to lowered heating needs, might be overcome by electricity cost increases.

If the change of population distribution is accounted for, the impacts are further exacerbated in the warmer region, while they are diminished in the colder areas. For example, the estimated change of annual building energy cost in Florida increases from +$2.7 billion (based on 2010 population) to +$3.9 billion (based on 2090 population), and the reserve margin further reduces from 5.1% to -1.9% corresponding.

The estimated cost differences for consumers and suppliers explored here can provide insight into a number of challenges associated with quantifying and prioritizing climate policy. For example, the impact of climate change on building energy supply and demand at these space/time scales can provide a more accurate estimate of impacts in calculations

of the climate change damages and social cost of carbon (Tol 2005). These costs, when combined with the analysis of climate change mitigation, can be further used to optimize the cost-benefit analysis and the pricing of carbon taxes (Roughgarden & Schneider 1999). Furthermore, the information presented here could also offer a prioritization of climate change mitigation that is sensitive to varying costs and savings across the US landscape.

Similar to some other researches (Tol 2005), the work presented here is based on the current society structure (e.g., population, economics, and policy). Although the framework used here is not flexible enough to account for the impacts of other factors such as policy and technology, it is useful to separate the pure effect of climate change and evaluate the cost of it. Hence, this work should be viewed as a sensitivity study focusing on *ceteris paribus* analysis. Finally, given the complex relationship between energy consumers and suppliers, further research is required to better understand how the energy suppliers will pass the extra cost to consumers, and how consumer behavior will change in response to higher cost.

5.5 Acknowledgements

We would like to thank the National Science Foundation CAREER award 0846358, the Department of Energy grant #DE-SC0006105 and Amazon cloud computing resources provided by Amazon Climate Research Grant Program.

CHAPTER 6

6 CONCLUSION

6.1 Summary of Research Findings

In this dissertation, I estimate the impact of climate change on US building energy consumption, and quantify the financial implications to energy users and suppliers. In particular, I focus on both the long-term mean changes and the change in extreme events in the future. I also test the sensitivity of these estimated impacts against a number of aspects of the climate change/building energy relationship that were not comprehensively explored, for example, the spatial and temporal scales, the balance point temperature, building type, and population distribution.

In chapter 2, I quantify the impact of climate change on long-term annual/monthly building energy consumption, and test the sensitivity of this impact to three elements of the analysis. First, I test the sensitivity of climate change impact to the space and time resolution. I show that there are large (up to +50% or -48%) building energy demand changes at the state spatial scale and the monthly/seasonal time scales which are masked by analysis at the national/annual scales. Second, I examine the sensitivity of the future impact to the balance point temperature methodology. I find that the use of a fixed 65 °F balance point temperature versus a state-specific value leads to an overestimate of the energy consumption changes in most states by about 2 percentage points. . Finally, I test the impact to population spatial distribution, finding that commonly-used projections of the population spatial distribution, when combined with modeled spatial projections of temperature, exacerbate the building energy demand increase in warmer states (e.g., enhancing the increase in Florida by 5.3 percentage points), while lessening the decreases

in colder states (e.g., reducing the decrease in Wyoming by 8.2 percentage points). As a result, the national total source energy consumption changes from a net decrease (less energy needed) without the incorporation of changing population/climate distribution to a net increase (more energy needed) when t these spatial changes are included.

In chapter 3, I develop a model that links electricity demand to temperature for the whole United States. Based on this model, I estimate the impact of more frequent and intense extreme climate change events (heat waves) on building electricity demand, finding that the most extreme electricity demand events (1-per-56 years) experienced in the last half-century (1-per-56 years) will increase 2600-fold, while the occurrence of the once per year extreme events increases more than 70 fold in the 2044-2099 time period under the RCP 8.5 scenario. In addition to the greater frequency of large electricity demand events, the extreme electricity demand events are more intense, increasing about 25% for different event frequency (ranging from 1-per-56-year to 1-per-year) by the end of this century. If the changes in population and AC saturation are also accounted for, the impact of climate change on building energy demand will be exacerbated. For example, the projected changes in population will increase the likelihood of the 1-per-56-year electricity demand by more than 1000 folds, while the AC saturation level change will increase the likelihood by 20 times around 2050 (2022-2077). By isolating the changes in temperature at the annual/monthly timescale from those in the sub-monthly domain, I find that the impact of sub-monthly temperature changes is small relative to the impact of the monthly/annual changes.

In chapter 4, I estimate the impact of climate change on the energy consumption of different building types at more than 900 U.S. locations, and explore the variations of these impacts at different spatial and temporal scales. I find a small national/annual energy consumption increase for residential building types, but a larger increase (up to 8%) for commercial building types by the decade of the 2090s. When examined at the monthly scale for sub-sectoral building type, I find the national energy consumption increases up to 39% in August for the *secondary school* building type, while *warehouse* building types show a decline up to 22% in January. At the hourly scale the variations are larger, with the *warehouse* building type exhibiting increases up to 110% at 5-6 pm in Summer. Similar variations are also found within and between building types, when impact is examined at sub-national spatial scales. At the climate zone scale, the RD value increases up to 21 % in the *secondary school* building type (climate zone 1A), while it decreases up to 17% in the *warehouse* building type (climate zone 7A). Larger variations are found across building types at the local scale, ranging from -20% to 24%. The clustering analysis suggests that large energy consumption changes are mainly clustered in areas with warm-humid (Southeast) climates. The variation of current CDD/HDD in different climate zones is the major driver of the spatial variation in energy consumption changes between climate zones, while the variation of local-scale temperature change is strongly related to the variation of local-scale energy consumption change within each climate zone.

In chapter 5, I evaluate the financial implications of climate change to energy consumers and suppliers based on the state-level monthly energy demand changes estimated in chapter 2. The residential sector sees a savings about $7 billion/year for the whole US,

while the commercial sector sees a net increase of $2.2 billion/year. At the average household level, changes in annual residential energy cost range from -$340/household in Vermont to +$231/household in Florida. To meet the increased electricity demand needed in summer while simultaneously maintaining safe reserve margins, utilities will need to add capacity. In order to meet the 15% reserve margin requirement, 80.6 GW capacity is needed for the whole US, which amounts to $19.2– $72.1 billion/year to build and operate this additional capacity. Were these costs passed to consumers, the net savings found in some states due to lowered heating needs, might be overcome by electricity cost increases. If the change of population distribution is accounted for, the impacts are further exacerbated in the warmer region, while they are diminished in the colder areas. For example, the estimated change of annual building energy cost in Florida increases from +$2.7 billion (based on 2010 population) to +$3.9 billion (based on 2090 population), and the reserve margin further reduces from 5.1% to -1.9% corresponding.

6.2 Limitations and Future Research

This research is a significant advance in studying the impact of climate change on building energy consumption, and it will provide useful information for policy makers, building designers, and scientists. However, it is important to note that, there are some limitations with this research, which may need further improvement.

Firstly, I only estimate the impacts of temperature change on building energy demands. In addition to temperature change, climate change consists of changes in other variables such as humidity and radiation. The changes in these variables, can affect the heat balance in buildings, which will further impact the space cooling/heating and energy

demands in buildings. Secondarily, the building technology is kept unchanged in the future due to the lack of available data. The potential improvements in future building technology, for example, more efficient HVAC system, and well-insulated walls and windows, can help to cut down space cooling and mitigate the impacts caused by higher temperature. Finally, building energy consumption is affected by a lot of other factors such as economy and policy, which are not considered in this research. These factors will not only affect building energy consumption, but also affect the projected temperature change through the impacts on anthropogenic greenhouse gas emission.

Based on the results in this research, there are also so interesting topics that worth further exploration. For example, with the advent of policy occurring at sub-national scales, such as the Clean Power Plan recently enacted in the US, the state-level climate change impacts estimated in this research may be used to quantify the state-specific goals of CO2 reduction. With the location-level spatio-temporal energy consumption changes estimated for different building types in this research, potential mitigation/adaptation strategies specific to the particularly vulnerable building types (e.g., restaurants) at the most vulnerable times of the year could be explored. The estimated changes in frequency and intensity of extreme electricity demands can probably be linked to the damage cost due to electricity scarcity and breakout. Finally, the financial costs of climate change can be further used to calculate the social cost of carbon and the pricing of carbon tax.

REFERENCES

Anselin, L., 1995. Local indicators of spatial association-LISA. *Geographical analysis*, 27(2), pp.93–115.

Baechler, M.C. et al., 2010. *High-performance home technologies: guide to determining climate regions by county*, Pacific Northwest National Laboratory.

Baumert, K. & Selman, M., 2003. Heating and cooling degree days. *World resources institute*.

Brekke, L. et al., 2013. Downscaled CMIP3 and CMIP5 climate projections: Release of downscaled CMIP5 climate projections, comparison with preceding information, and summary of user needs. *Prepared for archive at http://gdo-dcp-ucllnl. org/downscaled_cmip_projections/. Denver, CO: US Department of the Interior, Bureau of Reclamation*.

Burnham, K.P. & Anderson, D.R., 2004. Multimodel inference understanding AIC and BIC in model selection. *Sociological methods & research*, 33(2), pp.261–304.

Council, N.A.E.R., 2002. 1996 System Disturbances: Review of Selected 1996 Electric System Disturbances in North America.

Crawley, D.B. et al., 2001. EnergyPlus: creating a new-generation building energy simulation program. *Energy and buildings*, 33(4), pp.319–331.

De Dear, R. & Brager, G.S., 2001. The adaptive model of thermal comfort and energy conservation in the built environment. *International journal of biometeorology*, 45(2), pp.100–8. Available at: http://www.ncbi.nlm.nih.gov/pubmed/11513046.

Deru, M. et al., 2011. US Department of Energy commercial reference building models of the national building stock.

Deru, M. & Torcellini, P., 2007. Source Energy and Emission Factors for Energy Use in Buildings Source Energy and Emission Factors for Energy Use in Buildings.

Dirks, J.A. et al., 2015. Impacts of climate change on energy consumption and peak demand in buildings: A detailed regional approach. *Energy*, 79, pp.20–32. Available at: http://linkinghub.elsevier.com/retrieve/pii/S0360544214010469 [Accessed April 8, 2015].

DoE, U.S., 2012. Buildings energy databook. *Energy Efficiency & Renewable Energy Department*.

Douglas, J., 2000. Power for a digital society. *EPRI Journal*, 25(4), pp.18–25.

Edenhofer, O., 2014. *2014: Buildings. In: Climate Change 2014: Mitigation of Climate Change. Contribution of Working Group III to the Fifth Assessment Report of the Intergovernmental Panel on Climate Change*, Available at: http://scholar.google.com/scholar?hl=en&btnG=Search&q=intitle:Climate+change+2014:+Mitigation+of+climate+change.+Working+group+III+contribution+to+the+fifth+assessment+report+of+the+IPCC#0 [Accessed June 2, 2015].

Edenhofer, O. et al., 2014. Climate change 2014: mitigation of climate change. *Contribution of Working Group III to the Fifth Assessment Report of the Intergovernmental Panel on Climate Change*, pp.511–597.

Energy Star, 2011. ENERGY STAR Performance Ratings Methodology for Incorporating Source Energy Use.

Franco, G. & Sanstad, A.H., 2007. Climate change and electricity demand in California. *Climatic Change*, 87(S1), pp.139–151. Available at: http://www.springerlink.com/index/10.1007/s10584-007-9364-y [Accessed July 20, 2012].

Gaffen, D.J. & Ross, R.J., 1999. Climatology and Trends of U . S . Surface Humidity and Temperature. *Journal of Climate*.

Georgescu, M. et al., 2012. Summer-time climate impacts of projected megapolitan expansion in Arizona. *Nature Climate Change*, 3(1), pp.37–41. Available at: http://www.nature.com/doifinder/10.1038/nclimate1656 [Accessed November 19, 2013].

Georgescu, M. et al., 2014. Urban adaptation can roll back warming of emerging megapolitan regions. *Proceedings of the National Academy of Sciences of the United States of America*, (14), pp.1–6. Available at: http://www.ncbi.nlm.nih.gov/pubmed/24516126 [Accessed February 25, 2014].

Hadley, S.W. et al., 2006. Responses of energy use to climate change: A climate modeling study. *Geophysical research letters*, 33(17).

Hadley, S.W. et al., 2006. Responses of energy use to climate change: A climate modeling study. *Geophysical Research Letters*, 33(17), pp.2–5. Available at: http://www.agu.org/pubs/crossref/2006/2006GL026652.shtml [Accessed October 4, 2012].

Hamlet, A.F. et al., 2010. Effects of projected climate change on energy supply and demand in the Pacific Northwest and Washington State. *Climatic Change*, 102(1-2), pp.103–128.

Hamlet, A.F. et al., 2010. Effects of projected climate change on energy supply and demand in the Pacific Northwest and Washington State. *Climatic Change*, 102(1-2), pp.103–128. Available at: http://link.springer.com/10.1007/s10584-010-9857-y [Accessed April 21, 2013].

Hong, T., Chang, W.K. & Lin, H.W., 2013. A fresh look at weather impact on peak electricity demand and energy use of buildings using 30-year actual weather data. *Applied Energy*, 111, pp.333–350. Available at: http://dx.doi.org/10.1016/j.apenergy.2013.05.019.

Huang, J., 2006. The impact of climate change on the energy use of the US residential and commercial building sectors. *LBNL*.

Huang, J. & Gurney, K.R., 2015. The hidden spatiotemporal vulnerability of US building energy demand to climate change. *Environmental science & technology*.

Huang, Y.J., 2006. The impact of climate change on the energy use of the US residential and commercial building sectors. *Lawrence Berkeley National Laboratory, Report No. LBNL-60754*.

Isaac, M. & Van Vuuren, D.P., 2009. Modeling global residential sector energy demand for heating and air conditioning in the context of climate change. *Energy Policy*, 37(2), pp.507–521.

Jaglom, W.S. et al., 2014. Assessment of projected temperature impacts from climate change on the U.S. electric power sector using the Integrated Planning Model®. *Energy Policy*, 73, pp.524–539. Available at: http://dx.doi.org/10.1016/j.enpol.2014.04.032.

Jones, B. et al., 2015. Future population exposure to US heat extremes. *Nature Climate Change*, (May), pp.1–5. Available at: http://www.nature.com/doifinder/10.1038/nclimate2631.

Karl, T.R., 2009. *Global climate change impacts in the United States*, Cambridge University Press.

Kelso, J., 2012a. *2011 Buildings Energy Data Book*, Available at: http://scholar.google.com/scholar?hl=en&btnG=Search&q=intitle:2011+Buildings+Energy+Data+Book#2 [Accessed June 2, 2015].

Kelso, J., 2012b. 2011 Buildings Energy Data Book. *Department of Energy*.

Linder, K.P. & Inglis, M.R., 1989. The potential impact of climate change on electric utilities, regional and national estimates. *US Environmental Protection Agency, Washington, DC*.

Mansur, E.T., Mendelsohn, R. & Morrison, W., 2008. Climate change adaptation: A study of fuel choice and consumption in the US energy sector. *Journal of Environmental Economics and Management*, 55(2), pp.175–193.

Mazzei, P., Minichiello, F. & Palma, D., 2005. HVAC dehumidification systems for thermal comfort: A critical review. *Applied Thermal Engineering*, 25(5-6), pp.677–707.

McFarland, J. et al., 2015. Impacts of rising air temperatures and emissions mitigation on electricity demand and supply in the United States: a multi-model comparison. *Climatic Change*, pp.111–125. Available at: http://link.springer.com/10.1007/s10584-015-1380-8.

McNeil, M.A. & Letschert, V.E., 2008. Future air conditioning energy consumption in developing countries and what can be done about it: the potential of efficiency in the residential sector. *Lawrence Berkeley National Laboratory*.

Meehl, G. a & Tebaldi, C., 2004. More intense, more frequent, and longer lasting heat waves in the 21st century. *Science*, 305(5686), pp.994–997.

Mendelsohn, R. et al., 2000. Country-specific market impacts of climate change. *Climatic change*, 45(3-4), pp.553–569.

Mendon, V. V, Lucas, R.G. & Goel, S., 2013. *Cost-Effectiveness Analysis of the 2009 and 2012 IECC Residential Provisions: Technical Support Document*, Pacific Northwest National Laboratory.

Miller, N.L. et al., 2008. Climate, Extreme Heat, and Electricity Demand in California. *Journal of Applied Meteorology and Climatology*, 47(6), pp.1834–1844. Available at: http://journals.ametsoc.org/doi/abs/10.1175/2007JAMC1480.1 [Accessed May 19, 2015].

Muggeo, V.M.R., 2008. segmented : An R Package to Fit Regression Models with Broken-Line Relationships. , 8(May), pp.20–25.

Nakicenovic, N. & Swart, R., 2000. Special report on emissions scenarios. *Special Report on Emissions Scenarios, Edited by Nebojsa Nakicenovic and Robert Swart, pp. 612. ISBN 0521804930. Cambridge, UK: Cambridge University Press, July 2000.*, 1.

National Center for Environmental Prediction, 2014. National Center for Environmental Prediction's (NCEP) North American Regional Reanalysis (NARR) dataset.

National Oceanic and Atmospheric Administration, Average Mean Temperature Index by Month. National Oceanic and Atmospheric Administration. Available at: http://www.esrl.noaa.gov/psd/data/usclimdivs/tmp.state.19712000.climo.

De Nooij, M., Koopmans, C. & Bijvoet, C., 2007. The value of supply security: The costs of power interruptions: Economic input for damage reduction and investment in networks. *Energy Economics*, 29(2), pp.277–295.

North American Electric Reliability Corporation, 2008-2012, *Summer Reliability Assessment*

Pardo, A., Meneu, V. & Valor, E., 2002. Temperature and seasonality influences on Spanish electricity load. *Energy Economics*, 24(1), pp.55–70. Available at: http://linkinghub.elsevier.com/retrieve/pii/S0140988301000822.

Pendleton, L., Karl, T.R. & Mills, E., 2013. Economic growth in the face of weather and climate extremes: A call for better data. *Eos, Transactions American Geophysical Union*, 94(25), pp.225–226.

Rosenthal, D.H., Gruenspecht, H.K. & Moran, E.A., 1995. Effects of global warming on energy use for space heating and cooling in the United States. *The Energy Journal*, pp.77–96.

Roughgarden, T. & Schneider, S.H., 1999. Climate change policy: Quantifying uncertainties for damages and optimal carbon taxes. *Energy Policy*, 27(7), pp.415–429.

Ruth, M. & Lin, A.-C., 2006a. Regional energy demand and adaptations to climate change: methodology and application to the state of Maryland, USA. *Energy policy*, 34(17), pp.2820–2833.

Ruth, M. & Lin, A.-C., 2006b. Regional energy demand and adaptations to climate change: Methodology and application to the state of Maryland, USA. *Energy Policy*, 34(17), pp.2820–2833. Available at: http://linkinghub.elsevier.com/retrieve/pii/S0301421505001175 [Accessed August 15, 2011].

Sailor, D.J., 2003. Air conditioning market saturation and long-term response of residential cooling energy demand to climate change. *Energy*, 28(9), pp.941–951. Available at: http://linkinghub.elsevier.com/retrieve/pii/S0360544203000331 [Accessed July 20, 2011].

Sailor, D.J., 2001a. Relating residential and commercial sector electricity loads to climate—evaluating state level sensitivities and vulnerabilities. *Energy*, 26(7), pp.645–657.

Sailor, D.J., 2001b. Relating residential and commercial sector electricity loads to climate—evaluating state level sensitivities and vulnerabilities. *Energy*, 26(7), pp.645–657. Available at: http://linkinghub.elsevier.com/retrieve/pii/S0360544201000238.

Sailor, D.J. & Muñoz, J.R., 1997. Sensitivity of electricity and natural gas consumption to climate in the U.S.A. - Methodology and results for eight states. *Energy*, 22(10), pp.987–998.

Sailor, D.J. & Muñoz, J.R., 1997. Sensitivity of electricity and natural gas consumption to climate in the USA—methodology and results for eight states. *Energy*, 22(10), pp.987–998.

Sailor, D.J. & Pavlova, A.A., 2003. Air conditioning market saturation and long-term response of residential cooling energy demand to climate change. *Energy*, 28(9), pp.941–951.

Sailor, D.J., Rosen, J.N. & Muñoz, J.R., 1998a. Natural gas consumption and climate: a comprehensive set of predictive state-level models for the United States. *Energy*, 39(4), p.265. Available at: http://linkinghub.elsevier.com/retrieve/pii/S0140670198963895.

Sailor, D.J., Rosen, J.N. & Muñoz, J.R., 1998b. Natural gas consumption and climate: a comprehensive set of predictive state-level models for the United States. *Energy*, 23(2), pp.91–103.

Sailor, D.J., Rosen, J.N. & Muñoz, J.R., 1998c. Natural gas consumption and climate: a comprehensive set of predictive state-level models for the United States. *Fuel and Energy Abstracts*, 39(4), p.265. Available at: http://linkinghub.elsevier.com/retrieve/pii/S0140670198963895.

Salagnac, J.-L., 2007. Lessons from the 2003 heat wave: a French perspective. *Building Research & Information*, 35(4), pp.450–457.

Sathaye, J. a. et al., 2013. Estimating impacts of warming temperatures on California's electricity system. *Global Environmental Change*, 23, pp.499–511. Available at: http://linkinghub.elsevier.com/retrieve/pii/S0959378012001458 [Accessed February 28, 2013].

Scott, M.J., Wrench, L.E. & Hadley, D.L., 1994. Effects of climate change on commercial building energy demand. *Energy sources*, 16(3), pp.317–332.

Smeds, J. & Wall, M., 2007. Enhanced energy conservation in houses through high performance design. *Energy and Buildings*, 39(3), pp.273–278.

Solomon, S., 2007. *Climate change 2007-the physical science basis: Working group I contribution to the fourth assessment report of the IPCC*, Cambridge University Press.

Star, E., 2009. Energy star performance ratings methodology for incorporating source energy use. *Understanding Source and Site Energy. Environmental Protection Agency. Date Accessed*, 12(6), p.9.

Swan, L.G. & Ugursal, V.I., 2009. Modeling of end-use energy consumption in the residential sector: A review of modeling techniques. *Renewable and sustainable energy reviews*, 13(8), pp.1819–1835.

Swan, L.G. & Ugursal, V.I., 2009. Modeling of end-use energy consumption in the residential sector: A review of modeling techniques. *Renewable and Sustainable Energy Reviews*, 13(8), pp.1819–1835. Available at: http://linkinghub.elsevier.com/retrieve/pii/S1364032108001949 [Accessed March 4, 2013].

The World Climate Research Programme, 2014. The World Climate Research Programme's (WCRP's) Coupled Model Intercomparison Project phase 3 (CMIP3) multi-model dataset. Available at http://gdo-dcp.ucllnl.org/downscaled_cmip_projections/.

The World Climate Research Programme, The World Climate Research Programme's (WCRP's) Coupled Model Intercomparison Project phase 3 (CMIP3) multi-model dataset. Available at http://gdo-dcp.ucllnl.org/downscaled_cmip_projections/.

Tol, R.S.J., 2005. The marginal damage costs of carbon dioxide emissions: an assessment of the uncertainties. *Energy policy*, 33(16), pp.2064–2074.

U.S. Census Bureau, 2008-2012 American Community Survey 5-year estimates. Available at: http://www.census.gov/acs/www/data_documentation/2012_release/.

U.S. Census Bureau, 2010 U.S. Census 2010 population. Available at: http://www.census.gov/

U.S. Department of Energy, Commercial Buildings Energy Consumption Survey (CBECS). Energy Information Administration, US Department of Energy. Available at: http://www.eia.gov/consumption/commercial/.

U.S. Department of Energy, 2003. Commercial Buildings Energy Consumption Survey (CBECS). Energy Information Administration, US Department of Energy. Available at: http://www.eia.gov/consumption/commercial/.

U.S. Department of Energy, 2014. Natural Gas Consumption by End Use, Natural Gas Monthly. , p.http://www.eia.gov/naturalgas/.

U.S. Department of Energy, 2009. Residential Energy Consumption Survey (RECS). Available at: http://www.eia.gov/consumption/residential/.

U.S. Department of Energy, Residential Energy Consumption Survey (RECS). Energy Information Administration, US Department of Energy. Available at: http://www.eia.gov/consumption/residential/.

U.S. Energy Information Administration, 2014a. Form EIA-826 Data Monthly Electric Sales and Revenue Data.

U.S. Energy Information Administration, *Levelized Cost and Levelized Avoided Cost of New Generation Resources in the Annual Energy Outlook 2014*

U.S. Energy Information Administration, 2014b. State Energy Data System. Available at: http://www.eia.gov/state/seds/.

U.S. Energy Information Administration, State Energy Data System. Available at: http://www.eia.gov/state/seds/.

U.S. Environmental Protection Agency, 2012 Emissions & Generation Resource Integrated Database (eGRID). Available at: http://www.epa.gov/cleanenergy/energy-resources/egrid/index.html.

U.S. Environmental Protection Agency, 2010. ICLUS Tools and Datasets (Version 1.3 & 1.3.1). U.S. Environmental Protection Agency, Washington, DC, EPA/600/R-09/143F.

Van Vuuren, D.P. et al., 2011. The representative concentration pathways: An overview. *Climatic Change*, 109(1), pp.5–31.

Wan, K.K.W. et al., 2012. Impact of climate change on building energy use in different climate zones and mitigation and adaptation implications. *Applied Energy*, 97, pp.274–282. Available at: http://dx.doi.org/10.1016/j.apenergy.2011.11.048.

Wang, H. & Chen, Q., 2014. Impact of climate change heating and cooling energy use in buildings in the United States. *Energy and Buildings*, 82, pp.428–436. Available at: http://linkinghub.elsevier.com/retrieve/pii/S0378778814005726 [Accessed December 26, 2014].

Wilbanks, T. et al., 2008. *Effects of climate change on energy production and use in the United States*. U.S. Department of Energy.

Wilcox, S. & Marion, W., 2008. *Users manual for TMY3 data sets*, National Renewable Energy Laboratory Golden, CO.

Xu, P. et al., 2012a. Impacts of climate change on building heating and cooling energy patterns in California. *Energy*, 44(1), pp.792–804.

Xu, P. et al., 2012b. Impacts of climate change on building heating and cooling energy patterns in California. *Energy*, 44(1), pp.792–804. Available at: http://linkinghub.elsevier.com/retrieve/pii/S0360544212003921 [Accessed October 4, 2012].

Zhou, Y., Clarke, L., Eom, J., Kyle, P., Patel, P., Kim, S.H., et al., 2014. Modeling the effect of climate change on U.S. state-level buildings energy demands in an integrated assessment framework. *Applied Energy*, 113, pp.1077–1088. Available at: http://linkinghub.elsevier.com/retrieve/pii/S0306261913006776 [Accessed March 29, 2014].

Zhou, Y., Clarke, L., Eom, J., Kyle, P., Patel, P., Kim, S.H., et al., 2014. Modeling the effect of climate change on US state-level buildings energy demands in an integrated assessment framework. *Applied Energy*, 113, pp.1077–1088.

Zhou, Y., Eom, J. & Clarke, L., 2013a. The effect of global climate change, population distribution, and climate mitigation on building energy use in the U.S. and China. *Climatic Change*, 119(3-4), pp.979–992. Available at: http://link.springer.com/10.1007/s10584-013-0772-x [Accessed November 19, 2013].

Zhou, Y., Eom, J. & Clarke, L., 2013b. The effect of global climate change, population distribution, and climate mitigation on building energy use in the US and China. *Climatic change*, 119(3-4), pp.979–992.

APPENDIX A

SUPPORTING MATERIAL FOR CHAPTER 2

Section S2.1 Energy consumption data

The physical units of energy consumption are converted to equivalent energy units (heat content), so that the consumption for different energy types can be summed. The heat content for natural gas is 1023 MMbtu per MMcf, and the heat content for electricity is 3.142 MMbtu per MWh. The on-site energy consumption for all fuel types are further converted to source energy consumption using source-to-site ratios. The source-to-site ratio is 1.047 for natural gas, 1.01 for petroleum fuels (distillate fuel oil, propane and kerosene), and 1.0 for wood (Energy Star 2011). Because the source energy used for electricity generation varies by the power plant producing the electricity, the source-to-site ratio for electricity varies by state. The state-level source-to-site ratios of electricity (Table S2.1) are retrieved from the National Renewable Energy Laboratory (NREL) database (Deru & Torcellini 2007).

Table S2.1 State-level source-to-site ratios for electricity.

State	*Source-to-Site Ratio*
Alabama	3.155
Arizona	3.004
Arkansas	3.074
California	2.951
Colorado	3.117
Connecticut	3.160
Delaware	3.580
District of Columbia1	3.248
Florida	3.103
Georgia	3.231
Idaho	1.546
Illinois	3.360
Indiana	3.296
Iowa	3.427
Kansas	3.492
Kentucky	3.277
Louisiana	3.128
Maine	2.693
Maryland	3.248
Massachusetts	3.029
Michigan	3.285
Minnesota	3.348
Mississippi	3.273
Missouri	3.288

Montana	2.776
Nebraska	3.317
Nevada	3.079
New Hampshire	3.187
New Jersey	3.333
New Mexico	3.333
New York	3.011
North Carolina	3.172
North Dakota	3.402
Ohio	3.245
Oklahoma	3.095
Oregon	1.597
Pennsylvania	3.292
Rhode Island	2.495
South Carolina	3.258
South Dakota	2.320
Tennessee	3.056
Texas	3.357
Utah	3.251
Vermont	3.031
Virginia	3.439
Washington	1.692
West Virginia	3.183
Wisconsin	3.407
Wyoming	3.377

[1] *District of Columbia uses the ratio in Maryland, because the source-to-site ratio in DC is unusually high and more than 90% of the electricity consumption in DC is imported from other states.*

Section S2.2 CMIP5 Climate Models

Table S2.2 lists the 20 models used in the CMIP5 model inter-comparison from which results were retrieved and used in this study.

Table S2.2 The 20 climate models with available outputs under the RCP 8.5 scenario

ID	CMIP5 Models
1	ACCESS1-0
2	BCC-CSM1-1
3	BNU-ESM
4	CANESM2
5	CCSM4
6	CESM1-BGC
7	CNRM-CM5
8	CSIRO-MK3-6-0
9	GFDL-ESM2G
10	GFDL-ESM2M
11	INMCM4

12	IPSL-CM5A-LR
13	IPSL-CM5A-MR
14	MIROC-ESM
15	MIROC-ESM-CHEM
16	MIROC5
17	MPI-ESM-LR
18	MPI-ESM-MR
19	MRI-CGCM3
20	NORESM1-M

Section S2.3 Degree days and Balance Point Temperature

The HDD/CDD at the spatial scale of an individual US county are computed with the following equations:

$$HDD(c,m) = \sum_{d}^{m}[T_b - T(c,d)]\,; for\ all\ T(c,d) < T_b \quad \textbf{(S1)}$$

$$CDD(c,m) = \sum_{d}^{m}[T(c,d) - T_b]\,; for\ all\ T(c,d) > T_b \quad \textbf{(S2)}$$

where *T(c,d)* represents the daily mean temperature for US county, *c*, and day, *d*. The month is represented by, *m*, and T_b represents the balance point temperature. The balance point temperature is the outside temperature at which a building maintains a comfortable indoor temperature without using heating or cooling (Baumert & Selman 2003). At temperatures greater than the balance point and less than the balance point, greater energy is consumed. Hence, the balance point represents the outside temperature for which building space heating/cooling energy consumption is at a minimum. Because of thermal inertia and heat gain inside buildings (due to, for example, incoming solar radiation, heat loss from human metabolism, lighting, cooking, electrical appliances), the balance point

temperature is usually different from the "set point" temperature (the interior thermostat setting) of the heating, ventilation, and air conditioning (HVAC) system.

Because the HDD/CDD values are used in relationships with building energy consumption, the state HDD/CDD values are constructed as a population-weighted mean value from the county HDD/CDD and the proportion of county to state population statistics as follows:

$$HDD(s,m) = \sum_c^s \left[\frac{P(c)}{P(s)} HDD(c,m)\right] \quad \text{(S3)}$$

$$CDD(s,m) = \sum_c^s \left[\frac{P(c)}{P(s)} CDD(c,m)\right] \quad \text{(S4)}$$

The HDD/CDD values are hence, denoted as either *HDD(c)/CDD(c)* or as *HDD(s)/CDD(s)* for the county and state, respectively. Similarly, the population-weighted state temperature is calculated as:

$$T(s,m) = \sum_c^s \left[\frac{P(c)}{P(s)} T(c,m)\right] \quad \text{(S5)}$$

The value traditionally used as the balance point temperature is 65 °F which we denote as $T_b(65)$. (Baumert & Selman 2003) However, some research suggests that the balance point temperature varies by location, driven by differences in building characteristics (e.g. insulation, utility usage), weather conditions (e.g. solar radiation, wind speed), population demographics and social norms (e.g. race, age, preferences) (Ruth & Lin 2006b; de Dear & Brager 2001). An incorrect balance point temperature, when used to estimate energy demand independently from measured data, may result in poor model performance and bias.

In order to avoid this potential bias, a state-specific balance point temperature, $T_b(S)$, is estimated using total state building electricity consumption and population-weighted state temperature with a segmented regression method (Muggeo 2008). This reflects the fact that the relationship between site heating/cooling electricity consumption and external temperature can be represented by two segments or regimes: one associated with temperatures above a balance point temperature (the cooling segment) and one associated with temperatures below the balance point temperature (the heating segment). In both segments, energy consumption increases as temperatures move away from the balance point, resulting in a "V" plot of energy consumption versus external temperature. The segmented regression method simultaneously solves the separate regression segments iterating on the value of the balance point temperature. The best fit will optimize both the regression coefficients and the balance point temperature. The traditional balance point temperature, 65 °F, is used as initial value to run the segmented regression model for each state.

Because natural gas is not used for cooling, natural gas consumption cannot be used to isolate the balance point temperature. Hence, only building electricity consumption is used. Furthermore, to normalize the impact of building electricity consumption and temperature to variations in population, the temperature values are weighted by population. The population-weighted state temperature ($T(s,m)$) is calculated using equation (S5).

The segmented regression model is expressed as:

$$ELE(s,m) = \alpha + \beta * T(s,m) + \varepsilon \quad \text{(S6)}$$

where the total building electricity consumption, *ELE*, for state, *s*, and month, *m*, is related to the population-weighted air temperature, $T(s,m)$ via linear regression. The linear regression constant, slope and error terms are represented by α, β, and ε, respectively.

The relationship between the monthly mean, population-weighted air temperature and monthly total building electricity consumption for each state in addition to the segmented regression fit lines and the resulting state-specific balance point temperature are shown in Figures 2.1 and S2.1. The relationship between state balance point temperatures and state long-term average annual temperatures is shown in Figure S2.2.

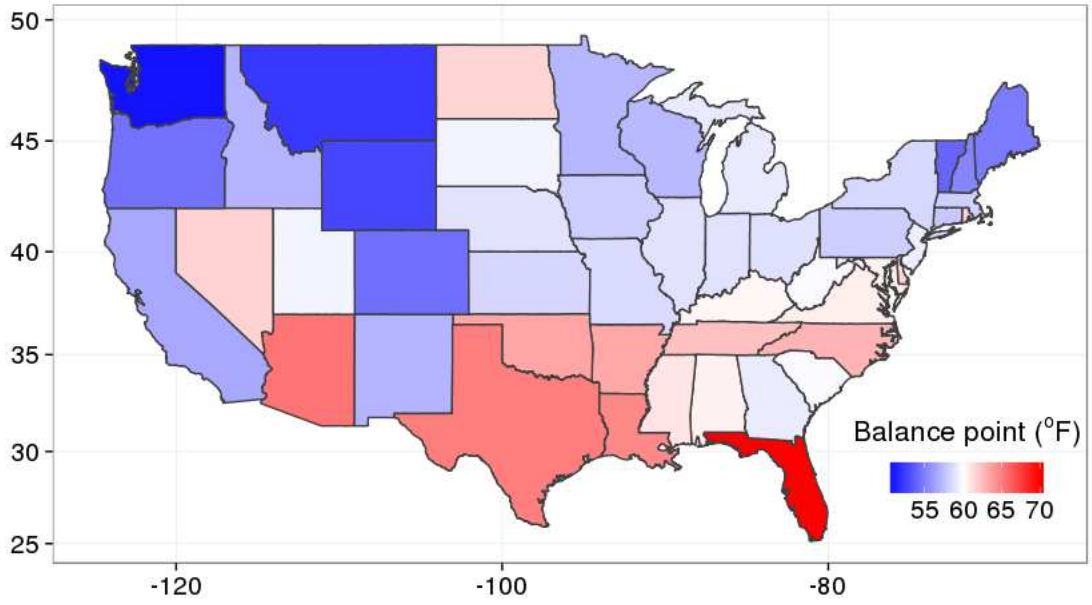

Figure S2.1 State-specific balance point temperatures derived from the segmented regression approach.

The $T_b(S)$ values range from 50.7 °F in Washington State to 70 °F in Florida. Because the "V" shape for the states of Oregon and Washington are curved and the bottoms and somewhat flat, a log transformation (log(E)) is used to estimate the balance point

temperature for these two states. In the approach used here, a single balance point temperature is estimated for each state. Two balance point temperatures (one for cooling and one for heating) is potentially more realistic in some states due to electricity consumption patterns. This was considered out-of-scope for the current research goals. A comparison of model performance with one versus two balance point temperature(s) is a useful topic for future research.

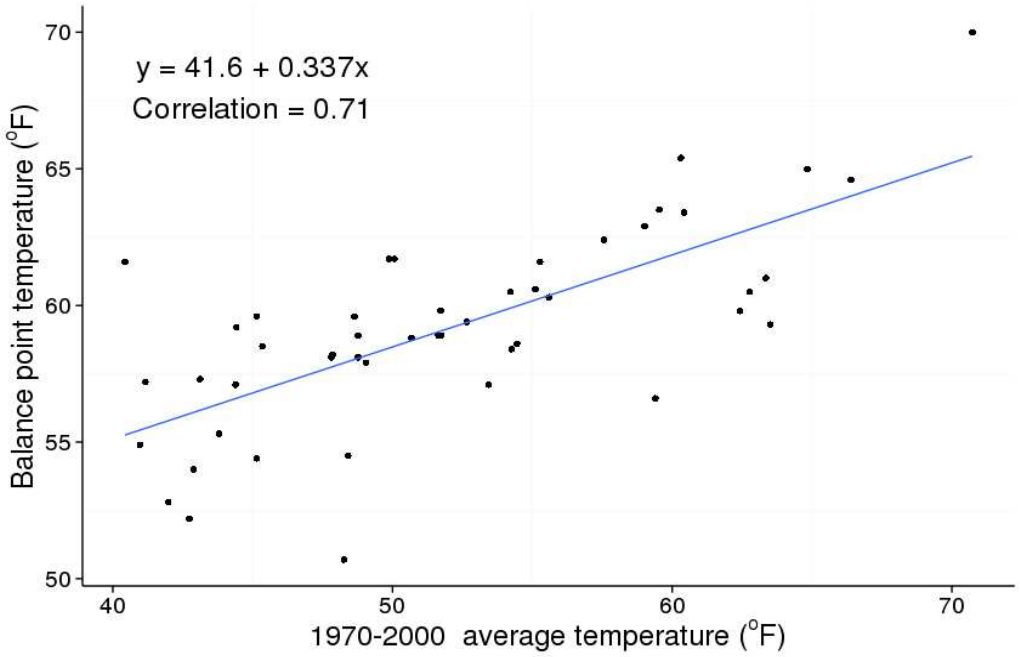

Figure S2.2 Correlation between long-term (1970-2000) average temperatures and balance point temperatures. Each point represents a US state.

To test for sensitivity to the state-specific balance point temperature in the current study, we compute HDD/CDD based on both $T_b(65)$ and $T_b(S)$ (see Section S6). The HDD/CDD, derived using $T_b(65)$, is abbreviated as HDD(65)/CDD(65), and the HDD/CDD derived using the $T_b(S)$ values is abbreviated as HDD(S)/CDD(S).

Section S2.4 Energy Demand Estimation Model

To quantify the relationship between HDD/CDD and building energy consumption, we utilize a regression modeling approach. Numerous studies have used HDD and CDD as independent variables in regression models aimed at estimating building energy consumption (Ruth & Lin 2006b; Alan F. Hamlet et al. 2010; David J. Sailor & Muñoz 1997; Sailor et al. 1998c; Sailor 2001b). Although many have availed of additional variables, HDD and CDD were found to be the most significant terms related to energy consumption. Sailor et al. [1998] reported that including non-temperature weather data into a building energy consumption regression model may cause multicollinearity with the temperature or temperature-derived variables (e.g. HDD/CDD), resulting in suspicious coefficients.

The details of the regression models can be found in the main paper, methods section. The HDD/CDD variables can represent the values calculated with either the $T_b(65)$ or $T_b(S)$. As pointed out by Sailor et al. (1998), space cooling/heating is significantly related to temperature, water heating is marginally related to temperature, and other building energy consumption is not related to temperature. Thus, the HDD/CDD variable reflects energy consumption devoted to space cooling/heating and a small portion of water heating; the constant, α, captures the energy consumption for other energy use; and trend term, m-1, captures the long-term linear change of energy consumption.

Table S2.3 Regression results associated with the per capita natural gas consumption model (main paper, equation (1)) using state-specific balance point temperatures.

State	*α*	*λ*	*β*	*γ*	*Adjusted- R2*	*NG Heating(%)1*
AL	439(**)	-0.6	2.52(**)	1.55(**)	0.96	57
AZ	460(**)	-0.04	1.57(**)	1.37(**)	0.98	70
AR	719(**)	4.89(**)	2.11(**)	2.68(**)	0.99	68
CA	988(**)	1.15	4.55(**)	0.77(**)	0.95	86
CO	909(**)	-2.39	6.27(**)	0.26(.)	0.99	84
CT	574(**)	6.17(**)	2.59(**)	1.14(**)	0.99	30

DE	593(**)	1.78	3.47(**)	0.43(**)	0.98	53
DC	2296(**)	-6.38(.)	10.94(**)	-0.01	0.97	53
FL	233(**)	0.56(**)	0.32(**)	0.26(**)	0.90	21
GA	566(**)	2.43(**)	5.01(**)	0.48(**)	0.99	77
ID	579(**)	2.73(*)	3.97(**)	-0.02	0.98	91
IL	1320(**)	-1.17	6.08(**)	1.41(**)	0.99	97
IN	804(**)	-2.28(.)	5.63(**)	0.19(*)	1.00	83
IA	1122(**)	-2.46	4.47(**)	0.88(**)	0.99	66
KS	845(**)	-2.47	4.52(**)	2.45(**)	0.98	93
KY	415(**)	-0.46	3.82(**)	0.52(**)	0.99	57
LA	529(**)	2.79(**)	2.89(**)	1.5(**)	0.98	68
ME	107(**)	3.3(**)	0.66(**)	0.06(.)	0.96	30
MD	782(**)	-0.77	4.47(**)	0.04	0.99	53
MA	775(**)	3.14(*)	4.35(**)	0.54(**)	0.99	56
MI	1142(**)	-2.84	5.91(**)	1.04(**)	0.98	88
MN	1034(**)	-0.88	4.41(**)	0.39(**)	0.99	66
MS	504(**)	1.19	3.14(**)	1.54(**)	0.98	57
MO	644(**)	-0.16	4(**)	1.65(**)	0.98	70
MT	705(**)	8.35(**)	4.75(**)	1.57(**)	0.97	91
NE	1135(**)	-1.95	2.88(**)	2.49(**)	0.97	93
NV	940(**)	1.71	2.95(**)	1.92(**)	0.98	93
NH	371(**)	-0.96(.)	1.68(**)	0.16(**)	0.99	30
NJ	1410(**)	3.45	6.77(**)	0.28	0.98	85
NM	897(**)	2.31	2.99(**)	3.22(**)	0.96	93
NY	1099(**)	2.16(.)	4.37(**)	0.77(**)	0.99	63
NC	264(**)	1.06	2.97(**)	-0.12(.)	0.99	56
ND	556(**)	2.62(*)	3.12(**)	0.02	0.99	66
OH	827(**)	0.38	5.97(**)	0.78(**)	1.00	83
OK	634(**)	-0.33	2.93(**)	3.12(**)	0.96	68
OR	422(**)	1.39	3.71(**)	1.11(**)	0.96	70
PA	668(**)	-0.27	4.22(**)	0.93(**)	0.99	49
RI	447(**)	1.25	2.87(**)	1.33(**)	0.93	30
SC	352(**)	1.27(*)	2.95(**)	0.35(**)	0.99	56
SD	666(**)	0.6	3.04(**)	0.46(**)	0.99	66
TN	435(**)	-0.94	2.99(**)	1.25(**)	0.98	67
TX	568(**)	1.09(*)	2.64(**)	1.65(**)	0.99	74
UT	578(**)	6.48	3.48(**)	1.48(**)	0.93	91
VT	213(**)	0.87	0.78(**)	0.5(**)	0.97	30
VA	535(**)	-0.22	3.71(**)	0	0.99	64
WA	687(**)	1.34	4(**)	0.95(**)	0.96	70
WV	814(**)	-0.47	3.93(**)	0.58(**)	0.99	53
WI	911(**)	-0.6	5.29(**)	-0.05	1.00	82
WY	849(**)	8.43(**)	4.28(**)	1.69(**)	0.97	91

[1] *NG heating(%) represents the percentage of heating consumption depends on natural gas*

Significance Codes: "**" represents $p<0.01$; "*" represents $p<0.05$; "." represents $p<0.1$

The regression model for natural gas (main paper, equation 1) fits the data well with adj-R^2 exceeding 0.9 for all states (Table S2.3). The regression analysis indicates that the HDD regression coefficient and the intercept are statistically significant in all states, the lagged HDD term is significant in roughly 85% of states, and the trend term is significant in about 1/3 of states at the 90% confidence level. The HDD and lagged HDD regression

coefficients represent the sensitivity of the per capita natural gas consumption to variations in HDD, contemporaneously and delayed by one month, respectively. Small HDD coefficients are most often associated with states where natural gas is not the primary heating fuel, for example, Florida, Maine, and Vermont (Table S2.3). Hence, few people are consuming natural gas for heating and the statewide per capita consumption is small and weakly related to the external temperature. By contrast, large coefficients are most often associated with states where natural gas is the dominant heating fuel, for example, the Midwestern states and Colorado.

The coefficient for the lagged HDD is usually smaller than the HDD, because heating demand is primarily affected by the contemporary temperature. However, in some states (Arkansas, Kansas, Nebraska, New Mexico, Oklahoma), the coefficients of the lagged HDD are similar to, or even larger than, HDD indicating a strong delayed response of heating demand to temperature. This could be a reflection of social norms, average building technology, or building thermal properties.

The regression model for electricity (main paper, equation 2) fits the data in each state well with adj-R^2 exceeding 0.9 for most states (Table S2.4). The regression analysis for electricity consumption indicates that the HDD/CDD and intercept variables are significant in all states, the lagged HDD/CDD term is significant in roughly 80% of states, and the trend term is significant in about 1/2 of states, all at the 90% confidence level.

Table S2.4 Regression results associated with the per capita electricity consumption model (main paper, equation (2)) using state-specific balance point temperatures.

State	□ *α*	□ *λ*	*β1*	*β2*	*γ1*	*γ2*	*Adjusted-R2*	*Electric Heating (%)*[1]
AL	579(**)	-0.81(**)	0.7(**)	0.76(**)	0.2(**)	0.23(**)	0.95	23

AZ	532(**)	-0.55(**)	0.36(**)	0.71(**)	0.05	0.1(**)	0.98	30
AR	520(**)	-0.34	0.3(**)	0.52(**)	0.25(**)	0.49(**)	0.96	21
CA	358(**)	-0.06	0.26(**)	0.2(**)	0.07	0.15(**)	0.84	9
CO	507(**)	-0.14	0.16(**)	0.32(**)	0	0.11(**)	0.92	3
CT	468(**)	-0.37(.)	0.19(**)	0.44(**)	0.04(*)	0.16(**)	0.86	2
DE	531(**)	-0.3	0.27(**)	0.64(**)	0.17(**)	0.4(**)	0.89	21
DC	1338(**)	-2.3(**)	0.63(**)	0.9(**)	-0.23(**)	-0.13(**)	0.92	21
FL	678(**)	-0.38	0.43(**)	0.76(**)	0.11(*)	0.36(**)	0.95	79
GA	564(**)	-0.7(*)	0.58(**)	0.62(**)	0.18(**)	0.21(**)	0.94	19
ID	540(**)	-0.08	0.41(**)	0.49(**)	0	-0.03	0.95	9
IL	477(**)	-0.53(**)	0.22(**)	0.5(**)	-0.02	0.12(**)	0.95	3
IN	509(**)	-0.69(**)	0.37(**)	0.64(**)	0	0.12(**)	0.96	8
IA	546(**)	-0.36	0.23(**)	0.47(**)	-0.01	0.05	0.86	6
KS	609(**)	-0.59(**)	0.31(**)	0.61(**)	-0.01	0.1(**)	0.97	7
KY	571(**)	-0.98(**)	0.5(**)	0.78(**)	0.1(**)	0.23(**)	0.97	23
LA	580(**)	0.41	0.49(**)	0.59(**)	0.42(**)	0.58(**)	0.96	21
ME	457(**)	-0.06	0.18(**)	0.3(**)	-0.06(**)	0.01	0.73	2
MD	601(**)	-0.34(.)	0.38(**)	0.74(**)	0.01	0.05(*)	0.96	21
MA	451(**)	-1.71(**)	0.16(**)	0.42(**)	-0.02	0.1(*)	0.79	3
MI	506(**)	-0.24	0.17(**)	0.6(**)	-0.05(**)	-0.04	0.91	2
MN	575(**)	-0.26	0.15(**)	0.43(**)	-0.01	0.03	0.90	6
MS	526(**)	-0.33	0.45(**)	0.47(**)	0.4(**)	0.48(**)	0.96	23
MO	634(**)	-1.11(**)	0.46(**)	0.68(**)	0.04(.)	0.13(**)	0.97	13
MT	562(**)	0.64(**)	0.25(**)	0.34(**)	0.17(**)	0.15(**)	0.92	9
NE	645(**)	-0.68(**)	0.27(**)	0.47(**)	0.07(**)	0.14(**)	0.93	7
NV	343(**)	-0.06	0.32(**)	0.7(**)	0.05	0.06(*)	0.97	7
NH	445(**)	-0.06	0.12(**)	0.27(**)	0.05(**)	0.21(**)	0.86	2
NJ	511(**)	-0.76(**)	0.2(**)	0.64(**)	-0.02	0.07(**)	0.96	1
NM	466(**)	0.45(**)	0.21(**)	0.3(**)	0.02(.)	0.09(**)	0.96	7
NY	431(**)	-0.08	0.14(**)	0.34(**)	0.01	0.17(**)	0.97	2
NC	594(**)	-0.49	0.45(**)	0.75(**)	0.13(**)	0.28(**)	0.91	27
ND	741(**)	2.79(**)	0.36(**)	0.47(**)	0.04(**)	0.1(*)	0.97	6
OH	513(**)	-0.28	0.34(**)	0.66(**)	-0.03(.)	0.06(*)	0.94	8
OK	633(**)	-0.27	0.4(**)	0.83(**)	-0.03	0.09(**)	0.97	21
OR	583(**)	-0.27	0.64(**)	0.63(**)	-0.01	-0.06	0.90	23
PA	487(**)	-0.82(**)	0.27(**)	0.45(**)	0.05(**)	0.13(**)	0.94	9
RI	459(**)	-0.13	0.13(**)	0.68(**)	-0.05(**)	-0.08(*)	0.89	2
SC	570(**)	-0.73(*)	0.71(**)	0.7(**)	0.2(**)	0.2(**)	0.95	27
SD	648(**)	0.93(**)	0.2(**)	0.36(**)	0.12(**)	0.17(**)	0.95	6
TN	570(**)	-0.94(**)	0.34(**)	0.59(**)	0.33(**)	0.61(**)	0.96	33
TX	463(**)	1.23(**)	0.38(**)	0.59(**)	0.27(**)	0.36(**)	0.98	22
UT	457(**)	0.58(**)	0.12(**)	0.55(**)	-0.03(*)	0.01	0.92	9
VT	458(**)	-0.24(.)	0.18(**)	0.3(**)	-0.03(*)	0.04(.)	0.87	2
VA	678(**)	-0.4(.)	0.56(**)	0.84(**)	-0.02	0.01	0.95	26
WA	635(**)	-0.03	0.47(**)	0.18(**)	0.31(**)	0.02	0.97	23
WV	576(**)	-0.43	0.6(**)	0.68(**)	0.03	0.15(**)	0.94	21
WI	544(**)	-0.2	0.18(**)	0.48(**)	-0.04(**)	-0.02	0.91	3
WY	837(**)	0.11	0.29(**)	0.19(**)	0.13(**)	0.06(.)	0.90	9

[1] *Electric heating (%) represents the percentage of heating fuel consumption depends on electricity*

Significance Codes: "**" represents p<0.01; "*" represents p<0.05; "." represents p<0.1

The coefficients for HDD (β_1) tend to be large in the South where there is more use of electricity for space heating, and are small in the areas where other fuels are used for space heating (e.g., New England and East North Central areas). The correlation

coefficient between β_1 and the percentage of electric heating is 0.6. The coefficients for CDD (β_2) tend to be large in warmer states where air-conditioners are prevalent, and are small in colder states where air-conditioning is less common. The correlation coefficient between β_2 and long term average state temperature is 0.57.

Section S2.5 Air-conditioning saturation

Past research suggests that the fraction of residential buildings with air-conditioning capability (referred to as the "saturation level") is directly related to the magnitude of CDD in a given locale (Sailor 2003; McNeil & Letschert 2008). The EIA's Residential Energy Consumption Survey (RECS) provides residential air-conditioning saturation levels in 27 spatial domains within the US (U.S. Department of Energy 2009). We use the 2009 RECS data to represent the saturation levels in the current period. For future time periods, we calculate saturation levels based on the saturation equation developed by Sailor et al. (2003) with data from 39 cities, and adjusted by McNeil et al. (2008) using RECS data for the whole United States:

$$SAT = 1 - 0.949 * e^{-0.00187*\mathrm{CDD}} \quad \textbf{(S7)}$$

where *SAT* is the air-conditioning saturation level (%), and *CDD* is the annual cooling degree days. Because the equation was developed based on a 65 °F balance point temperature, we calculate the SAT using the same 65 °F balance point temperature. We calculated the saturation level difference between future and current time periods, and added it to the 2009 RECS data to get the adjusted future saturation:

$$SAT'_{ft} = SAT_{RECS} + (SAT_{ft} - SAT_{cr}) \quad \text{(S8)}$$

where SAT_{RECS} is the air-conditioning saturation level derived from 2009 RECS data, SAT_{cr} and SAT_{ft} are current (*cr*) and future (*ft*) saturation levels calculated with equation (S7), and SAT'_{ft} is the adjusted future saturation level. The combination of equation (S7) and (S8) guarantees that SAT'_{ft} matches with the real 2009 RECS survey data when the CDD difference between future and current period is zero. The SAT'_{ft} calculated with this method may be larger than unity in some cases, so the upper limit is set to unity to constrain the saturation values. Table S2.5 shows that the contemporary residential air-conditioning saturation level is usually high in warmer states (e.g., AR, LA, and OK), and low in colder states (e.g., OR and WA). The air-conditioning saturation level in some colder states (e.g., VT, OR, and RI) increases over 20% from 2008-12 to 2080-99.

Table S2.5 Air-conditioning saturation levels (%) in current and future periods

State	***2008-12***	***2020-39***	***2040-59***	***2060-79***	***2080-99***
AL	97.2	97.8	98.2	98.6	98.7
AZ	93.5	93.6	93.6	93.7	93.7
AR	97.4	98.3	98.8	99.1	99.2
CA	56.4	59.3	62.1	63.8	64.9
CO	48.3	57.5	66.1	73.6	78.4
CT	64.8	72.5	78.1	82.8	85.4
DE	93.8	96.8	98.8	100.0	100.0
DC	93.8	95.8	97.3	98.3	98.7
FL	96.3	96.4	96.4	96.4	96.4
GA	96.9	97.7	98.3	98.7	98.9
ID	72.1	80.8	90.0	96.3	100.0
IL	90.3	94.0	96.5	98.4	99.2
IN	83.7	87.4	89.8	91.8	92.7
IA	86.7	91.3	94.2	96.4	97.6
KS	96.1	97.6	98.3	98.8	99.1
KY	97.2	99.6	100.0	100.0	100.0
LA	97.4	97.6	97.7	97.8	97.8
ME	64.8	76.0	86.5	96.4	100.0
MD	93.8	96.8	98.8	100.0	100.0
MA	78.6	86.7	92.8	98.0	100.0
MI	81.4	88.4	94.1	98.2	100.0
MN	86.7	95.5	100.0	100.0	100.0
MS	97.2	97.6	97.8	98.0	98.1

MO	97.0	98.9	99.7	100.0	100.0
MT	72.1	83.6	97.2	100.0	100.0
NE	96.1	99.4	100.0	100.0	100.0
NV	67.6	68.0	68.4	68.5	68.7
NH	64.8	76.1	85.4	94.1	99.1
NJ	93.0	98.1	100.0	100.0	100.0
NM	67.6	71.4	74.0	76.1	77.4
NY	73.2	78.8	82.8	86.0	87.6
NC	95.5	97.0	98.0	98.8	99.1
ND	86.7	98.5	100.0	100.0	100.0
OH	83.7	88.6	92.1	94.8	96.1
OK	97.4	98.1	98.4	98.6	98.7
OR	43.4	52.1	65.8	76.8	87.0
PA	89.3	95.5	99.9	100.0	100.0
RI	64.8	73.5	79.9	85.6	88.9
SC	95.5	96.2	96.6	97.0	97.1
SD	86.7	93.2	98.0	100.0	100.0
TN	97.9	99.5	100.0	100.0	100.0
TX	96.4	96.5	96.6	96.7	96.7
UT	72.1	77.9	82.9	86.2	88.7
VT	64.8	76.3	87.2	97.4	100.0
VA	94.0	96.3	98.0	99.3	99.9
WA	43.4	50.9	63.0	74.8	86.8
WV	93.8	99.3	100.0	100.0	100.0
WI	77.7	86.1	93.1	98.0	100.0
WY	72.1	83.3	94.4	100.0	100.0

Results for the current time period (2008-12) are derived from RECS 2009 data. Results for the four future time periods represent the median of 15 climate models driven by the IPCC A2 emissions scenario.

The future commercial building air-conditioning saturation levels are unchanged because air-conditioning saturation levels are near 100% in most commercial building types(U.S. Department of Energy 2003). Building types with less cooling demand, for example, vacant buildings and warehouses (Table S2.6) are an exception. Because these two building types account for a relatively small amount of total commercial building energy consumption and there is little research to support changes in the saturation air-conditioning level, saturation levels are kept constant.

Table S2.6 Commercial building air-conditioning statistics, derived from CBECS 2003

Building type	***Total floorspace (Million square feet)***	***Cooled floorspace (Million square feet)***	***Energy consumption (trillion Btu)***	***Air-conditioning saturation (%)***
Education	9874	9200	820	0.93
Food Sales	1255	1198	251	0.95
Food Service	1654	1583	427	0.96
Health Care	3163	3157	594	1.00
Lodging	5096	4841	510	0.95
Retail (Other Than Mall)	4317	4079	319	0.94

Office	12208	12032	1134	0.99
Public Assembly	3939	3477	370	0.88
Public Order and Safety	1090	1043	126	0.96
Religious Worship	3754	3301	163	0.88
Service	4050	3261	312	0.81
Warehouse and Storage	10078	7295	456	0.72
Other	1738	1636	286	0.94
Vacant	2567	836	54	0.33
Total	64783	56939	5822	0.88

It is assumed that the coefficients for CDD (β_2) and lagged CDD (γ_2) in the electricity regression model (main paper, equation 2) increase linearly with air-conditioning saturation level. Thus, β_2 and γ_2 are multiplied by an inflation factor to account for the residential air-conditioning saturation level change in future periods:

$$IF = 1 + \frac{SAT'_{ft} - SAT_{RECS}}{SAT_{RECS}} \times \frac{ELE_{res}}{ELE_{res} + ELE_{com}} \quad \text{(S9)}$$

where, *IF* is the inflation factor for β_2 and γ_2, and *ELE* is the electricity consumption for the residential sector, *res*, or commercial sector, *com*. $(SAT'_{ft} - SAT_{RECS})/SAT_{RECS}$ represents the residential air-conditioning saturation level relative difference between the future and current period, and $ELE_{res}/(ELE_{res} + ELE_{com})$ represents the ratio of residential electricity consumption to total building sector electricity consumption during 2008-2012. For example, if the residential air-conditioning saturation level increases 10%, and the residential sector accounts for 60% of total building sector electricity consumption, the *IF* will be (1 + 0.1 * 0.6 = 1.06). The *IF* is calculated for each future period in each state, which is further used to adjust β_2 and γ_2 and calculate future electricity consumption.

Figure S3 shows that the relative difference of source electricity consumption is mainly caused by direct impact of climate change on buildings. The additional air-conditioning

capacity added in future years and its interaction with climate change has a much smaller impact on the building energy consumption change than the pre-existing air-conditioning stock.

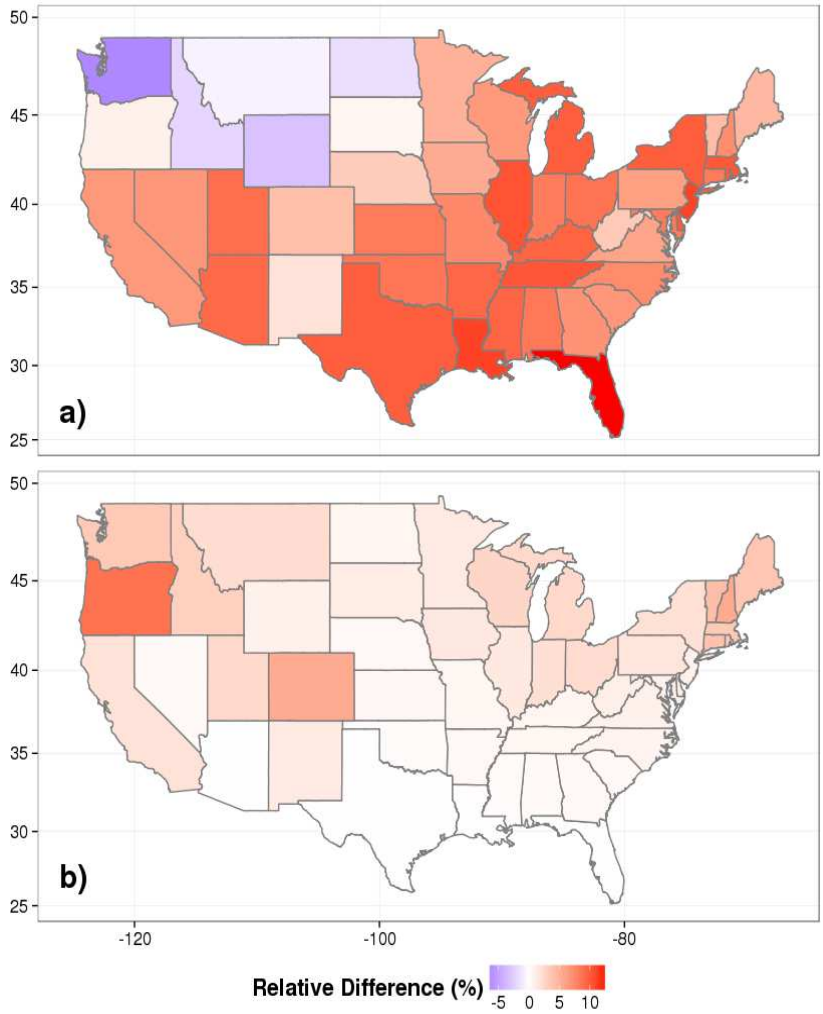

Figure S2.3 Annual state building electricity consumption relative difference (%) between the 2080-99 time period and 2008-2012. Results represent the median of 20 climate models: **a)**, difference without the addition of air-conditioning capacity; and **b)**, difference due to additional air-conditioning. The sum of **a)** and **b)** is equal to main paper, Figure 2.3a.

Section S6. Sensitivity to balance point temperature

The impact of climate change on building energy consumption presented in the main paper utilizes a state-specific balance point temperature to empirically derive the change in both electricity and non-electric demand. The same analysis can be performed but using a fixed balance point temperature. This will offer insight into the importance of using a state-specific balance point temperature to the study results. To demonstrate this difference, Tables S2.7-S2.9 reflect the same information provided in Tables S2.3, S2.4 and main paper Table 2.1.

The comparison of regression results shows that the regression coefficients differ substantially between the model based on the fixed 65 °F and those based on state-specific balance point, and the intercept terms are negative in some states, which is physically unexplainable. The bias of the coefficients further suggests the potential misallocation of end-use energy consumption based on 65 °F balance point.

Table S2.7 Regression results associated with the per capita natural gas consumption model (main paper, equation (1)) using a 65°F balance point temperature.

State	*α*	*λ*	*β*	*γ*	*Adjusted-R2*
AL	381(**)	-0.73	2.01(**)	1.23(**)	0.96
AZ	463(**)	-0.05	1.62(**)	1.41(**)	0.98
AR	684(**)	4.91(**)	1.96(**)	2.52(**)	0.98
CA	861(**)	1.17	2.62(**)	0.29	0.91
CO	372(**)	-1.91	4.8(**)	0.08	0.97
CT	377(**)	5.88(**)	2.1(**)	0.93(**)	0.96
DE	514(**)	1.55	3.1(**)	0.38(**)	0.97
DC	1833(**)	-8.61(**)	7.8(**)	-0.48(.)	0.98
FL	242(**)	0.53(*)	0.46(**)	0.39(**)	0.83
GA	465(**)	2.14(*)	3.89(**)	0.23(*)	0.99
ID	315(**)	2.57	3.25(**)	-0.04	0.97
IL	983(**)	-2.22	5.26(**)	1.19(**)	0.98
IN	577(**)	-2.98	4.8(**)	0.12	0.98
IA	834(**)	-3.19(.)	3.89(**)	0.73(**)	0.99
KS	591(**)	-2.72	3.66(**)	2(**)	0.97
KY	308(**)	-0.77	3.26(**)	0.43(**)	0.98
LA	524(**)	2.8(**)	2.82(**)	1.46(**)	0.98
ME	28	3.33(**)	0.53(**)	0.05	0.95
MD	667(**)	-1.11	3.87(**)	-0.01	0.98
MA	484(**)	2.91	3.62(**)	0.44(*)	0.97
MI	763(**)	-3.28	5.15(**)	0.95(**)	0.97
MN	678(**)	-1.53	3.9(**)	0.29(*)	0.99
MS	448(**)	1.24	2.55(**)	1.22(**)	0.98

MO	450(**)	-0.67	3.27(**)	1.35(**)	0.97
MT	-131	8.43(*)	3.73(**)	1.08(**)	0.94
NE	894(**)	-2.34	2.49(**)	2.18(**)	0.97
NV	885(**)	1.73	2.54(**)	1.63(**)	0.98
NH	195(**)	-0.9	1.32(**)	0.15(*)	0.97
NJ	1155(**)	2.87	5.74(**)	0.16	0.96
NM	650(**)	3.13	2.12(**)	2.48(**)	0.96
NY	852(**)	1.75	3.63(**)	0.64(**)	0.98
NC	236(**)	0.99	2.74(**)	-0.14(.)	0.98
ND	425(**)	2.57(.)	2.99(**)	0	0.99
OH	540(**)	-0.39	5.03(**)	0.67(**)	0.99
OK	586(**)	-0.24	2.75(**)	2.96(**)	0.96
OR	-117	0.95	2.64(**)	0.79(**)	0.92
PA	426(**)	-0.71	3.47(**)	0.74(**)	0.98
RI	305(*)	1.32	2.63(**)	1.23(**)	0.92
SC	295(**)	1.14(*)	2.34(**)	0.18(**)	0.99
SD	492(**)	0.3	2.78(**)	0.38(**)	0.99
TN	382(**)	-1.09	2.71(**)	1.13(**)	0.97
TX	568(**)	1.09(*)	2.64(**)	1.65(**)	0.99
UT	373(.)	6.31	2.99(**)	1.34(**)	0.91
VT	67(*)	0.97	0.61(**)	0.41(**)	0.96
VA	450(**)	-0.48	3.21(**)	-0.06	0.98
WA	87	0.71	2.57(**)	0.45(**)	0.95
WV	645(**)	-0.61	3.39(**)	0.47(**)	0.99
WI	553(**)	-1.44	4.52(**)	-0.06	0.98
WY	223(.)	8.49(**)	3.33(**)	1.17(**)	0.97

Significance Codes: "**" represents p<0.01; "*" represents p<0.05; "." represents p<0.1

Table S2.8 Regression results associated with the per capita electricity consumption model (main paper, equation (2)) using a 65°F balance point temperature

State	*α*	*λ*	*β1*	*β2*	*γ1*	*γ2*	*Adjusted-R2*
AL	622(**)	-0.95(**)	0.5(**)	0.91(**)	0.14(**)	0.28(**)	0.94
AZ	526(**)	-0.55(**)	0.38(**)	0.7(**)	0.06	0.1(**)	0.98
AR	538(**)	-0.4	0.26(**)	0.55(**)	0.22(**)	0.52(**)	0.95
CA	390(**)	-0.05	0.12(**)	0.31(**)	-0.01	0.21(**)	0.83
CO	540(**)	-0.27(.)	0.1(**)	0.6(**)	-0.02	0.22(**)	0.90
CT	492(**)	-0.54(*)	0.13(**)	0.78(**)	0.02	0.33(**)	0.81
DE	554(**)	-0.52	0.23(**)	0.79(**)	0.14(**)	0.51(**)	0.87
DC	1440(**)	-2.83(**)	0.32(**)	1.41(**)	-0.18(**)	-0.2(*)	0.89
FL	596(**)	-0.39(.)	0.72(**)	0.61(**)	0.31(**)	0.34(**)	0.95
GA	608(**)	-0.87(**)	0.38(**)	0.79(**)	0.11(**)	0.29(**)	0.93
ID	511(**)	-0.18	0.33(**)	0.91(**)	0.01	0.04	0.91
IL	514(**)	-0.9(**)	0.16(**)	0.69(**)	-0.03(.)	0.19(**)	0.91
IN	547(**)	-1.12(**)	0.28(**)	0.9(**)	-0.01	0.2(**)	0.90
IA	585(**)	-0.76(*)	0.17(**)	0.64(**)	-0.02	0.09	0.76
KS	667(**)	-0.9(**)	0.2(**)	0.74(**)	-0.02	0.15(**)	0.94
KY	597(**)	-1.24(**)	0.39(**)	1.01(**)	0.08(**)	0.35(**)	0.94
LA	586(**)	0.42	0.47(**)	0.6(**)	0.41(**)	0.58(**)	0.96
ME	469(**)	-0.2	0.13(**)	0.93(**)	-0.05(**)	0.08	0.64
MD	624(**)	-0.56(*)	0.3(**)	0.97(**)	0	0.11(*)	0.92
MA	469(**)	-1.85(**)	0.12(**)	0.8(**)	-0.02	0.23(**)	0.77
MI	532(**)	-0.46(*)	0.12(**)	0.89(**)	-0.04(*)	-0.01	0.85
MN	604(**)	-0.55(*)	0.11(**)	0.74(**)	-0.01	0.03	0.82
MS	571(**)	-0.39	0.31(**)	0.53(**)	0.29(**)	0.57(**)	0.95
MO	685(**)	-1.56(**)	0.33(**)	0.88(**)	0.02	0.2(**)	0.92
MT	523(**)	0.38	0.19(**)	1.09(**)	0.12(**)	0.65(**)	0.87

NE	668(**)	-1.05(**)	0.22(**)	0.62(**)	0.05(**)	0.23(**)	0.91
NV	373(**)	-0.06	0.24(**)	0.77(**)	0.03	0.07(*)	0.97
NH	464(**)	-0.21	0.08(**)	0.78(**)	0.03(.)	0.59(**)	0.78
NJ	547(**)	-0.95(**)	0.13(**)	0.9(**)	-0.02	0.13(**)	0.94
NM	494(**)	0.4(**)	0.13(**)	0.42(**)	0	0.15(**)	0.96
NY	455(**)	-0.22(.)	0.1(**)	0.54(**)	-0.01	0.29(**)	0.93
NC	609(**)	-0.56	0.4(**)	0.84(**)	0.11(**)	0.32(**)	0.90
ND	731(**)	2.62(**)	0.35(**)	0.68(**)	0.04(**)	0.13(*)	0.97
OH	544(**)	-0.64(*)	0.25(**)	0.98(**)	-0.02	0.15(*)	0.88
OK	650(**)	-0.32	0.36(**)	0.87(**)	-0.03	0.1(**)	0.96
OR	525(**)	-0.09	0.41(**)	2.97(**)	0.01	0.12	0.79
PA	505(**)	-1.06(**)	0.2(**)	0.73(**)	0.03(.)	0.28(**)	0.88
RI	470(**)	-0.17	0.11(**)	0.91(**)	-0.05(**)	-0.09(.)	0.87
SC	604(**)	-0.86(*)	0.51(**)	0.89(**)	0.13(**)	0.27(**)	0.94
SD	654(**)	0.65(**)	0.18(**)	0.5(**)	0.11(**)	0.26(**)	0.93
TN	591(**)	-1.08(**)	0.29(**)	0.68(**)	0.28(**)	0.71(**)	0.94
TX	463(**)	1.23(**)	0.38(**)	0.59(**)	0.27(**)	0.36(**)	0.98
UT	478(**)	0.56(**)	0.08(**)	0.76(**)	-0.03(.)	0.05	0.89
VT	466(**)	-0.39(*)	0.12(**)	1.01(**)	-0.02(.)	0.24(*)	0.75
VA	698(**)	-0.61(.)	0.44(**)	1.08(**)	-0.02	0.05	0.90
WA	489(**)	0.01	0.31(**)	1.49(**)	0.23(**)	0.77(**)	0.93
WV	578(**)	-0.76(*)	0.5(**)	1.06(**)	0.03	0.29(**)	0.91
WI	579(**)	-0.57(*)	0.13(**)	0.78(**)	-0.04(*)	0	0.81
WY	792(**)	-0.11	0.22(**)	0.54(**)	0.1(**)	0.33(**)	0.87

Significance Codes: "**" represents p<0.01; "*" represents p<0.05; "." represents p<0.1

Table S2.9 Annual national (site and source) energy consumption differences between four future time periods and the 2008-12 time period, based on A 65 °F balance point. Results represents the relative difference (%, upper line), and difference (Trillion btu, lower line). The value outside of the parenthesis represents the median, and the values within the parenthesis represent minimum and maximum based on 20 climate models.

	Site Electricity	Source Electricity	Site Non-electricity	Source Non-electricity	Total Site	Total Source
2020-39	1 (-0.6, 2.6) 91 (-59, 242)	1 (-0.7, 2.7) 296 (-202, 775)	-8.6 (-14.3, -2.2) -866 (-1429, -219)	-8.7 (-14.3, -2.2) -900 (-1484, -228)	-3.8 (-7.1, -1.2) -727 (-1364, -239)	-1.5 (-3.2, -0.1) -583 (-1262, -41)
2040-59	3.9 (1.1, 6) 362 (99, 557)	3.9 (1.1, 6) 1145 (311, 1741)	-14.7 (-21.6, -7.1) -1476 (-2160, -709)	-14.7 (-21.6, -7.1) -1533 (-2243, -738)	-5.4 (-9.1, -2.8) -1043 (-1762, -531)	-0.6 (-3.2, 0.3) -254 (-1275, 124)
2060-79	7.6 (4.2, 10.4) 701 (387, 961)	7.6 (4.1, 10.2) 2201 (1191, 2963)	-20.5 (-28.8, -11.7) -2050 (-2881, -1170)	-20.5 (-28.8, -11.7) -2130 (-2993, -1216)	-7 (-10.5, -4) -1339 (-2024, -770)	-0.1 (-2.1, 1.5) -22 (-840, 601)
2080-99	12 (6.2, 16.3) 1112 (574, 1511)	11.9 (6.1, 16.2) 3463 (1776, 4687)	-26.7 (-37.2, -17.9) -2671 (-3728, -1790)	-26.7 (-37.2, -17.9) -2774 (-3872, -1859)	-7.7 (-11.5, -6.2) -1492 (-2217, -1198)	1.6 (-1.1, 4.1) 649 (-452, 1632)

Section S2.7 Population redistribution

Population patterns are projected to differ from current population distribution and the intersection of these pattern changes with the spatial pattern associated with climate change projections is an important element of the quantification of future building energy

demand under climate change. Figure S2.4 represents the population ratio between 2090 and 2010 for each state. In this figure, the 2090 national total population is held at the 2010 level. Thus, it only represents the effect of population redistribution.

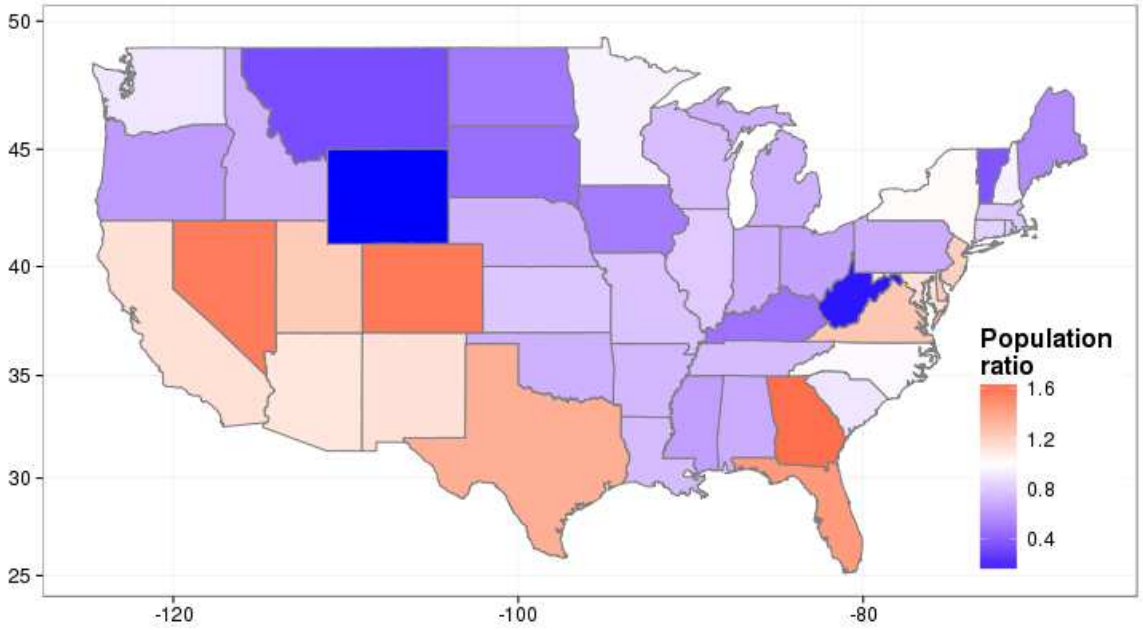

Figure S2.4 Ratio of population distribution in 2090 to 2010.

APPENDIX B

SUPPORTING MATERIAL FOR CHAPTER 3

Table S3.1 CMIP5 climate models

	Models
1	ACCESS1-0
2	BCC-CSM1-1
3	BNU-ESM
4	CANESM2
5	CCSM4
6	CESM1-BGC
7	CNRM-CM5
8	CSIRO-MK3-6-0
9	GFDL-ESM2G
10	GFDL-ESM2M
11	INMCM4
12	IPSL-CM5A-LR
13	IPSL-CM5A-MR
14	MIROC-ESM
15	MIROC-ESM-CHEM
16	MIROC5
17	MPI-ESM-LR
18	MPI-ESM-MR
19	MRI-CGCM3
20	NORESM1-M

Table S3.2 lm(formula = y ~ C + BD + T + xc0 + xc1 + xc3 + xc6 + xh0 + xh2 + xc1_2) adjusted R2 = 0.9823

	Estimate	Standard Error	t value	Pr(>|t|)
C	9.608e+06	3.816e+04	2.518e+02	0.000e+00
BD	1.099e+06	1.179e+04	9.326e+01	0.000e+00
T	-9.351e+04	2.700e+03	-3.464e+01	2.681e-193
PAC_{d+1}	3.036e-04	1.888e-05	1.607e+01	9.845e-54
PAC_{d}	2.052e-04	3.092e-05	6.638e+00	4.451e-11
PAC_{d-2}	1.017e-04	1.257e-05	8.091e+00	1.218e-15
PAC_{d-5}	5.122e-05	8.513e-06	6.016e+00	2.243e-09
PH_{d+1}	1.013e-04	1.314e-05	7.714e+00	2.215e-14
PH_{d-1}	1.063e-04	1.391e-05	7.642e+00	3.804e-14
PAC_{d}^{2}	6.827e-14	3.593e-15	1.900e+01	2.955e-72

Table S3.3 Frequency, period, and quantile

Frequency (event/56-year)	Frequency (event/year)	Period (year/event)	Quantile (%)
1	0.02	56	99.995
2	0.04	28	99.99

3	0.05	18.67	99.985
4	0.07	14	99.98
5	0.09	11.2	99.976
6	0.11	9.33	99.971
7	0.12	8	99.966
8	0.14	7	99.961
9	0.16	6.22	99.956
10	0.18	5.6	99.951
11	0.2	5.09	99.946
12	0.21	4.67	99.941
13	0.23	4.31	99.936
14	0.25	4	99.932
15	0.27	3.73	99.927
16	0.29	3.5	99.922
17	0.3	3.29	99.917
18	0.32	3.11	99.912
19	0.34	2.95	99.907
20	0.36	2.8	99.902
21	0.38	2.67	99.897
22	0.39	2.55	99.892
23	0.41	2.43	99.888
24	0.43	2.33	99.883
25	0.45	2.24	99.878
26	0.46	2.15	99.873
27	0.48	2.07	99.868
28	0.5	2	99.863
29	0.52	1.93	99.858
30	0.54	1.87	99.853
31	0.55	1.81	99.848
32	0.57	1.75	99.844
33	0.59	1.7	99.839
34	0.61	1.65	99.834
35	0.62	1.6	99.829
36	0.64	1.56	99.824
37	0.66	1.51	99.819
38	0.68	1.47	99.814
39	0.7	1.44	99.809
40	0.71	1.4	99.804
41	0.73	1.37	99.8
42	0.75	1.33	99.795
43	0.77	1.3	99.79
44	0.79	1.27	99.785
45	0.8	1.24	99.78
46	0.82	1.22	99.775
47	0.84	1.19	99.77
48	0.86	1.17	99.765
49	0.88	1.14	99.76
50	0.89	1.12	99.756
51	0.91	1.1	99.751
52	0.93	1.08	99.746
53	0.95	1.06	99.741
54	0.96	1.04	99.736
55	0.98	1.02	99.731
56	1	1	99.726

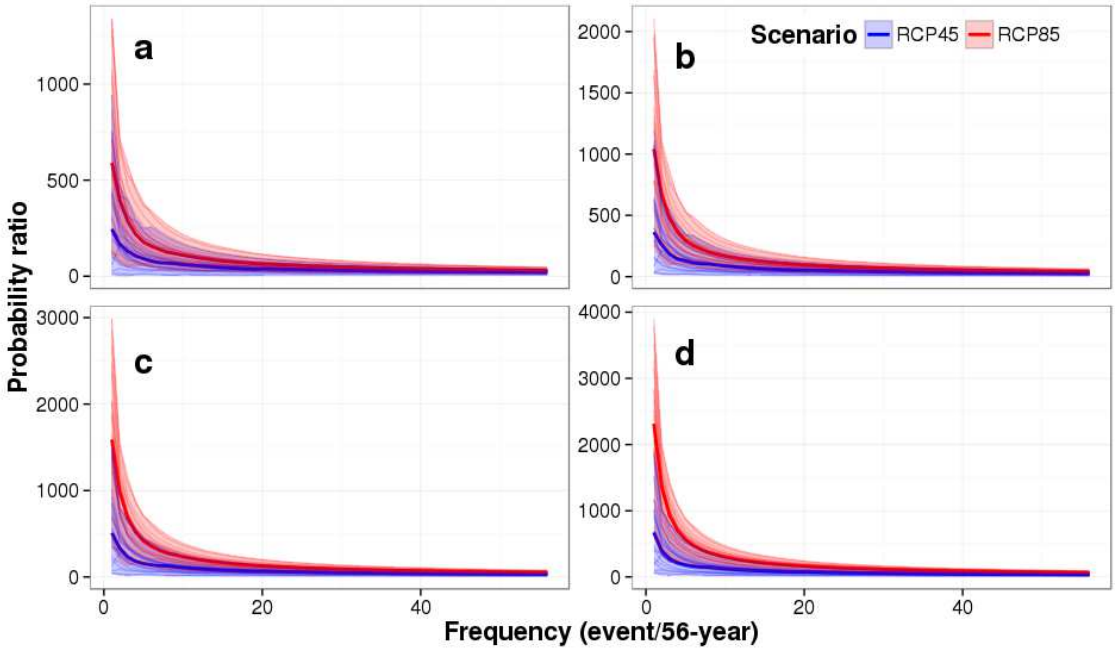

Figure S3.1 Probability ratio of extreme electricity demand in future periods relative to the 1950-2005 time period. Each thin line represents the estimate for a single climate model. The thick line represents the median estimate, and the shaded area represents the range of estimates for all climate models. Panels represent four chosen 56-year time periods: **a.** 2010-2065, **b.** 2020-2075, **c.** 2030-2085, and **d.** 2040-2095

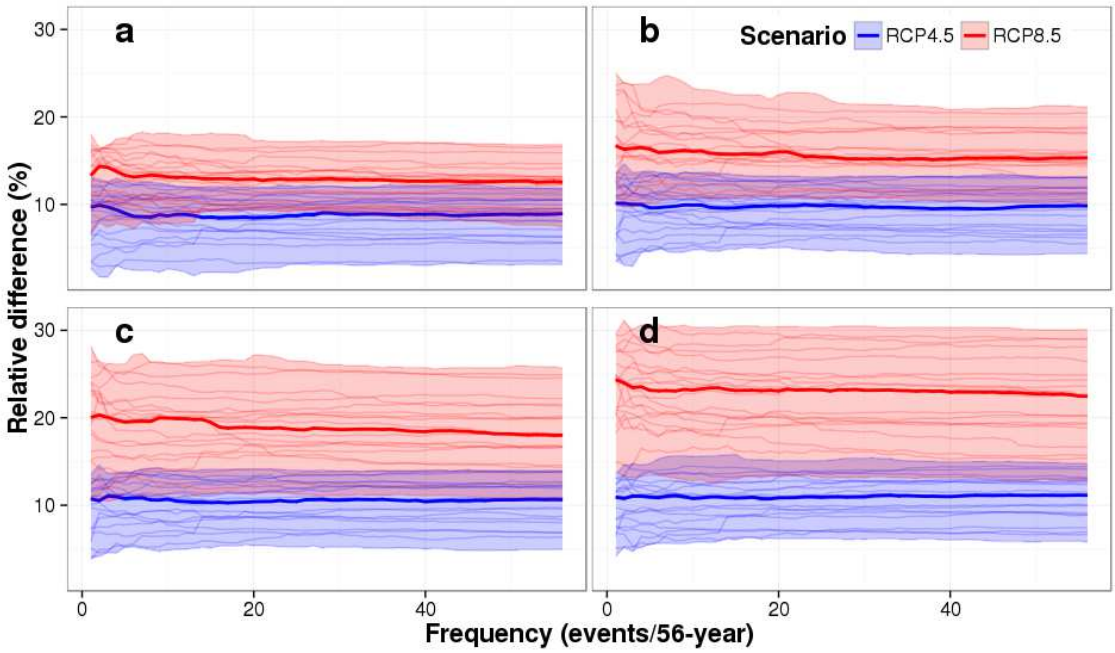

Figure S3.2 Relative difference of extreme electricity demand between future periods and the 1950-2005 time period. Each thin line represents the estimate for a single climate

model. The thick line represents the median estimate, and the shaded area represents the range of estimates for all climate models. Panels represent four chosen 56-year time periods: **a.** 2010-2065, **b.** 2020-2075, **c.** 2030-2085, and **d.** 2040-2095.

APPENDIX C

SUPPORTING MATERIAL FOR CHAPTER 4

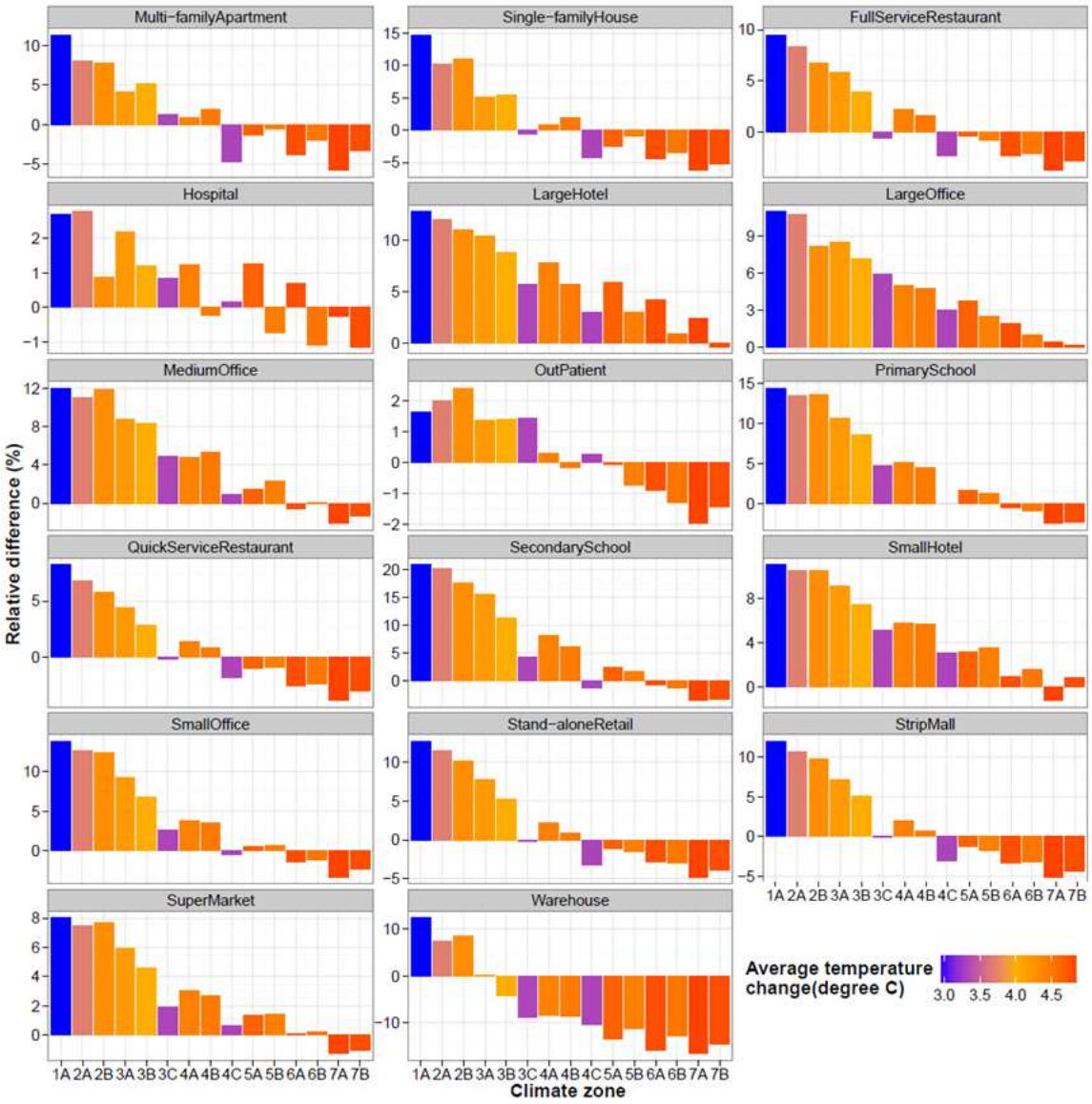

Figure S4.1 Climate-zone level annual building energy consumption relative difference (%) between the 2090s and the 1991-2005 time period under the A2 emission scenario for residential and commercial building types. The bar color represents the average temperature change of all locations within each climate zone.

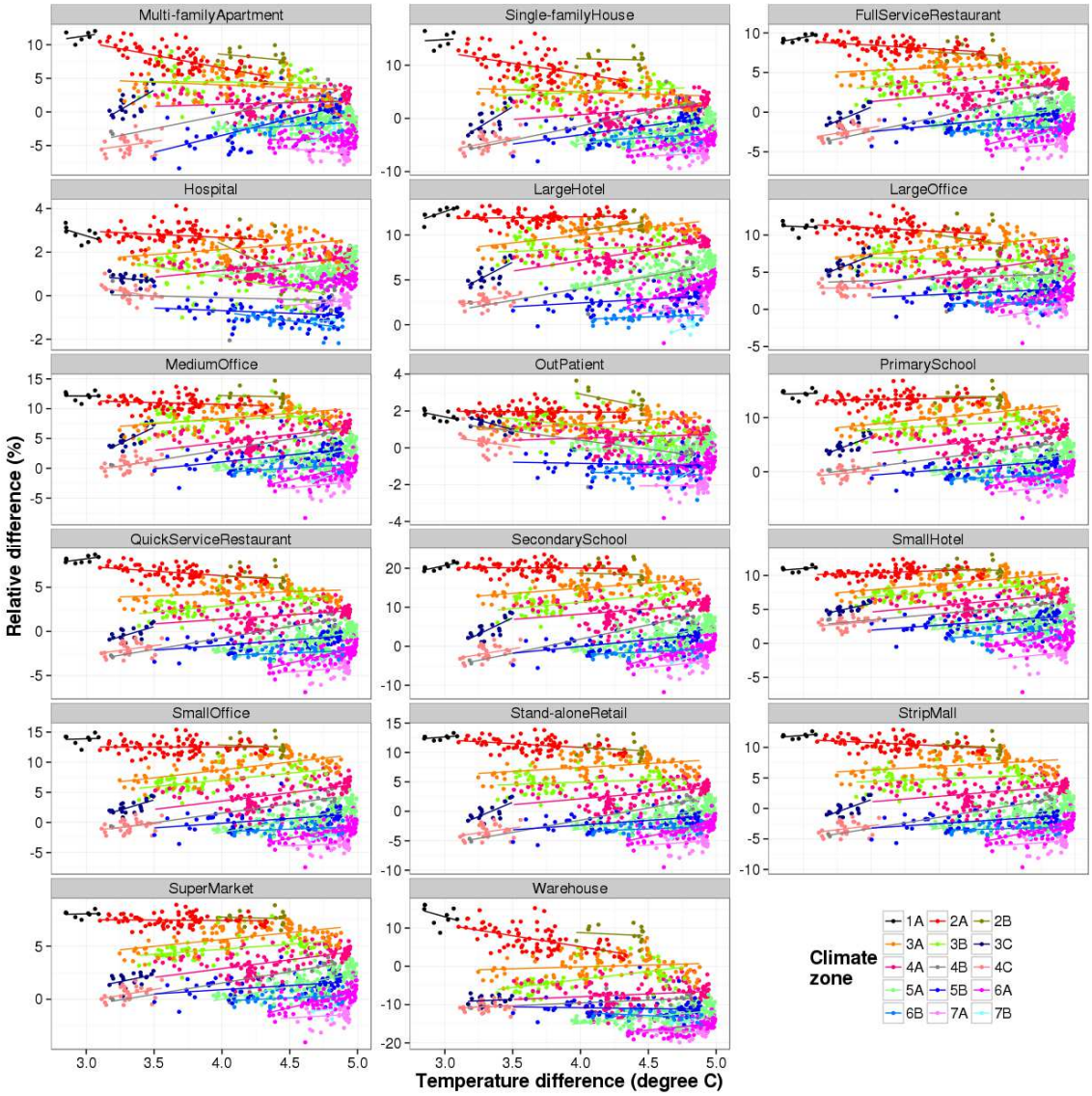

Figure S4.2 Relationship between the location-level relative difference (%) of annual building energy consumption and temperature change for all commercial and residential building types. Results represent the differences (changes) between the 2090s and the 1991-2005 time period under the A2 emission scenario.